RECLAMATION

Managing Water in the West

Evaluation of Numerical Models for Simulating Embankment Dam Erosion and Breach Processes

DSO-2017-02

Dam Safety Technology Development Program

U.S. Department of the Interior
Bureau of Reclamation
Technical Service Center
Denver, Colorado

August 2017

Mission Statements

Protecting America's Great Outdoors and Powering Our Future.

The Department of the Interior protects and manages the Nation's natural resources and cultural heritage; provides scientific and other information about those resources; and honors its trust responsibilities or special commitments to American Indians, Alaska Natives, and affiliated island communities.

Acknowledgments

The Working Group on Embankment Dam Erosion and Breach Modeling was organized under the Dam Safety Interest Group of CEATI International to conduct research on improved methods for modeling the failure of embankment dams. The working group included CEATI-member utilities and non CEATI-member organizations with strong research programs in this area. The late Gary Salmon was the Technical Coordinator of the DSIG during the first phase of this project and contributed greatly to our work. Other key contributors to the research included the following: Chris Hayes (CEATI International); Greg Hanson, Darrel Temple, and Ron Tejral (USDA-ARS); Mark Morris (HR Wallingford); Jean-Robert Courivaud (Electricité de France); Jeff McClenathan, Johannes Wibowo, and Michael Gee (U.S. Army Corps of Engineers); and Réne Kahawita (Ecolé Polytechnique de Montréal). The work was supported financially by each of the respective team member's organizations and by many other CEATI-member utilities.

Disclaimer:

The information provided in this report is believed to be appropriate and accurate for the specific purposes described herein, but users bear all responsibility for exercising sound engineering judgment in its application, especially to situations different from those studied. References to commercial products do not imply endorsement by the Bureau of Reclamation and may not be used for advertising or promotional purposes.

REPORT DOCUMENTATION PAGE		Form Approved OMB No. 0704-0188

PLEASE DO NOT RETURN YOUR FORM TO THE ABOVE ADDRESS.

1. REPORT DATE *(DD-MM-YYYY)*	**2. REPORT TYPE**	**3. DATES COVERED** *(From - To)*
August 2017		2007 – 2012

4. TITLE AND SUBTITLE

Evaluation of Numerical Models for Simulating Embankment Dam Erosion and Breach Processes

5a. CONTRACT NUMBER

5b. GRANT NUMBER

5c. PROGRAM ELEMENT NUMBER

6. AUTHOR(S)

Working Group on Embankment Dam Erosion and Breach Modeling, CEATI International Dam Safety Interest Group

5d. PROJECT NUMBER

5e. TASK NUMBER

5f. WORK UNIT NUMBER

7. PERFORMING ORGANIZATION NAME(S) AND ADDRESS(ES)

Department of the Interior, Bureau of Reclamation
Technical Service Center, Denver Federal Center
PO Box 25007 (86-68560)
Denver, CO 80225-0007

8. PERFORMING ORGANIZATION REPORT NUMBER

DSO-2017-02

9. SPONSORING/MONITORING AGENCY NAME(S) AND ADDRESS(ES)

Department of the Interior, Bureau of Reclamation
Dam Safety Office, Denver Federal Center
PO Box 25007 (84-44000)
Denver, CO 80225-0007

10. SPONSOR/MONITOR'S ACRONYM(S)

BOR/USBR: Bureau of Reclamation
DOI: Department of the Interior
DSO: Dam Safety Office

11. SPONSOR/MONITOR'S REPORT NUMBER(S)

DSO-2017-02

12. DISTRIBUTION/AVAILABILITY STATEMENT

13. SUPPLEMENTARY NOTES

14. ABSTRACT

The Working Group on Embankment Dam Erosion and Breach Modeling was organized under the Dam Safety Interest Group of CEATI International to conduct research on improved methods for modeling the failure of embankment dams. From approximately 2007-2009 the group conducted an evaluation of numerical breach models using data from five large-scale laboratory tests and two real dam failures. The evaluation focused primarily on two models, SIMBA, developed by the USDA-Agricultural Research Service (USDA-ARS), and HR BREACH, developed at HR Wallingford. Both models performed well on 5 of the 7 test cases, with the exceptions caused by a lack of high quality data on the embankment properties, failure scenarios, and resulting floods. The evaluation showed that the ability to obtain accurate estimates of soil erodibility was crucial to achieving good model performance, with direct measurements made through lab or field-based testing being most preferable. The evaluation also showed that there is a pressing need for research that can determine whether embankment materials are likely to erode predominantly through surface erosion or headcutting mechanisms.

15. SUBJECT TERMS

Dam breach, erosion, headcut, modeling, erodibility

16. SECURITY CLASSIFICATION OF:			**17. LIMITATION OF ABSTRACT**	**18. NUMBER OF PAGES**	**19a. NAME OF RESPONSIBLE PERSON**
					Tony L. Wahl
a. REPORT	**b. ABSTRACT**	**c. THIS PAGE**	SAR	91	**19b. TELEPHONE NUMBER** *(Include area code)*
UL	UL	UL			303-445-2155

Bureau of Reclamation

Dam Safety Technology Development Program

86-68560

DSO-2017-02

Evaluation of Numerical Models for Simulating Embankment Dam Erosion and Breach Processes

Tony L. Wahl

Digitally signed by TONY WAHL
Date: 2017.08.12 14:27:21 -06'00'

Prepared by: Working Group on Embankment Dam Erosion and Breach Modeling
CEATI International Dam Safety Interest Group
Chair: Tony L. Wahl, P.E., Hydraulic Investigations and Laboratory Services Group, 86-68560

ROBERT EINHELLIG

Digitally signed by ROBERT EINHELLIG
Date: 2017.09.15 14:24:05 -06'00'

Technical Approval: Robert F. Einhellig, P.E.
Manager, Hydraulic Investigations and Laboratory Services Group, 86-68560

BRUCE FEINBERG

Digitally signed by BRUCE FEINBERG
Date: 2017.08.24 09:43:17 -06'00'

Peer Review: Bruce D. Feinberg, P.E.
Hydraulic Engineer, Geographic Applications and Analysis Group, 86-68260

Contents

Tables

Figures

Acronyms and Abbreviations

HERU	Hydraulic Engineering Research Unit
NRCS	Natural Resources Conservation Service
NWS	National Weather Service
SIMBA	Simplified Breach Analysis
USDA	U.S. Department of Agriculture
USDA-ARS	USDA-Agricultural Research Service
WinDAM	Windows Dam Analysis Modules

Executive Summary

The Working Group on Embankment Dam Erosion and Breach Modeling was organized under the Dam Safety Interest Group of CEATI International to conduct research on improved methods for modeling the failure of embankment dams. The working group included CEATI-member utilities and non CEATI-member organizations with strong research programs in this area. The first phase of the project from 2004 to 2007 identified promising numerical models under development and collected data from real dam failures and large-scale laboratory tests that could be used to test those models. The second phase of the project included two major tasks, an evaluation of methods for measuring erodibility of the cohesive soils encountered in embankment dams (see report DSO-08-05), and an evaluation of numerical breach models using data from five large-scale laboratory tests and two real dam failures. The latter activity to evaluate numerical breach models is the subject of this report.

The model evaluations were performed from about 2007-2009, and development of the evaluated models has continued since that time. The two models that were the focus of the evaluation were SIMBA, developed by the USDA-Agricultural Research Service (USDA-ARS), and HR BREACH, developed at HR Wallingford. SIMBA was an internal-use research tool that led to the development of the WinDAM B dam breach model, publicly-released in 2011. HR BREACH development has led to two present-day models, the full-featured EMBREA model and the AREBA simplified model for homogeneous embankments. A third model originally identified by the working group for evaluation was FIREBIRD, developed at Montréal Polytechnic, but this model proved more difficult to use than the other two and has not been developed further.

The SIMBA and HR BREACH models were evaluated using data from two real dam failures, Oros Dam (Brazil, failed 1960), and Banqiao Dam (China, failed 1975). In addition, data from five large-scale embankment breach tests were used, two tests performed by USDA-ARS at Stillwater, Oklahoma (approx. 2-m-high embankments), and three performed in Norway as part of the European IMPACT Project (6-m-high embankments). The USDA-ARS tests were very well documented, with minimal uncertainties in the data used for the model evaluation work (beyond those associated with natural variability of soils in earthen embankments). Although the first phase of the CEATI project strived to identify case studies with high-quality data for evaluation purposes, the quality of the data for the real dam failures and the Norway tests proved to be a significant issue.

The Oros and Banqiao cases suffered from issues that plague almost all real dam failures. With no expectation of failure prior to the events, there is never an established plan for collecting data to document dam failure processes. Data that can be obtained after a failure are often spotty, inconsistent, and of questionable accuracy, and eyewitnesses to the event are focused on survival and damage-control, rather than accurate reporting for research purposes.

The Norway dam breach tests provided useful data, but with more uncertainty than the USDA-ARS tests. Two of the embankments were constructed in difficult weather conditions leading to very poor and uncertain compaction in one case and potentially a frozen embankment in the

second case. This makes evaluation of the erodibility of the soils in these tests very difficult. In addition, based on photo and video records there are questions about the exact materials that were placed in the embankments and the accuracy with which the embankment sections were constructed. Finally, the other problem that affected the Norway tests was poor control of the inflow to the site during each test. The tests were performed in a river reach located a short distance downstream from a reservoir whose releases could be regulated. Researchers attempted to control the inflow so that the reservoir upstream from the test embankments would be maintained at a constant head for a long period of time, simulating the boundary condition of a large-volume reservoir. Unfortunately, the magnitude and timing of the inflow could not be controlled with enough accuracy to achieve the objective and the result was a highly variable boundary condition. In contrast, the USDA-ARS tests were performed with a constant inflow and no attempt to maintain the pool elevation. As such the results were representative of small reservoirs, but the inflow was a small fraction of the peak breach discharge for the highly erodible cases, so the effect of the breach was readily discernible. This arrangement was easy to regulate and performed very well.

The model evaluation results showed that the SIMBA and HR BREACH models both performed well on 5 of the 7 test cases. The Banqiao Dam case was poorly modelled by both programs, but the quality of the input and observed data are questionable for this case. The Norway gravel dam case was judged to be impossible to model because of uncertainties regarding material erodibility and artificial manipulations of test conditions. The evaluators were unable to successfully run the FIREBIRD model on most of the test cases. In addition, the legacy National Weather Service BREACH model was considered a point of reference for the study and some attempts were made to run it on the various test cases. Although detailed results are not presented in this report, the evaluators typically found it difficult to produce realistic results with NWS-BREACH using reasonable material property inputs.

The ability of SIMBA and HR BREACH to predict the peak breach outflow was good in initial model runs and very good in improved runs where evaluators were allowed to make reasonable adjustments to input parameters and modeling options. Predictions of final breach width were good also, even though both models were somewhat restricted in their capabilities during the evaluation process. Specifically, SIMBA was operated only with its stress-based headcut erosion model (its energy-based model was disabled), and HR BREACH was intentionally run primarily in surface erosion mode, although it also includes an energy-based headcut erosion model.

Predictions of parameters related to time (breach widening rate, breach initiation time and breach formation time) were less accurate for both models, especially in the initial model runs. The improved model runs exhibited significant improvement, and the errors between predicted and observed values were generally one half order of magnitude or less. Although large, this is better than the prediction errors typically associated with breach formation times obtained from regression equations, which commonly range up to ±1 order of magnitude (Wahl 2004). Prediction errors in the initial runs were comparable to those obtained with regression equations.

Headcut erosion was the dominant feature for most of the case studies, although the Norway gravel dam and composite dam contained non-cohesive materials that were amenable to modeling with HR BREACH's surface erosion mode. The SIMBA model's stress-based headcut model performed very well and exhibited appropriate sensitivity to soil parameters. HR

BREACH's energy-based headcut erosion model also performed well and could readily be adjusted to represent a wide range of soil erodibility characteristics. The Oros case study test highlighted the importance of drowning effects on breach formation. The valley immediately downstream of the Oros Dam poses a tight constriction. In the HR BREACH model, inclusion of this constriction and the subsequent drowning of the breach during the formation process produced prediction results far closer to the observed data than without consideration of drowning effects. The SIMBA model did not provide a means to directly simulate a high tailwater condition, but reducing the soil erosion rate coefficient produced similar results. SIMBA's successor, WinDAM B, can account for tailwater effects.

Sensitivity of both models to changes in soil erodibility parameters was appropriate and consistent with observed variations in breach development during laboratory tests in which erodibility was directly measured. Some model runs were very sensitive to specific parameters when it affected the relative timing of the peak of the inflow hydrograph and the completion of the breach initiation phase. This is a real phenomenon which is often dramatic when trying to simulate a laboratory test where the inflow hydrograph has been matched with the timing of the breach development.

Some other important findings from the model evaluation process are:

- The usability of models is extremely important. Extensive testing of model sensitivity was important for this evaluation and will also remain important in any real-world use of the models. This requires the ability to readily and efficiently make multiple program runs and manage associated input and output data.
- User expertise is critical for identifying key physical processes and correctly applying the models, since numerous modeling options and parameters are available.
- The distinction between headcut erosion and surface erosion can be important, and there is a need for additional research to help delineate when each process occurs.

The model evaluation helped to highlight the fact that in 2009 the HR BREACH model was a more complex model than SIMBA in several ways:

- It allowed the internal erosion failure mode
- It allowed modeling of zoned embankments
- It allowed a wider range of erosion models
- The model simulates flow and erosion at multiple cross sections down the full length of the flow path, not just at the critical-depth flow section

These differences combine to make HR BREACH a somewhat slower model to execute (although run times are still just a matter of seconds to a few minutes on modern computer hardware). They also make HR BREACH more complex to configure and operate, since there are many modeling options and parameters.

Both of these models are worthy of further development, and that development has been continuing since this model evaluation work was performed. There is often value in having models that are simpler to configure and run, and thus HR BREACH development has followed two paths since 2009. A simpler AREBA model was developed for rapid breach modeling of

homogeneous embankments, while development of additional modeling capabilities for zoned embankments has led to the EMBREA model (replacing HR BREACH).

All three of the models that have evolved from the SIMBA and HR BREACH lines of development (WinDAM B, EMBREA, and AREBA) significantly improve our ability to model erosion and breach processes for embankment dams. Each is capable of functioning as a stand-alone model to produce breach outflow hydrographs that could serve as input to a variety of flood routing tools. Each also offers technology that could potentially be integrated into flood routing tools as an alternative to breach parameters developed from simple regression-based equations. The final section of this report discusses the specific components of the models, their similarities and differences, and how they could be combined and integrated to create next generation embankment dam breach modeling tools.

Introduction

In 2004 the Dam Safety Interest Group of CEATI International initiated a research project aiming to advance the state of practice for computer modeling of embankment dam erosion and breach processes. A working group was formed with representatives from CEATI-member utilities with a strong interest in this topic, including several pursuing dam breach modeling research programs of their own. Non CEATI-member organizations with strong research programs on this topic were also invited to join and participate in the working group. The resulting collaboration brought together many of the most active researchers and organizations working on this topic worldwide.

Table 1.—Members of the CEATI Working Group, and other project sponsors.

Organization	Roles
Electricité de France	Assemble case studies of real dam failures. Erodimeter and piping erosion research.
Hydro Québec / Ecolé Polytechnique Montréal	Review of numerical models for simulating dam breach, development of FIREBIRD breach model.
Bureau of Reclamation	Review of laboratory physical hydraulic modeling programs. Investigation of erodimeters.
USDA-Agricultural Research Service	Large-scale laboratory testing and development of SIMBA/WinDAM models. Development and investigation of erodimeters.
HR Wallingford	Small- and large-scale physical model testing (IMPACT project), developers of HR BREACH model
US Army Corps of Engineers	Erodimeter evaluation, breach model evaluation, future integration of breach modeling technology into HEC-RAS suite
Elforsk AB	Numerical breach model evaluation

Other sponsors: BC Hydro, Churchill Falls, Elforsk AB, EoN Vasserkraft, Great Lakes Power, Manitoba Hydro, New York Power Authority, Ontario Power Generation, Seattle City Light, Scottish & Southern Energy

The working group adopted a phased approach. The first phase reviewed the history of physical modeling of dam breach processes in laboratory environments (Wahl 2007) and reviewed efforts to develop improved numerical models (Kahawita 2007). Laboratory test data were compiled (Wahl 2007), especially results from recent, large-scale physical model tests, and data from real-world case studies of dam failure were also collected (Courivaud 2007). The review of current model-development programs revealed three computer models that the working group chose to evaluate in a second phase of the project using the assembled lab and real-world case study datasets. The model evaluations were performed from about 2007-2009, and the models have

continued to develop since that time. This report provides the detailed results of the model evaluation and provides updated information on further development of two of the models from 2010 to the present day (2017). Although these models have continued to develop and other dam breach models have also appeared in recent years, the results of the evaluation still provide insight for further development of next-generation technology for numerically modeling embankment dam erosion processes leading to dam breach, and potentially for the integration of that technology into existing dam-break flood routing models. A parallel activity in the second phase of the project was the evaluation of alternative methods for measuring erodibility of the cohesive soils encountered in embankment dams, and development of user guidance for estimating material parameters for modeling use. Reports on those research efforts were made separately.

The development and integration of next-generation dam breach modeling tools into dynamic flood routing models and the continued improvement of those models going forward is the long-term objective of the CEATI-sponsored project. The model evaluation described in this report is focused on the overtopping failure mode and relatively simple embankment geometries, but continued development of these models is addressing internal erosion and complex embankment geometries. These capabilities are expected to continue to improve over time.

Dam Breach Modeling Overview

The scientific desire and practical need to simulate the hydraulics of dam failure and resulting floods dates back to the earliest days of hydraulic engineering (e.g., Ritter 1892). As the Industrial Revolution ushered in the era of large dam construction, sometimes catastrophic dam failures accompanied it, such as Johnstown Dam (constructed 1853, failed 1889). Early attempts to model the floods resulting from dam failure assumed instantaneous failure of dams and focused mostly on understanding the dynamics of reservoir release and flood-wave propagation through downstream channels (Wahl 2007). In the 1970s several dramatic dam failures causing catastrophic loss of life and property damage led to legislation requiring careful assessment of the hazard potential of dams and prediction of expected areas of inundation in the event of the failure of high-hazard dams (those whose failure would threaten human life). Because early legislation was focused on a simple requirement to determine the inundated area (i.e., flood inundation map), first modeling efforts were aimed at prediction of the magnitude of the outflow hydrograph, especially the peak outflow, and less effort was devoted to determining the timing of the hydrograph, which is largely dependent in most cases on the rate of increase in the erosion rate during the breach initiation phase of a failure. The last decade has seen research focused on understanding and modeling the physical processes involved in erosion, breach initiation and breach development, as it was recognized that accurate simulation of details of failure processes could dramatically affect predictions of loss of life.

Wahl (2010) presented an overview of dam breach modeling methods and their evolution from the 1960s to the present. The primary modeling approach used during most of this period has been based on regression analysis using real-world case study data, either to predict peak dam breach outflow directly or to predict geometric and temporal parameters of breach development so that computer models could then determine breach outflow analytically, given a prescribed breach development scenario. The deficiency of these approaches is their primary focus on the

breach formation process and their inability to provide information about the duration of the *breach initiation* process, or their lack of distinction between the two phases when predicting breach time parameters. This stemmed partly from the nature of the case study data available for creating predictive regression equations, partly from the fact that early routing models (e.g., NWS-DAMBRK by Fread [1977; 1984]) simulated only the breach formation process and thus needed to know only the breach formation time, and partly from a lack of appreciation until recently for the distinct features and importance of each phase (Wahl 1998). The two distinct phases of the breach process can be described as follows:

- **Breach initiation** - The breach initiation phase begins with the first flow of water over or through a dam that produces observable erosion with the potential to progress and cause dam failure. During the breach initiation phase, the zone of active erosion is downstream from the point of hydraulic control of the flow, so outflow rate changes only in response to changes in the driving reservoir conditions, not as a result of erosion. As breach initiation proceeds, the zone of active erosion generally moves upstream (e.g., headcut or surface erosion during overtopping flow). The breach initiation phase ends when the active erosion front reaches the crest and upstream face of the dam, thereby producing a rapidly accelerating breach outflow and typically unstoppable failure of the dam.

- **Breach formation** - The breach formation phase begins at the end of the breach initiation phase, when erosion begins to cause enlargement of the channel cross section that serves as the hydraulic control of the outflow rate. The breach formation phase continues until the breach has enlarged to its approximate maximum dimensions. The breach formation period may include processes of both deepening and widening of the breach. Because breach enlargement may continue slowly as a reservoir drains, various means can be used to define a practical end to the breach formation phase (e.g., graphically). The breach formation phase could alternately be described as the *breach development* or *breach enlargement* phase.

Figure 1 illustrates a timeline for the dam breach process, with definition of key time-related terms. Note that the peak outflow can occur anywhere within the breach formation phase, including before the breach has enlarged to its ultimate dimensions, depending on factors such as the rate of erosion and the size of the reservoir. Also note that for a case of internal erosion failure, there may be a period of defect development preceding the first noticeable increased outflow that begins the breach initiation time. This time may be very long relative to the time for breach initiation and enlargement (weeks, months, or even years).

Procedures for estimating loss of life due to dam failure have been developed and refined over the last several decades (e.g., Brown and Graham 1988, DSO-99-06, and RCEM 2014 all developed at the Bureau of Reclamation). Today, simulation models such as LifeSim and the Life Safety Model are also used. From review of experiences during past dam failures and other large flood events, the key parameter affecting loss of life is the warning and evacuation time available to the population at risk. Once a problem at the dam is noticed, in most cases, the breach initiation phase comprises the majority of the available warning and evacuation time. When populations are a significant distance downstream from the dam there may be an additional warning time due to the travel time of the flood from the dam to the inundated area, but in most cases the breach initiation time and warning and evacuation times are closely coupled.

The second area of deficiency in the models available during the 1970s to 2000s for simulating dam breach processes was their inability to simulate the erosion processes observed in real world case studies, primarily headcut erosion and associated failures of large soil masses, and their inability to incorporate measurable parameters related to erodibility of embankment materials. These problems made it difficult for simulation models to reproduce the high degree of variability observed in real world failures between cases of highly erodible versus very erosion-resistant materials. Models that relied on sediment transport relations developed for rivers and considered erodibility to be solely a function of material particle size could not reproduce variations of real-world erosion rate that spanned several orders of magnitude. These variations of erodibility are often the result of differences in compaction effort and soil conditions (primarily water content) at the time of compaction (Hanson and Hunt 2007).

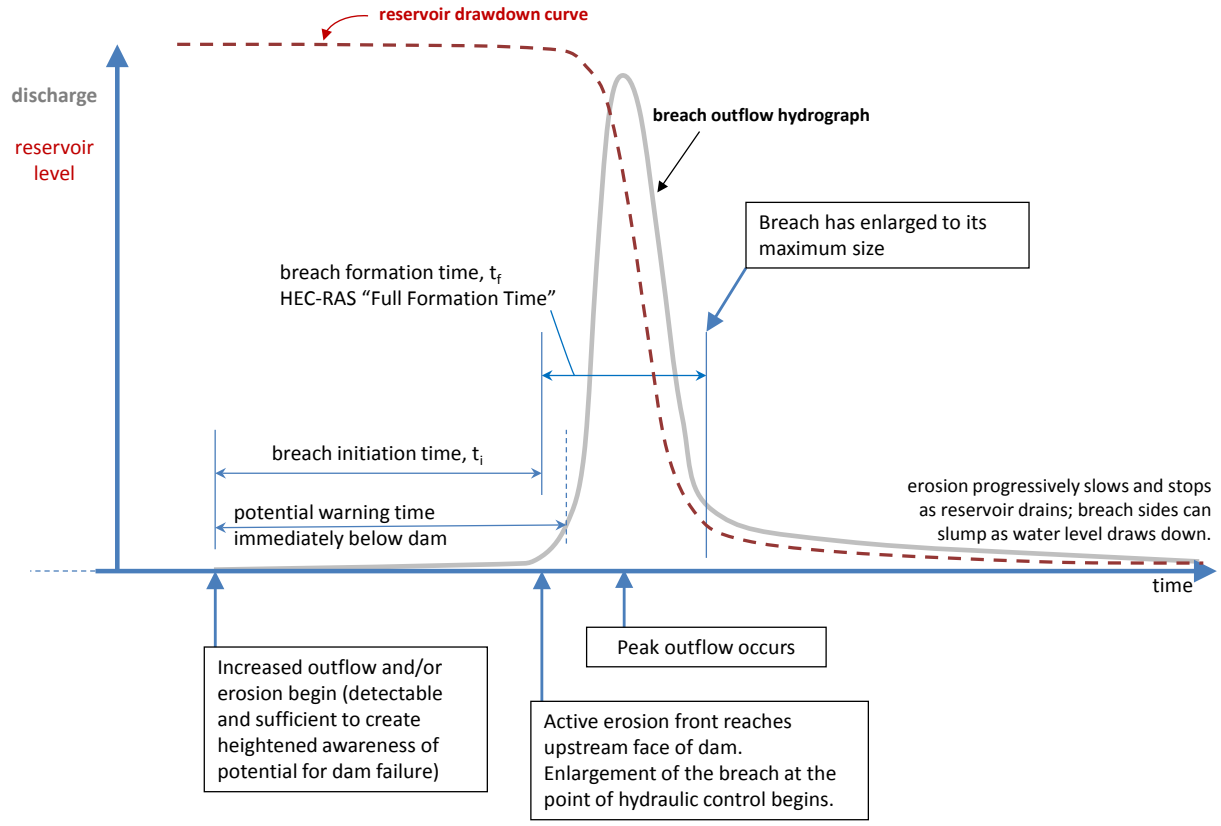

Figure 1.—Timeline showing key milestones in the development of a typical dam breach.

Value of Process-Based Models

With this background, it is clear that dramatic improvements in our ability to model the consequences of dam breach floods are possible with the use of process-based models that simulate observed erosion phenomena, utilize material erodibility parameters that better reflect observed erosion rates, and make the distinction between the breach initiation and breach

formation phases. In addition to providing more accurate information on the length of the breach initiation phase and hence the warning and evacuation time (although detection of breach initiation does not always lead directly to issuance of warning), these models also offer the potential to answer the basic question of whether a dam is likely to fail under a specified set of circumstances. Traditional approaches have been unable to address this essential question, since they have not modeled the process leading up to failure, but instead assumed that failure will occur and focused their modeling efforts on the process of accelerating breach enlargement that takes place after failure has commenced. Answering this question is of great importance for risk assessment studies, for emergency action planning, and for the design of rehabilitation features that might make dams more resistant to breach initiation and subsequent dam failure.

Research Strategy

The first phase of this project (Kahawita 2007) identified three candidate numerical models that were presently under development and had the potential to satisfy the needs described above. The models are all process-based and simulate both the breach initiation and breach formation phases, with further subdivisions of those phases that are unique to the particular models. The models utilize quantitative erodibility parameters and simulate the erosion processes observed in case studies and laboratory tests. The models all have the capability to simulate erosion and breach of embankments that are primarily composed of cohesive materials. The models have varying abilities to analyze embankments with complex internal geometries (i.e., zoned construction). The models all consider erosion caused by overtopping flow, and some have limited capability to also consider internal erosion.

The three models considered at the beginning of the study were:

- SIMBA – SIMplified Breach Analysis – Developed by the USDA-ARS Hydraulic Engineering Research Unit, Stillwater, Oklahoma. (Temple et al. 2005, Hanson et al. 2005a). This is a research-focused model used to analyze data from large-scale laboratory tests for the purpose of developing and refining algorithms needed for the creation of an application-focused model, WinDAM B. WinDAM B Version 1.0 was officially released in August 2011, and the most recent release is Version 1.1.
- HR BREACH – Under development at HR Wallingford, Great Britain (Mohammed 2002, Mohamed et al. 2002). This model has been under continuous development in connection with several European Union initiatives related to flood modeling, including CADAM, IMPACT, FLOODsite, and the latest, FloodProBE. Work undertaken in parallel with the DSIG project analyses (Morris 2011) details the development of new zoned embankment breach modeling functionality.
- FIREBIRD – Developed at the Polytechnic School of Montreal through a collaboration with Hydro Quebec. (Wang and Kahawita 2002, Wang et al. 2006). The development of this model has not continued since about 2009.

As the model evaluation work proceeded, the FIREBIRD model was found to be difficult to use compared to the other two models and often exhibited simulation results that were unrealistic. As a result, the bulk of the model evaluation effort was focused on the SIMBA and HR BREACH models.

To evaluate the models, they were tested using a set of seven case study dam failures. Two of these dam breaches were real, historic events, and five were large-scale controlled laboratory tests. For each case study, the breach models were run by multiple members of the working group and results were assembled to allow a comparison of model results and observed data from the case studies.

Overview of Breach Models

Before discussing the application of the models to the test cases, it is worthwhile to review some of the recent history of the development of computational breach models and then the characteristics of each of the models evaluated here, especially their treatment of the erosion processes and mechanisms that lead to dam breach. Any effort to reduce a complex phenomenon like dam breach to a simpler model that is amenable to analysis and computation will, by necessity, involve simplifying assumptions about the processes that affect breach development, the material properties that serve as inputs to each modeled process, and the logic and relationships that control how the different processes interact with one another in parallel or in sequence. Understanding the internal details of each model aids in the validation of results and confirms that observed model behaviors are consistent with the modeling approaches employed.

Dam Breach Modeling History

The earliest observations of real dam failures and laboratory physical model simulations showed that erosion was the basic process at work in causing development of a dam breach. Despite this obvious fact, erosion was only reasonably understood in the early twentieth century in the context of more common and familiar flow situations, such as sediment transport in canals and rivers and scour and deposition around hydraulic structures. Dam failures were so infrequent and difficult to study that little was known about erosion during dam-break flow conditions and the quality of the data that were available was limited. The first dam break flood routing models simulated the breach of a dam by simple parameterization of the process of opening a breach in an embankment, often assuming that breach dimensions increased linearly over time to a prescribed final size, estimated by regression analysis. This is still a common approach today, although most models now also allow for non-linear erosion rates.

Attempts to simulate actual erosion processes began in the 1960s and gained momentum in the 1970s and 1980s. The National Weather Service (NWS) BREACH model developed by Fread (1988) became the most widely recognized of the early physically-based breach models, due in part to its free availability, consistent support from Dr. Fread and the National Weather Service, and a relatively high profile through its association with National Weather Service DAMBRK, the first widely used dam-break flood routing model. EROSIF is the name of the NWS-BREACH model as implemented in France, where it has seen significant use. In the UK the model was used as part of the DAMBRK-UK package. While the DAMBRK flood routing component was adjusted for UK conditions, the breach modeling component remained unchanged and was used in dambreak analyses during the 1980-1990s.

Early physically-based dam breach models utilized sediment transport equations originally developed for estimating bed load in riverine environments, either the Schoklitsch formula (Harris and Wagner 1967; BRDAM model by Brown and Rogers 1981), Einstein-Brown (BEED model by Singh and Scarlatos 1985; Singh 1996), or the Meyer-Peter and Müller formula (Lou 1981; Ponce and Tsivoglou 1981). The NWS-BREACH model utilized a modified form of Meyer-Peter and Müller developed by Smart (1984) for flow in channels as steep as 20% slope.

The NWS-BREACH model, like most early physically-based dam breach models, was based on a conceptual view of dam breach as a process driven by sediment transport erosion in a channel passing over the dam or a pipe passing through the dam. For overtopping flow, erosion takes place in an initially small rectangular gully in the downstream face of the dam. While this may seem conceptually similar to a pilot channel, the initial gully does not pass through the crest of the dam like the pilot channels provided in many laboratory breach experiments. Rather, the crest of the dam is level and the gully exists only in the downstream face. This must be accounted for when setting up the NWS-BREACH model to simulate a lab experiment conducted with a pilot channel. (The dam crest length should be defined as the width of the pilot channel instead of the true length of the dam, and the maximum allowable breach width must be specifically defined to match the true length of the dam. The dam crest elevation should be made equal to the pilot channel invert elevation.) This breach channel erodes perpendicularly into the downstream embankment face uniformly over its length, always remaining parallel to the original downstream embankment slope. The rate of erosion is based on the Smart sediment transport relation, with erosion assumed to take place uniformly over the wetted perimeter of the channel. The width of the channel is also adjusted as a function of the critical depth at the channel entrance and the angle of the channel side slopes can adjust as the initially vertical sides experience slope-stability failures. Eventually, the channel erodes through the crest of the dam, after which continued erosion of the channel causes lowering of the hydraulic control and a rapid increase in breach outflow. Tejral et al. (2009) graphically illustrated this process (Figure 2).

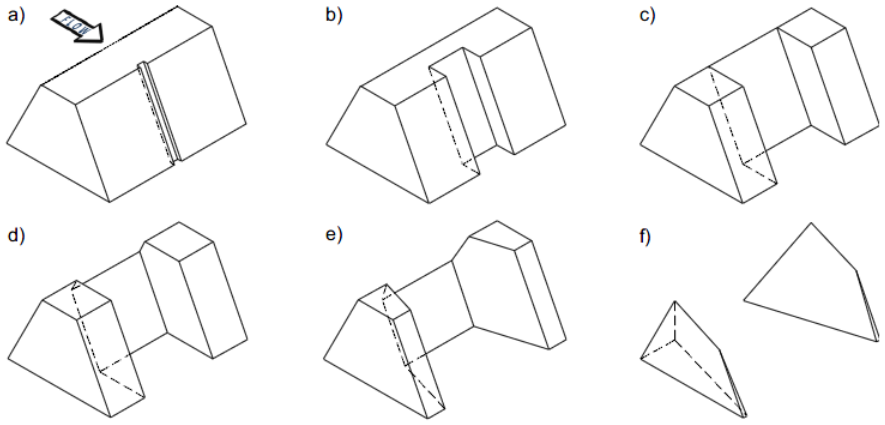

Figure 2.—Conceptual sequence of breach development for an overtopped dam, as modeled in NWS-BREACH. Flow is from is from top left to bottom right for each figure. (a) Initially, a small rectangular channel exists on the downstream dam face. (b) The channel erodes downward always parallel to the downstream face, and (c) erodes through the entire crest width. (d) The channel continues to deepen and widen. (e) Channel sides may collapse if they are determined to be unstable. (f) Breach opening may continue to widen through further collapses and continued flattening of side slopes (Tejral et al. 2009).

In addition to overtopping flow, the NWS-BREACH model also allowed for breach initiation by internal erosion, or piping. For a piping failure, the erosion sequence begins with flow through a rectangular duct or pipe of specified size and elevation. The sediment transport equation is used to determine a transport rate and the pipe enlarges by simultaneous and equal enlargement of the top, bottom and sides of the duct. Based on empirical criteria, the bridge over the pipe eventually collapses, changing the flow condition to a weir-controlled outflow and initiating the overtopping erosion sequence with the crest of the dam located at the pipe invert elevation.

The NWS-BREACH model also allows for the possibility of a sudden collapse of upper portions of the dam as the erosion channel enlarges and removes some of the mass that would otherwise help to prevent a sliding failure along horizontal planes through the dam. All mass-failure events modeled in NWS-BREACH produce pauses in the progress of erosion, as the displaced material must be transported out of the breach channel at the rate computed by the sediment transport equation (albeit with greatly increased flow rate in the case of a pipe collapse or sudden collapse of the crest of the dam).

The sediment transport equation is a key element of the NWS-BREACH model. Fread (1988) states that the critical material properties of the dam affecting the analysis are the internal friction angle, cohesive strength, and average (median) grain size (D_{50}). Examination of the sediment transport equation by Tejral et al. (2009) also confirms that D_{50} is one of the most important parameters in the model. The influence of D_{50} comes about through the fact that it can be used to compute the value of Manning's n in the breach channel using the Strickler equation, and Manning's n is in turn an influential parameter in the Smart sediment transport equation.[1] In fact, NWS-BREACH also allows the direct specification of the Manning's n value in the breach channel. When run in this way many users have seen that the peak breach outflow is highly sensitive to the value of Manning's n, if n values are changed dramatically. However, the original description of the model by Fread (1988) suggests that n values should not vary greatly and notes that allowing direct user specification of n creates the potential for misapplication of this parameter.

NWS-BREACH accommodates both piping and overtopping flow as modes of breach initiation. NWS-BREACH also allows for limited modeling of non-homogeneous embankment sections, although the modeled solution assumes an average of the section parameters which can lead to inaccurate predictions. The embankment may be defined to consist of a main embankment zone, with material properties of particle size (D_{50}), unit weight, friction angle, and cohesive strength; a core with similarly specified material properties; and a protective layer on the downstream slope of the embankment consisting of either vegetation or an earthen material with a larger grain size than the main embankment. For dams that are primarily composed of cohesive

[1] A confusing situation related to these parameters has developed in recent years, as the NWS-BREACH model is no longer supported by the National Weather Service, but a non-authorized version of NWS-BREACH is available on the Internet. While the model itself seems to be the authentic NWS-BREACH model, the accompanying documentation contains a typographical error in the Strickler equation that relates Manning's n to D_{50}. The correct equation is $n=0.013(D_{50})^{0.167}$, with D_{50} given in mm. In the erroneous formula, the value of the exponent is changed from 0.167 to 0.67. User's who compute their own values of Manning's n should ensure that the correct exponent is used.

materials, the plasticity index (PI) can be specified and is used in the sediment transport equation to define the threshold for initiating erosion.

Today, the NWS-BREACH model is no longer commonly used, although its algorithms have been adopted to some extent in newer models. In recent years there has been recognition that the fundamental mechanics simulated by NWS-BREACH did not adequately represent the behavior of many dams, especially those composed of cohesive materials. The SIMBA and HR BREACH models that are the focus of the remainder of this report are two models that represent the next generation of physically-based tools for simulating erosion and breach of embankment dams.

SIMBA

The Simplified Breach Analysis (SIMBA) model was developed at the Hydraulic Engineering Research Unit of the USDA-Agricultural Research Service, located in Stillwater, Oklahoma. SIMBA development began in the late 1990s following USDA's development of technology for simulating headcut erosion in earthen spillways. SIMBA was developed for the purpose of analyzing earth embankment breach test data collected from the HERU's outdoor laboratory (Hanson et al. 2005b; Hanson et al. 2010a), with the objective of improving the understanding of the underlying physical processes of breach of an overtopped earth embankment. As such, SIMBA is a research tool that has been modified routinely to test the sensitivity of the output to various submodels and assumptions. For the purpose of this evaluation, a fixed version of SIMBA was utilized in which many optional and experimental analysis routines were disabled. Since these evaluations were performed, the technology in SIMBA has been integrated by USDA into the Windows Dam Analysis Modules (WinDAM B) software that is available to the public and to end users within USDA. This is one of several envisioned WinDAM releases that will gradually incorporate additional erosion and breach modeling technologies. USDA has conducted both overtopping and piping breach tests in their laboratory and is working toward integrating piping erosion into the WinDAM model in the future.

The research underlying the SIMBA/WINDAM model development is driven by the need to evaluate existing NRCS dams. The majority of these dams are homogeneous earth fill. The large number of dams involved and the limited resources available for evaluation of each dam require that the final tool be as simple to use as possible while retaining the ability to simulate the dominant physical processes utilizing reasonably available inputs including the description of the embankment material. Temple et al. (2006) provide additional discussion of the SIMBA/WINDAM development.

The version of SIMBA evaluated here was limited to simulating overtopping of homogeneous earth embankments with negligible protection on the downstream face. WinDAM B adds the capability to simulate downstream embankment face protection consisting of vegetation or riprap, which are common on NRCS dams. The model simulates the four stages of the failure process observed for these embankments. These stages are: 1) surface erosion leading to development of a headcut on the downstream face of the embankment, 2) headcut advance through the crest to initiate the breach, 3) breach formation as the headcut advances into the reservoir, and 4) breach expansion during reservoir drawdown. The version of SIMBA used for this evaluation and described herein is the subset of the research model that appeared at the time

of this work to best represent the processes associated with these stages in the simplest possible form.

Tejral et al. (2009) illustrated the differences in the assumed breach morphology for the NWS-BREACH and SIMBA models (Figure 3). Rather than eroding layers of the downstream face of the dam, SIMBA creates headcut steps in the downstream face and then tracks the upstream advance of these headcuts through the embankment. The actively eroding face of the headcut remains essentially vertical as the headcut moves through the embankment. Failures of wedges depicted in Figure 3d are also possible, which will periodically flatten the slope of the headcut face, but the eroding headcut face tends to remain nearly vertical throughout the breach initiation process.

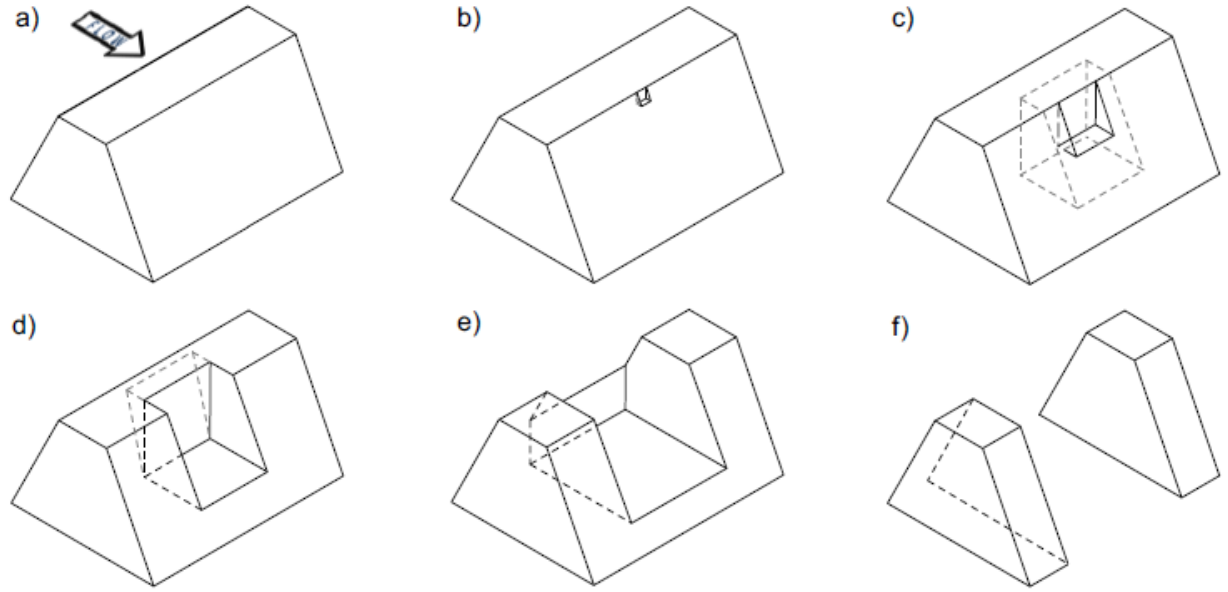

Figure 3.—Conceptual sequence of breach development in SIMBA. Flow is from top left to bottom right in each figure. (a) The simulation initiates with embankment intact. (b) A headcut forms at edge of downstream crest, (c) where it deepens and widens. Advance into crest (dashed lines) occurs when headcut height reaches critical depth of flow. (d) Headcut continues to deepen and widen and advances upstream when vertical face of headcut becomes unstable and collapses (dashed lines). (e) Breach formation occurs as headcut enters reservoir. (f) Breach opening may continue to widen after dam has been eroded to base (Tejral et al. 2009).

Unlike the NWS-BREACH model which computes erosion rates using sediment transport relations, SIMBA computes erosion rates with an excess stress equation for the soil detachment rate. The erosion rate is proportional to the stress applied in excess of the critical shear stress needed to initiate soil detachment. Erosion is presumed to be controlled by the rate at which soil can be detached by the flow, and the transport rate is always assumed to be great enough to move the material rapidly downstream once it has been detached. The excess stress equation is

$$\varepsilon = k_d (\tau - \tau_c)^a$$

where ε is the volumetric rate of erosion per unit area, τ and τ_c are the applied shear stress and critical resistive shear stress of the soil, k_d is the detachment rate coefficient, and a is an exponent

usually assumed equal to 1. Values of τ_c and k_d may be obtained by direct measurement using techniques such as the submerged jet erosion test (Hanson and Cook, 2004), or they may be estimated based on soil properties (Hanson et al. 2010b). The value of τ_c is often taken to be zero.

Another notable difference from NWS-BREACH is the geometry of the breach opening, which is assumed to always be rectangular in SIMBA (vertical sides). This is intended to mimic the observed behavior from laboratory tests of cohesive embankments in which breach sides remain essentially vertical throughout the period of breach enlargement.

Inputs to the SIMBA model consist of a reservoir inflow hydrograph, a stage-storage table for the reservoir, an outflow rating table for all reservoir outflow other than that associated with overtopping of the dam, a description of the dam cross section and the area to be overtopped, and a description of the soil material in the embankment. The initial elevation of the water surface in the reservoir is also an input along with the time step to be used in routing the flow through the reservoir and computing the extent of erosion. The inflow hydrograph is entered in elapsed time format with a starting time of zero. The use of elapsed time, user control of the computational time step, and entry of the characteristics of a depressed area (i.e., a pilot channel) where overtopping is to take place reflect the fact that SIMBA is a research tool designed to simulate laboratory experiments, rather than a field application model.

Model output includes information related to the outflow hydrographs, the timing of the breach, and the breach width and headcut position during the breach process. Graphical output is provided, taken from a generated text file table.

Computational Structure

The SIMBA model and an example application are discussed by Temple et al. (2005) and Hanson et al. (2005a). With the exception of the headcut advance model being used, these discussions are consistent with the evaluation version of the model. The 2005 discussions focused on an energy-based headcut advance model whereas the model evaluated for this project utilizes a stress-based headcut advance prediction.

SIMBA uses a level reservoir water surface assumption to route the inflow hydrograph through the reservoir. The change in reservoir storage is computed as the difference between the volume of average inflow and outflow over the time step. Inflow and spillway outflows are interpolated from provided inflow hydrograph and rating tables. Outflow over the dam and through the breach area is computed from the current eroded geometry and the elevation of the reservoir water surface. The width of the eroding area is initially zero, with widening taking place as embankment erosion progresses. If the eroding area is computed to have widened to the entire width of the overtopped length of the embankment (i.e., the width of the pilot channel) before the headcut enters the reservoir (completion of stage 2) then the eroding area is restricted to the overtopped width until the headcut enters the reservoir (beginning of stage 3). The width is not restricted during stages 3 and 4.

In computing the rates of erosion and the progression of the breach through the 4 stages, SIMBA uses a stepwise steady state approximation. The reservoir water surface elevation, the geometry of the eroded area, and the associated outflow are considered known at the beginning of each time step. The erosion rates are computed based on this initial condition and applied over the time step to obtain a new eroded geometry. This geometry (hydraulic control elevation and width in the eroding area) is used in computing outflow at the end of the time step when balancing inflow and outflow. The result is the condition at the beginning of the next time step. A check of inflow-outflow magnitude consistency is used to prevent numerical instability in the computed hydrograph.

Erosion is considered to be in stage 1 of the breach process when the headcut is not formed to a height greater than the critical depth of flow and is located within or downstream from the crest. The initial location of headcut formation is conservatively taken as the downstream edge of the crest. The erosive attack for this stage is computed from the approximation of a normal depth of flow on the slope with a Manning's *n* value for soil of 0.02. The applied hydraulic shear can then be calculated and the rate of material removal computed through use of an excess shear detachment rate relation. The material parameters governing this action are the erosion rate coefficient (rate of detachment per unit of excess stress) and the critical stress (stress below which no detachment occurs). The rate of widening of the breach area is taken as 1.4 times the rate of deepening of the headcut, not to be confused with the rate of crest lowering.

When the headcut height exceeds the critical depth of flow, the flow is considered plunging, and the headcut will advance upstream as well as deepen. Stage 2 is the advance of the headcut upstream through the level crest of the dam. Stage 2 ends when the headcut has advanced to the upstream edge of the crest. The evaluated version of SIMBA uses the stress-based headcut advance model described by Hanson et al. (2001), modified to limit the advance rate computed for unstable headcut heights. Stresses at the base of the overfall and on the face of the headcut are computed using the relations given by Robinson (1992) for a non-aerated condition.

As the headcut enters the reservoir (stage 3) the elevation of the hydraulic control is dependent on the position of the headcut. The relations used to compute the headcut advance are the same as those described in the preceding paragraph. The rate at which the hydraulic control would be lowered by the hydraulic stress associated with critical flow over the brink is also computed. When this rate exceeds that associated with headcut advance, then this downward erosion of the hydraulic control is considered to govern. Note that when headcut height is less than critical depth, the rate of headcut advance is zero. When stress governs the erosion process, the widening of the breach is kept proportional to the stress-generated detachment rate.

Once the embankment is locally removed to the elevation of the toe of the embankment (base of the headcut is limited to being at or above this elevation in preceding stages) (stage 4), then only widening can occur. The widening is assumed to be proportional to the applied stress for critical flow conditions, similar to the stress controlled portion of stage 3. The stress on the banks is considered to be 0.7 times the maximum stress that would be computed for the bed section in the rectangular breach opening. Thus, for small values of critical stress, the widening rate would be approximately 1.4 times the detachment rate associated with stress on the bed.

Limitations

As indicated in the preceding discussion, SIMBA is a research tool, and the evaluated version incorporated what were currently thought to be the best available descriptions of the dominant processes for the applicable range of conditions. Some key limitations of the model are summarized below.

- SIMBA was developed to evaluate homogeneous earth embankments constructed from cohesive materials. Parameters used to describe the embankment material are the total unit weight, the undrained shear strength, and a critical shear stress associated with the initiation of detachment. If it is not possible to effectively represent the embankment as homogeneous with the material described by these parameters, the value of the output will be limited.
- SIMBA computations are based on a uniform time step with a maximum of 5000 time steps. The user controls the time step, but values must be within this limit.
- SIMBA assumes a bare slope initial condition that will allow immediate erosion of the downstream slope, leading to headcut formation at the top of the slope. If the slope is protected such that the failure initiation is delayed or the critical point of headcut formation is other than on the slope near the crest, adjustments are required.

HR BREACH

The HR BREACH model was first developed at HR Wallingford in 2001 and has been updated since the original version via a sequence of research initiatives, and in particular through the European CADAM, IMPACT, FLOODsite, and FloodProBE projects. These research efforts included many laboratory and large-scale outdoor breach tests, and information from these tests has been utilized in the development of the model. The model is based on the principles of hydraulics, sediment transport, and soil mechanics. It predicts breach growth through embankment structures, providing breach characteristics such as size, shape and outflow hydrographs. The model has been developed to predict the following processes:

- Initial erosion of any embankment surface protection (grass or rock cover preventing initiation of breach erosion)
- Breach growth through overtopping flow of homogeneous embankments (cohesive or noncohesive materials - including consideration of head cut and the analysis of breach side slope instability)
- Breach growth through overtopping flow of simple composite embankment structures (i.e. simple zoned structures – core, embankment body and surface protection layers)
- Breach growth through pipe formation through, and subsequent collapse of, embankments (including collapse of the pipe roof leading to open breach growth).

The model allows the use of different equations and simulation processes for the breaching of cohesive, non-cohesive and composite (i.e. zoned) structures. Additional features can include Monte Carlo simulation using distributed values for key parameters and / or fuzzy factors of safety to represent varying soil and/or construction conditions.

Like SIMBA and unlike many existing models that have been calibrated against specific data sets, this model has not been calibrated to reproduce any specific data sets. The model has been tested using both experimental and real failure data, with modeling results showing good agreement with observed values for a range of different conditions.

Failure Processes

Fundamentally, HR BREACH allows the modeling of two types of embankments. Homogeneous embankments are primarily comprised of a single material, while composite embankments are assumed to contain an erosion-resistant core. Breach growth in the outer zone of a composite embankment and the entirety of a homogeneous embankment is assumed to take place through *surface erosion processes,* or the user may alternately opt to use a headcut migration model patterned after the energy-based headcut migration model in early versions of SIMBA (Temple et al. 2005, Hanson et al. 2005a). Breach development through the core of a composite embankment is allowed to occur by assuming structural failure of the core and wasting of large soil masses. In addition, either type of embankment can include a thin, surface protection layer composed of riprap, plain vegetation, or reinforced vegetation. The methods for modeling erosion and breach development in each of these zones are described below.

Erosion of Surface Protection Layers

Earth embankments are often protected against initial erosion by vegetation or hard measures, such as placed stone. The effect of these protection measures is to prevent or limit erosion – typically until limit conditions are exceeded. Three types of surface protection are simulated by the HR BREACH model, including:

- Plain and reinforced grass (Hewlett et al 1987)[2]
- Riprap (Chang 1998)

Performance of the protection layer is assessed by calculating the hydraulic loading applied by the predicted embankment overflow. When the hydraulic load exceeds the design performance conditions (as specified in the respective references) then the surface protection is considered to have failed and erosion of the embankment body is permitted to begin.

In addition to use of rock, grass or reinforced grass performance curves, the model also allows the user to define a time of surface cover failure. This can be very useful when undertaking a forensic analysis of a failure to see how the timing of initiation affects the overall breach process. Delays in initiation (as a result of more complex surface failure processes for example) can significantly affect the rate of breach growth.

[2] Note that in more recent work it was found that the CIRIA 116 grass protection design guidance (Hewlett et al 1987) contained factors of safety intended to support the design process. However, when the performance curves are used for reliability analysis (as in the case of breach modelling) the factors of safety work in the opposite sense leading to a prediction of failure that is too rapid. Recognizing this, current guidance for breach modeling is to use the earlier CIRIA Technical Note 71 data instead (Whitehead et al, 1976).

Breach Growth – Homogeneous

For homogeneous embankments the HR BREACH model allows the user to choose between overtopping failure arising from surface erosion or overtopping arising from headcut. These processes are physically quite different, and can result in different breach flood hydrographs. Headcut erosion tends to occur in more cohesive, erosion resistant material and surface erosion in less cohesive, more erodible material. The exact transition between processes remains unclear, but is clearly very dependent upon the soil erodibility. Since this in turn depends upon soil type and state (moisture content, compaction etc.) then it is possible to see both processes occur in materials that would typically demonstrate one or other process.

Clarification of the driving physical process in relation to soil type and state is a key area of ongoing research, hence for current breach prediction the user is required to make a judgment as to which process might dominate. It was for this reason that the HR BREACH model, which was originally developed as a surface erosion model, was developed to include a headcut modeling process as well, allowing the user to choose or compare both processes.

Surface Erosion

In surface erosion mode, the HR BREACH model uses a combination of continuous surface erosion and discrete mass instability to model breach growth through non cohesive homogeneous embankments. Continuous erosion is due to the erosive action of the overflowing water. This action gradually deepens and widens the breach. Unlike SIMBA which focuses on conditions at the critical-flow section, HR BREACH calculates flow and erosion conditions at multiple cross sections through the embankment. Conditions are calculated at discrete time steps at each section, and the section profiles are allowed to develop freely. Hence, there is no predefined erosion process driving the breach growth other than the flow and resulting erosion conditions at each cross section.

Surface flow conditions are initially calculated for flow traveling across a defined notch in the crest and downstream face. Erosion only occurs for submerged sections within the notch, resulting in vertical sides being undercut. At a certain point within the erosion process, mass instability of a side slope takes place, resulting in failure of the side slopes and consequently a step change in the breach width. Simulation of the vertical and undercut sides of the breach reproduce observations from both field and laboratory tests. Failure of the breach side slopes is allowed to occur either through shear or bending failure. The most likely mode is selected through analysis of the forces and moments acting on the side slope soil mass (Figure 4). A probabilistic approach can also be used to take into account the uncertainties associated with the computed factor of stability of the breach side slopes.

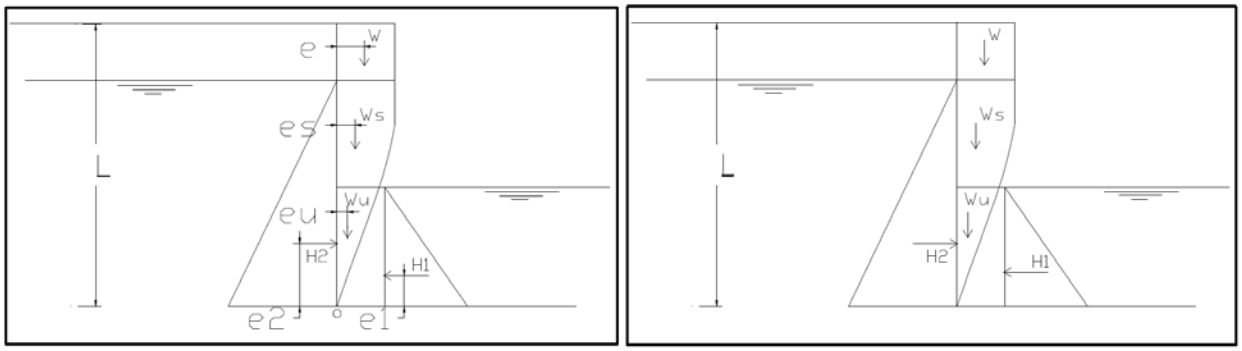

Figure 4.—Illustration of side slope undercutting and resulting moments for bending failure and forces for shear failure of side slope soil masses in HR BREACH.

Headcut Erosion

A headcut migration model has been incorporated into the HR BREACH model. The headcut migration uses the energy-based approach that was originally employed in SIMBA (Temple et al. 2005, Hanson et al. 2005a). The headcut migration model controls both the rate of upstream headcut advance and the rate of headcut widening. The use of headcut migration is likely to be appropriate for cohesive soils, and perhaps also for soils that have traditionally been considered noncohesive, but which exhibit headcut-type erosion during embankment breach. Soils in this category can include materials that are non-plastic, but have 5 percent or more fines and 70 percent or less sand (Greg Hanson, personal communication).

When using the headcut model, the headcut advance rate and widening rates are predicted as with the SIMBA approach; breach side slope stability is not considered. The headcut model can only be applied to the prediction of breach through a homogeneous embankment. For composite or zoned structures, surface erosion must be used.

Breach Growth through Composite Structures

Often, embankment dams contain a core within the embankment body. This core is typically made of clay and is more resistant to erosion than the surrounding material. The erosion of the material of the downstream layer affects the stability of the core and if eroded can eventually lead to its failure. The HR BREACH model allows simulation of breach through a composite dam with a thin core. Erosion of the core supporting material is simulated with potential failure mechanisms for the core itself including cracking and failure through:

- Sliding
- Overturning
- Bending

The HR BREACH model considers potential sliding and overturning failure of a core by computing the core factor of stability. A simplified analysis of the bending mechanism is applied in the absence of a detailed analytical solution. The loading and failure processes assumed are shown in Figure 5. After failure of the core down to the embankment base level, lateral growth of the breach is modeled using the continuous erosion and discrete mass instability method explained above for homogeneous breach growth.

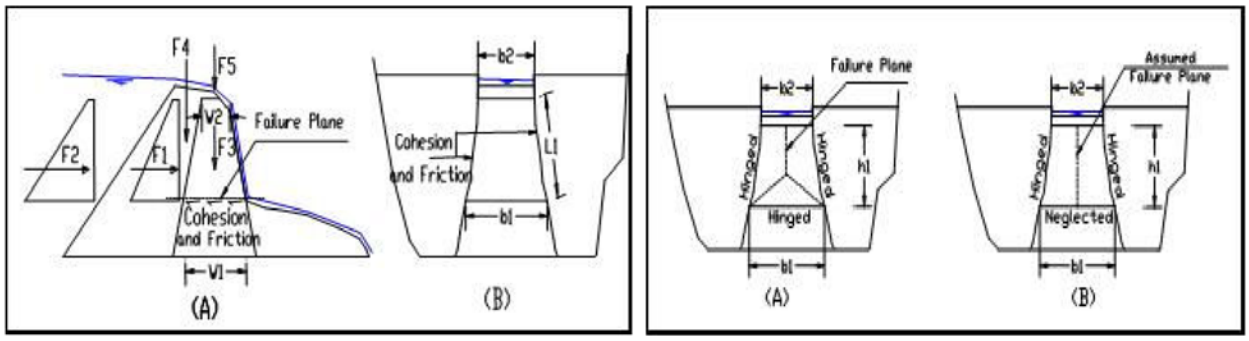

Figure 5.—Loading and failure processes considered for core failure in HR BREACH.

In Europe, dikes and levees have sometimes been constructed with a zoning geometry that is inverted from the case just described. The core of the embankment is non-cohesive, while the outer zone is cohesive and more erosion resistant. HR BREACH as presently configured is not capable of analyzing this type of zoning[3].

Breach Growth through Pipe Formation

To simulate breach growth through pipe formation (internal erosion), an initial assumption is made that a finite size of pipe has already been established through the embankment. The HR BREACH model then simulates growth of this pipe using the following processes:

- Erosion of material in the pipe (i.e. growth of the pipe diameter and hence flow through the embankment)
- Slumping of the downstream embankment face material above the pipe (simulating the cut back of the pipe exit in the downstream embankment face)
- Collapse of the embankment body above the pipe, either under its own weight or the water pressure forces, and
- Following collapse of a pipe, erosion of the embankment body as described for the overtopping failure of embankments.

Modeling Equations

The following sections provide a brief description of the key equations and assumptions used to model breach growth through overtopping failure.

Reservoir Hydraulics

To compute the breach outflow, both an upstream reservoir or water level and downstream water level must be known. HR BREACH allows the direct specification of an upstream head vs. time boundary condition, or alternately, an upstream reservoir may be modeled using level-pool routing calculations with a specified inflow hydrograph to the reservoir. Outflow from the reservoir through defined discharge structures as well as via breach growth can also be specified.

[3] Work undertaken after the DSIG breach modelling project by Morris (Morris 2011) has developed capabilities within HR BREACH that allow for breach simulation through zoned embankments.

Downstream water level conditions are used to determine any submergence effect. Downstream conditions may be defined using head vs time boundary conditions or using a normal depth calculation based upon downstream valley section and longitudinal slope.

Flow Computations and Submergence Effect

Flow through the breach opening is computed using a simple weir equation, with a correction for submergence made when necessary. The location of the control section in the breach channel (i.e., position at which critical depth occurs), moves according to the section by section evolution arising from the section erosion predictions. Estimation of the position of the control section can be undertaken using a number of techniques including through minimum flow and bed slope calculations. The water depth and velocity profile in the breach channel is calculated in the upstream direction in the sub-critical flow zone and in the downstream direction in the supercritical flow zone by solving the gradually varied flow equation (Chow 1959).

Drowning (submergence) of the breach is calculated using the Villemonte equation (Villemonte, 1947). As flow through the breach drowns, the discharge is reduced, the flow shear stresses reduce and hence the rate of breach erosion is reduced. This can have very significant effects on the breach prediction results, changing the timing, size and hence outflow from a breach.

To truly benefit from prediction of the effects of breach drowning it is also necessary to adjust the downstream water level condition as the flow from the breach varies. This creates a dependency between breach prediction and downstream level prediction which can only truly be simulated by using an integrated breach and flow routing model. For this reason, the HR BREACH model was also integrated within the InfoWorksRS flow modeling software.[4]

Sediment Transport and Erosion Equations

For flexibility, the HR BREACH model has been coded with the option to choose from a variety of sediment transport and erosion equations when operating in surface erosion mode. Sediment transport equations focus on the capacity of the flow to move sediment from one location to another, assuming it can be readily detached from its starting position. Erosion equations focus on the capacity of the flow to detach sediment from its initial location, presuming that this will limit the rate of sediment movement.

When HR BREACH was first developed (around 2000) many breach models used sediment transport equations. It was subsequently shown to be more appropriate to use an erosion equation, such as the excess stress equations developed by Chen or Hanson. While the options remain to use sediment transport equations, the recommendation is generally to use an erosion equation where the modeler also defines the soil erodibility. This allows for consideration of the embankment material state as well as type, which has a critical effect on the rate of erosion and hence breach growth.

[4] The integrated version of the HR BREACH model was not used for the DSIG modelling work. For the case studies where drowning was important, analysis of the data was undertaken to determine an event-specific downstream head time relationship.

The erosion rate can be calculated using one of several different equations: Visser (1995), Yang (1979), Chen and Anderson (1986), the Smart (1984) modification of the Meyer-Peter and Müller equation (Fread 1988), or Hanson et al. (2005a). The Visser, Yang, and Meyer-Peter and Müller equations were developed from the study of equilibrium transport rates of already detached sediment particles in steady flows. The Hanson equation and the three Chen equations (one for sand, one for low plasticity clay, one for higher plasticity clay) are based on the concept of predicting sediment detachment rates as a function of applied shear stress versus soil erosion resistance. The Hanson equation is the same excess stress equation utilized in several parts of the SIMBA model, with the user specifying the detachment rate coefficient and critical shear stress value. The Chen equations are also similar in form, but with fixed values of the detachment rate coefficient and specific values (different from 1.0) for the exponent on the stress term, depending on the soil type. The HR BREACH developers recommend the use of one of the latter so-called "erosion equations" as the default starting point for most simulations.

Choice of Modeling Approach for DSIG Test Cases

While the HR BREACH model allowed for the choice of headcut or surface erosion physical processes, the decision was made to use the surface erosion option for most initial runs so that the effect of this modeling approach could be compared to the headcut approach used by SIMBA. For some DSIG test cases the headcut erosion option was used for "improved" runs.

FIREBIRD

Although the FIREBIRD model was not extensively tested because of difficulties encountered during the evaluation process, a short description of the model is provided here.

The FIREBIRD breach model (Wang and Kahawita, 2002) was developed to model breach formation in an earthfill or rockfill dam due to overtopping. The model simultaneously solves the one dimensional unsteady flow St. Venant equations and the Exner equation for sediment transport. The numerical algorithm used for the hydraulics component is sufficiently robust to handle transcritical flows, i.e. flows passing from subcritical to supercritical and back. The reservoir water level is modeled with a simple level pool routing technique. The embankment is considered to be homogeneous; the effect of an erosion resistant core is not modeled. Lateral stability of the side slopes is evaluated with a simple geotechnical analysis that considers a simple sliding failure along an inclined face.

The FIREBIRD model contains no specific provision for modeling headcut development or migration, so in this respect it functions similarly to the surface erosion modeling option in HR BREACH. The critical input to the model is the choice of erosion formula. Four erosion formulas are supported in the model:

- Smart (1984) (modified Meyer-Peter and Müller)
- Wilson (1987)
- Cheng (2002)
- DOT – (FHWA Hydraulic Engineering Circular 15)

The Smart, Wilson, and Cheng equations are based on bed load sediment transport concepts. The DOT formula as implemented in FIREBIRD is similar to the excess stress equation for soil detachment used in SIMBA and HR BREACH (Hanson equation option), except that the exponent on the stress term is allowed to vary from 1.

Models Applied to Case Studies

To evaluate the performance of the numerical breach models, a set of 7 case studies was assembled, comprising 5 large-scale laboratory tests and 2 real dam failures. Data for these case studies were compiled during the first phase of the CEATI project (Wahl 2007; Courivaud 2007). Project participants were briefed on two different occasions to become familiar with the case studies and the use of the different dam breach models and to discuss potential input parameters, especially those relating to soil properties. Participants then ran the models more or less independently over a period of months to generate predictions of erosion, breach development, and hydrograph characteristics. Consultation among the seven evaluators and with model developers was permitted during the evaluation process, but each evaluator was also free to use their own best judgment when developing input parameters and choosing modeling options. Each evaluator was asked to attempt at least two runs with each model, one utilizing initial best-estimate selections of model options and input parameters and one utilizing refined or improved inputs intended to match model performance to observed breach behavior. The first runs were meant to represent the ability of the model to be applied in the future for predictive purposes on dams that have not failed. The second set of runs would reflect the ability of the model to achieve better results when more refined input data are available, such as actual field measurements of soil erodibility properties. Model evaluators were asked to consider whether the necessary adjustments to achieve improved model performance were sensible. Although a rigorous sensitivity analysis was not performed, evaluators were also asked as they worked with the models to consider whether they exhibited appropriate sensitivity to model inputs. In many cases, evaluators only completed an initial model run, especially when the initial effort provided reasonably satisfactory results, but at least one evaluator completed an improved run for each case study. Most evaluators were able to complete runs using the SIMBA and HR BREACH models, and some also completed runs using the NWS-BREACH model.

In the sections below, each case study situation is described and the application of the different breach models is discussed. Representative results from one simulation with each model are shown. Following the presentation of individual results, the performance each model will be shown as applied by all evaluators across all case studies.

The various laboratory tests and case studies and the modeling efforts to simulate them took place across many decades, continents, and countries and utilized both the U.S customary and S.I. units systems. The study team grappled with units issues during some of the early modeling efforts and ultimately decided to utilize both unit systems, as necessary.

Laboratory Tests

USDA-1

Two outdoor laboratory tests of embankment overtopping were carried out in June and July 1999 at the USDA Hydraulic Engineering Research Unit (HERU) near Stillwater, Oklahoma. In the first test, designated here as USDA-1, embankment breach occurred; in the second test, USDA-2, overtopping erosion occurred, but did not progress far enough to complete the breach initiation process. Both of these tests are described by Hanson et al. (2005b). The USDA-1 test is identified in that paper as embankment 1 constructed from soil 1.

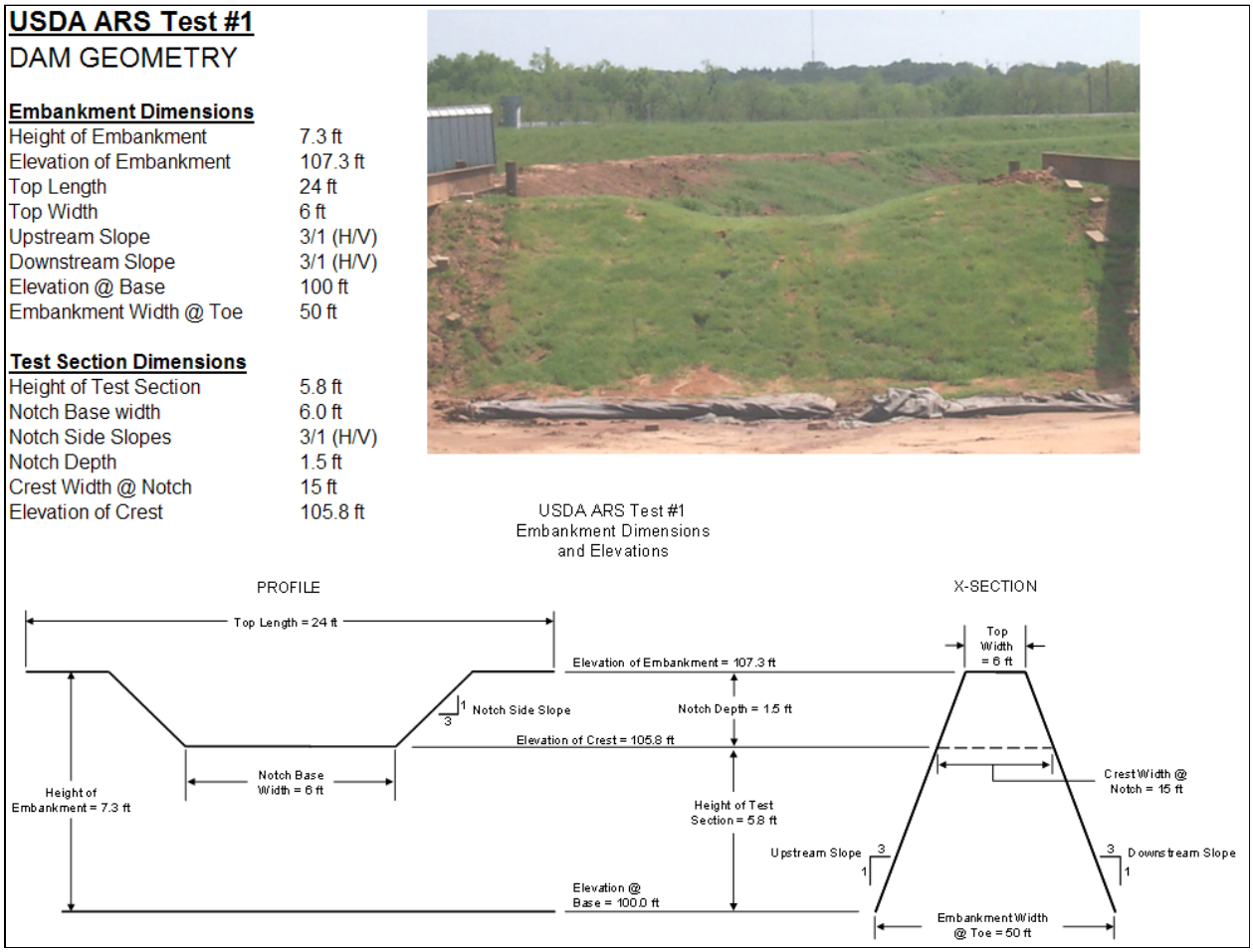

Figure 6.—Geometry of USDA-1 embankment. The photo is taken looking upstream toward the embankment and reservoir. Sketches of the pilot channel notch and dam cross section are not to scale.

Figure 6 shows the embankment geometry. The embankment was constructed approximately 9 months prior to testing. The surface was seeded with fescue to protect against surface erosion due to minor rainfall, but the stand was young and of poor quality at the time of the test, so the vegetation provided little to no protection against embankment erosion due to overtopping flow.

The soil used to construct USDA-1 was a non-plastic silty sand (SM) with 70% sand, 25% silt, and 5% clay (< 0.002 mm). Water content at the time of placement was 8.9 percent, approximately optimum. Erodibility of the material was measured by submerged jet erosion tests during construction and after the test. The embankment had a high detachment rate coefficient, k_d = 10.3 cm^3/(N-s), and the threshold shear stress to initiate erosion was estimated to be τ_c=0.14 Pa, which is very near zero considering the magnitude of the effective stress.

The reservoir upstream from the embankment held about 3.1 ac-ft of water at the invert elevation of the pilot channel. The test was performed by filling the reservoir on the day of the test and then overtopping the embankment through the pilot channel. Flow rate into the reservoir was measured, as were reservoir water levels and the flow rate downstream from the embankment. Erosion of the embankment and development of the breach was monitored with photographs and by physical measurements carried out from a movable carriage over the test section. Figure 7 shows the inflow and outflow hydrographs, with first overtopping occurring at t = 52 min and breach initiating about 34 min later at t = 86 min.

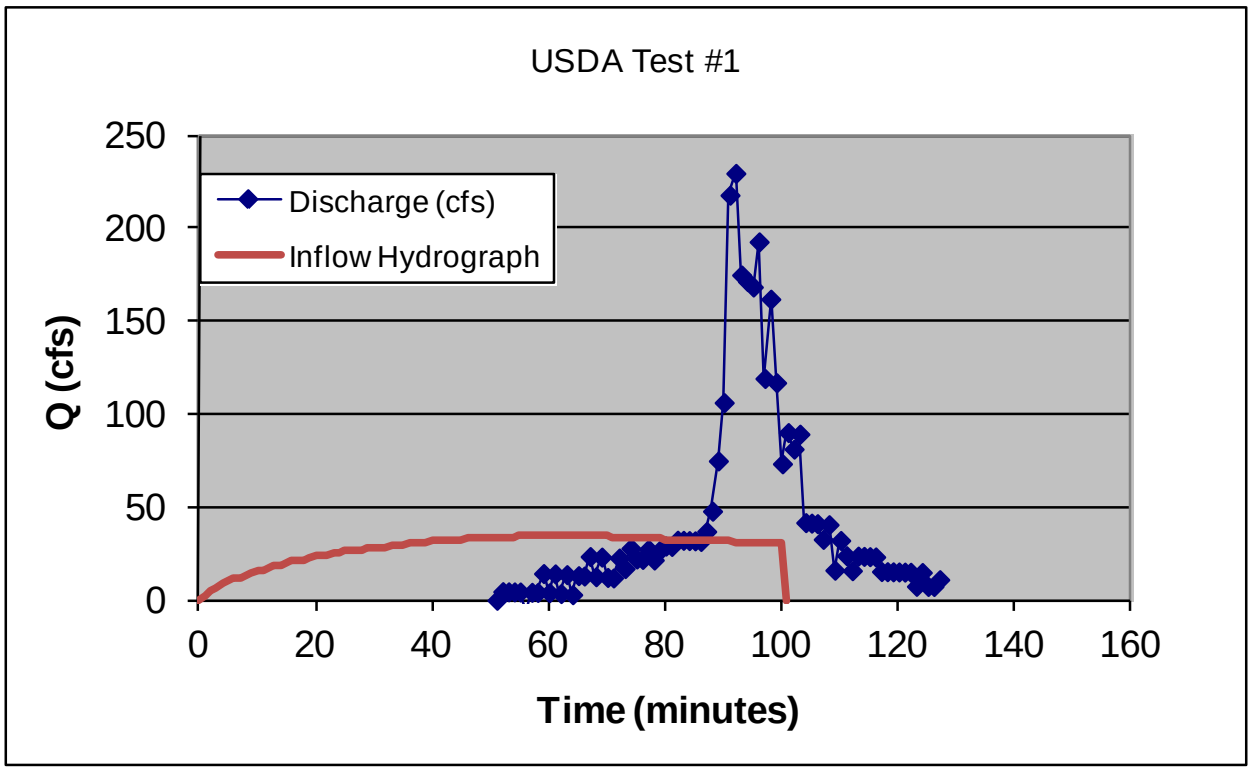

Figure 7.—Inflow and outflow hydrographs resulting from the test of the USDA-1 embankment.

In addition to the inflow and outflow hydrographs, measurements of headcut position and breach width were made during the tests by physical probing from a movable carriage mounted above the test section.

Modeling with SIMBA

The SIMBA model was applied using the soil erodibility parameters that were determined by submerged jet erosion testing. This produced a very good match to the observed data, as shown in Figure 8. Predicted outflow hydrographs and reservoir water surfaces match very closely,

both in magnitude and in time. This indicates that both the size of the breach and the rate of advance of the headcut are accurately reproduced. Rates of increase of the breach width are similar, although there is a mismatch of the actual breach width values, due to differences in how breach width is defined computationally in SIMBA versus how it was observed in the test. The offset is also related to the fact that the pilot channel in the test gives the initial breach width a finite value of about 6 ft (1.83 m), but in the SIMBA simulation the breach width grows beginning from zero when a headcut first forms on the downstream slope. In the run shown, the option to include an external tailwater rating was not used, and this may account for the divergence of reservoir water levels late in the test, as the reservoir drained.

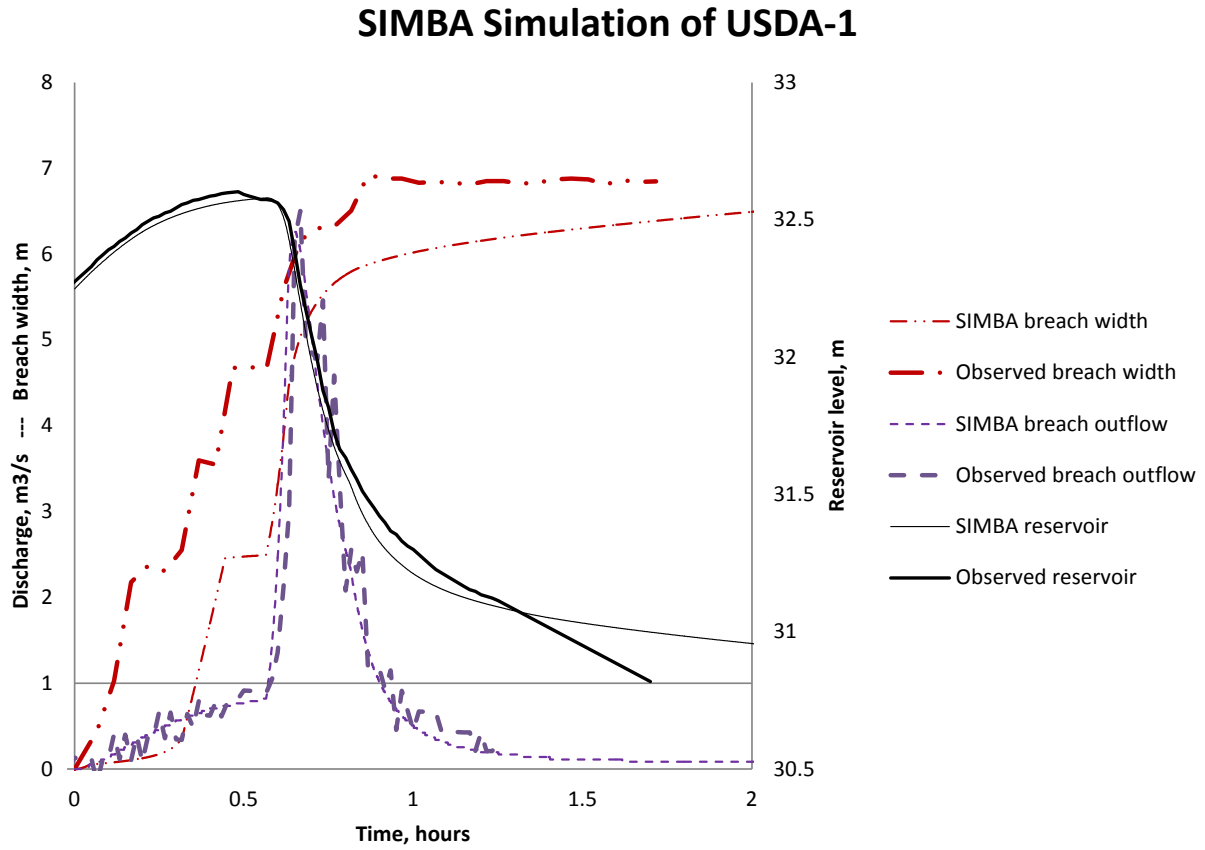

Figure 8.—SIMBA simulation of USDA-1 breach test.

Modeling with HR BREACH

The HR BREACH model was used in surface erosion (rather than headcut) mode; headcut mode is the same concept as SIMBA and hence would duplicate the simulation process. HR BREACH allows for progressive surface erosion, following removal of any surface protection – such as grass. The flow calculation also takes into account the downstream water level and hence any drowning of flow through the breach. Both surface protection and drowning effects proved to be significant for the HR BREACH predictions.

HR BREACH allows the modeler to select an appropriate erosion equation for the surface erosion process. The Chen sand equation was used initially, and then for comparative purposes, a model run was also undertaken using the Hanson equation.

The initial run (i.e., that which would be undertaken without seeing the observed results) gave a predicted outflow hydrograph that was broadly consistent with the observed peak, but about 10 min early. The timing of the breach initiation was dictated by the combination of delay from assumed grass cover protection and the rate of surface erosion predicted by use of the Chen sand equation. A second issue created by the timing delay was related to tailwater effects. The observed downstream conditions from the test were initially used in HR BREACH to provide a head-time boundary condition. However, when the simulated breach timing differs from the observed, the boundary condition became unrealistic for the simulation. This was remedied by using the observed data from the test to develop a tailwater rating curve that could be applied as the downstream boundary condition.

A far better fit with the same erosion equation (Chen sand) was achieved by dictating the time of initiation of erosion. When this was done, the outflow hydrograph proved very similar, albeit lacking observed variability on the falling limb (which is probably partially due to inherent uncertainty in the measurements used to calculate observed discharge).

The predicted versus observed reservoir level results were consistent with the discharge results (i.e., the initial run gave results that were early compared to observed; the improved run results offered a good match).

Breach width results differ, but the breach width predicted by HR BREACH relates to the critical flow section of the model rather than a measurement of width at a fixed location. As such, this result is generally smaller than the fixed location observation. However, the rate of breach width growth was comparable.

A model run performed using the Hanson erosion equation, with a k_d value of 25.5 $cm^3/(N\text{-}s)$ gave a similar result as the Chen sand equation when the time of breach initiation was specified.

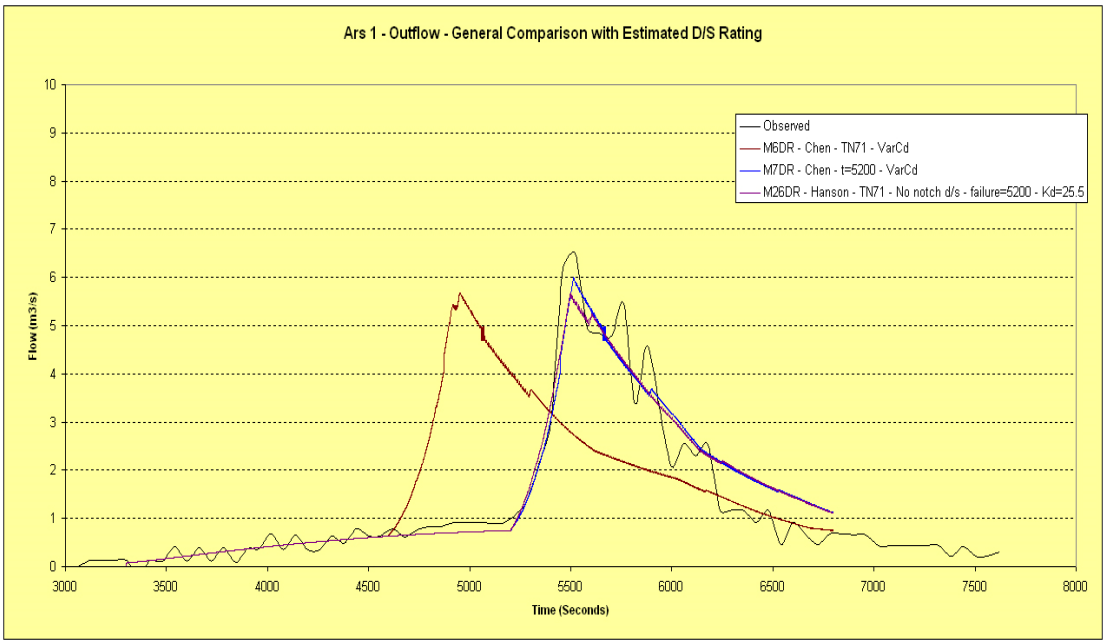

Figure 9.—Plot of breach outflow for HR BREACH initial and improved model runs, USDA-1 test case.

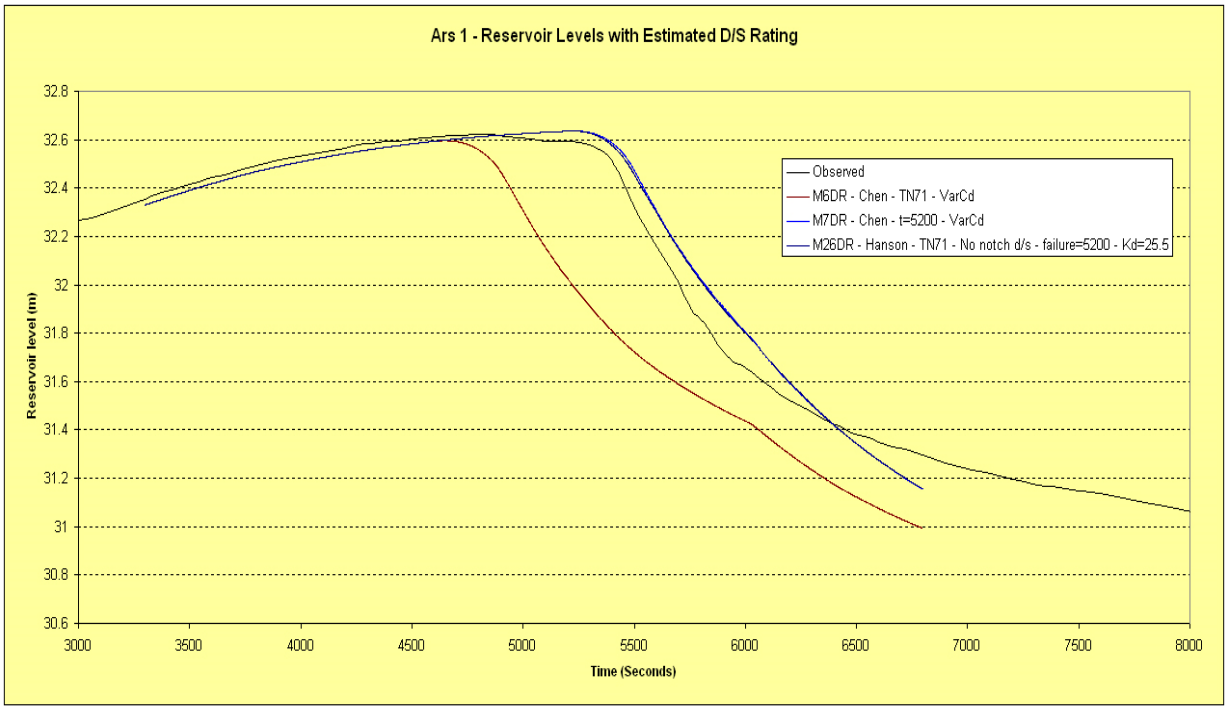

Figure 10.—Plot of reservoir water level for HR BREACH initial and improved model runs, USDA-1 test case.

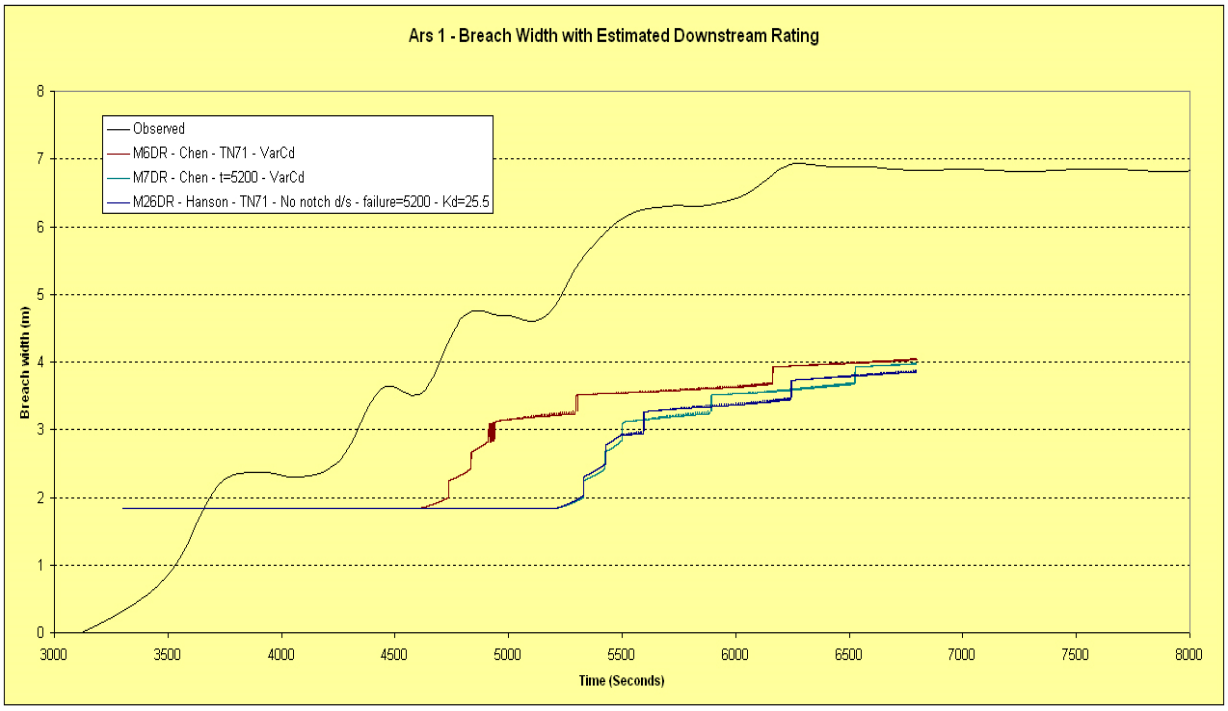

Figure 11.—Plot of breach width development versus time for HR BREACH initial and improved model runs, USDA-1 test case.

USDA-2

The USDA-2 test is identified in Hanson et al. (2005b) as embankment 1 constructed from soil 3. The geometry is nearly identical to USDA-1, except for a 1 ft increase in the crest width and base width of the embankment to 16 ft and 51 ft, respectively. A young, poor stand of fescue was again present but offered little to no resistance to erosion by overtopping flow.

The soil used for USDA-2 was a lean clay with sand, (CL)s, containing 25% sand, 49% silt and 26% clay. The soil was plastic with a liquid limit of 34 and plasticity index of 17. Water content at the time of placement was 16.4 percent, more than 2% wetter than the optimum water content of 14 percent. Erosion resistance of the material was much greater than the USDA-1 embankment, with a detachment rate coefficient, k_d = 0.039 cm^3/(N-s), and a critical shear stress value of τ_c=15 Pa. This detachment rate coefficient is 2.4 orders of magnitude less than the value for the USDA-1 test.

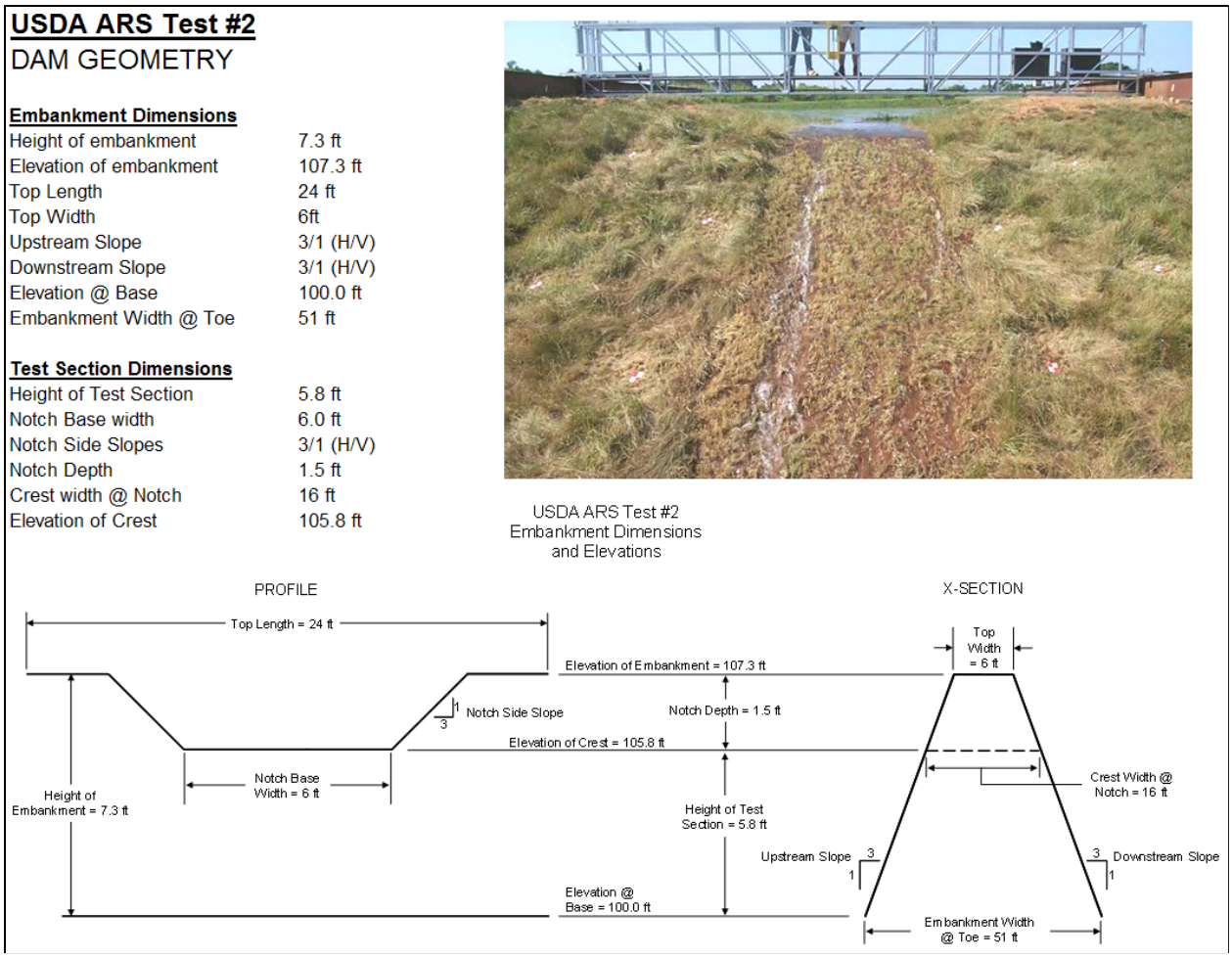

Figure 12.—Geometry of USDA-2 embankment. The photo shows the start of overtopping flow through the pilot channel. Sketches of pilot channel and dam cross section are not to scale.

The USDA-2 embankment was subjected to an overtopping flow of about 33 ft^3/s for 20.5 hours. The unit discharge through the pilot channel was about 5.5 ft^3/s/ft. Headcut erosion took place on the downstream slope, but the headcut migrated less than two thirds of the way through the

crest. The estimated time required to complete breach initiation would have been over 33 hours, based on the observed headcut migration rate.

This particular test case offers the opportunity to see whether models can successfully predict slow erosion that does not lead to failure. The test embankment was constructed with a high soil strength and high resistance to erosion, and thus erosion leads to the formation of a headcut rather than a gradually lowering or flattening of the downstream slope of the embankment.

Modeling with SIMBA

An initial SIMBA model run was undertaken using the soil parameters listed above, with the detachment rate coefficient measured by submerged jet erosion testing. Results from this run indicated very little erosion occurring and the outflow over the dam approximately matching the inflow hydrograph. From the standpoint of predicting dam breach outflow and reservoir conditions, this result was fully satisfactory. However, the most useful parameter to examine is the headcut position versus time, which was measured during the test and is provided in the SIMBA output. With the initial soil parameters, the SIMBA simulation showed essentially zero advance of the headcut after over 20 hrs, but the observed advance in the test was approximately 8 ft (2.7 m). Thus, an effort was made to adjust the soil erodibility parameters to better match the observed behavior. A good agreement was obtained with τ_c=0 and k_d=1.59 cm^3/(N-s). Thus, while the embankment construction did produce an erosion resistant soil, the observed headcut advance shows that the erosion resistance was not as great as indicated by the reported soil erodibility parameters. Although the adjustment made here was substantial (k_d increased by a factor of about 40), the new value still indicates significant erosion resistance and is not unreasonable for this soil. The fact that the embankment was constructed with the soil in a wetter than optimum state may have caused some difficulty during construction that led to less effective compaction, although it is somewhat surprising that this was not more accurately indicated in the jet tests that were carried out in situ as the embankment was being constructed.

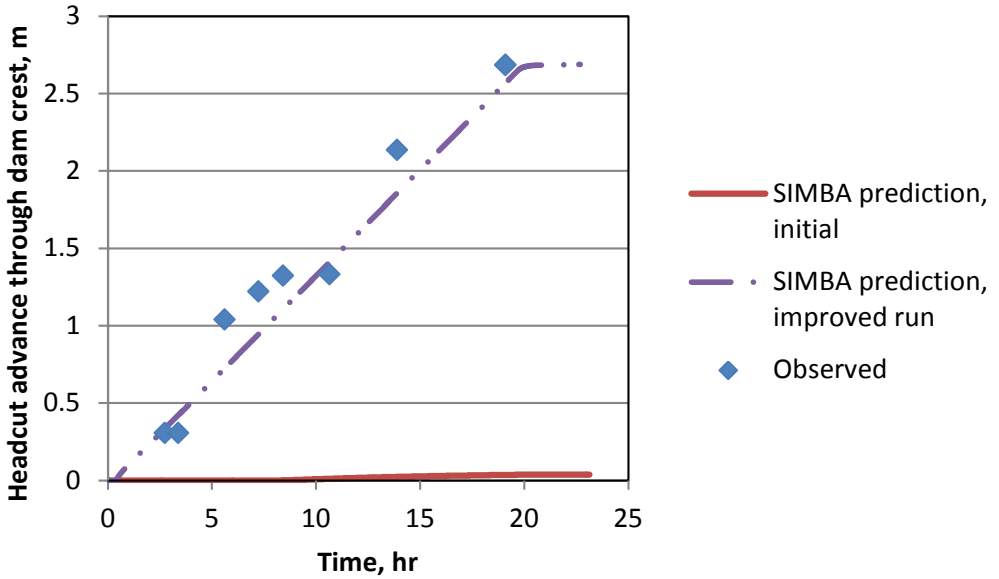

Figure 13.—Observed and predicted locations of advancing headcut for USDA-2 embankment modeled with SIMBA.

Modeling with HR BREACH

Two runs are shown for HR BREACH – the initial run and an improved run. The initial run uses the Hanson equation with k_d=0.039 cm^3/(N-s), but with a zero critical shear stress and mode of erosion set to surface erosion, although it was anticipated that the headcut erosion mode would be better suited to this test case. The model does not predict failure, and the outflow hydrograph matches the observed very well. This is because the model predicts overflow of the embankment, with outflow more or less matching inflow, which was the case.

A slight difference between modeled and observed reservoir level can be seen for the initial run results. This is because the simulation predicts slow surface erosion and hence a progressive, albeit small, lowering of the embankment crest that allows the reservoir level to also drop slowly.

The improved model run uses the same erosion equation (Hanson) but adopts a headcut approach rather than surface erosion. The outflow comparisons are identical (because the models are simply matching outflow to inflow), but this time the reservoir level is steady. This is because erosion takes place from the toe of the downstream slope, advancing toward the reservoir, but the predicted headcut does not advance far enough into the embankment to allow breach initiation to begin.

Breach width predictions remain close to the initial starting value. The initial run shows a slight widening, reflecting the progression of surface erosion, however the headcut shows no widening since breakthrough into the reservoir does not occur. Note that the breach width recorded here is the width of the critical flow section within the model (which moves upstream as headcutting progresses), not the width at a single fixed location.

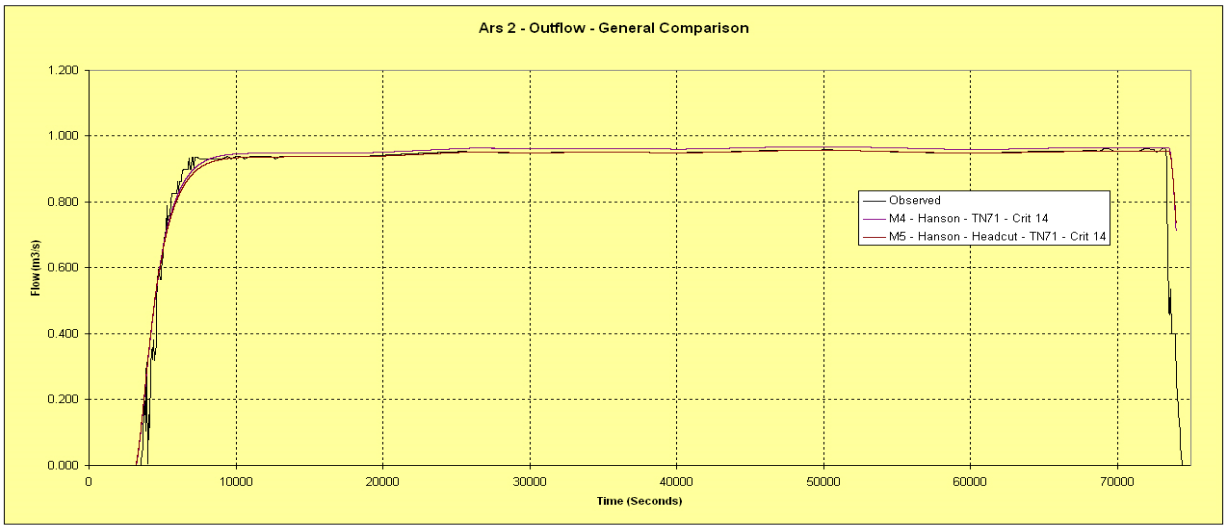

Figure 14.—Plot of Outflow – HR BREACH initial and improved runs for USDA-2 test case.

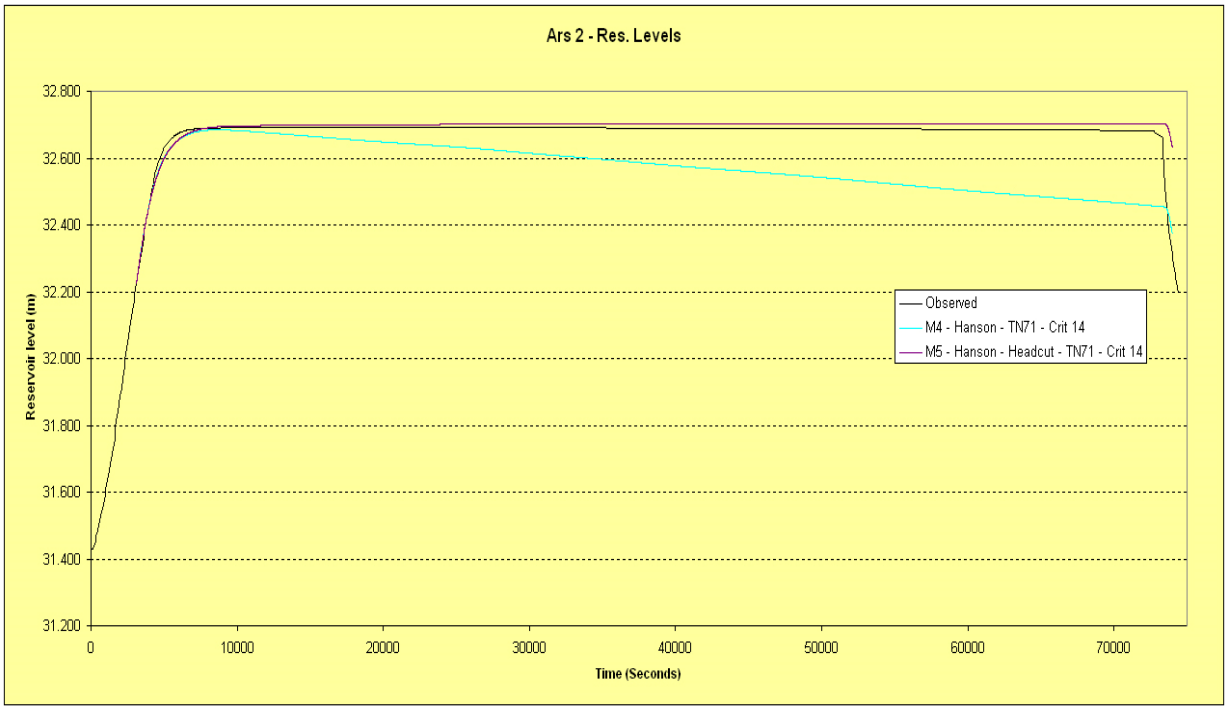

Figure 15.—Plot of Water level – HR BREACH initial and improved runs for USDA-2 test case.

Norway 1-02 (Clay Dam)

Three large-scale (approx. 6-m high) embankment breach tests conducted in Norway in connection with the European IMPACT project (www.impact-project.net) were included in the evaluation. These tests were performed by a consortium of Norwegian organizations and data were provided to HR Wallingford, coordinator of the IMPACT project and work package leader for the breach studies. Discrepancies in data provided through different avenues led to a review of the data and a summary report by Hassan and Morris (2008). In this report, the overtopping breach test of a homogeneous clay embankment was designated as test 1-02. The embankment for this test was constructed and tested in late 2002 (Figure 16). The embankment height was 5.9 m with 2:1 (H:V) upstream and downstream slopes and a crest thickness of 2 m. A 0.45-m deep by 5.5-m wide pilot channel was excavated through the crest so that the effective height of the test section was 5.45 m. The embankment material contained about 30% clay (< 0.002 mm) and less than 15% sand. The internal friction angle and cohesion strength of the soil were reported, but Atterberg limits and other typical properties of a cohesive soil were not reported. Due to prolonged rainy weather, the material was placed in a very wet condition (approximately 28-33 percent water content), and compaction techniques were changed (thicker lifts and less compaction effort) midway through construction, so the erodibility of the embankment was probably not uniform.

The test site was located in a sizable river about 600 m downstream from a dam and reservoir whose outflow could be regulated to produce the inflow hydrograph needed for the test. The travel time between release of water and arrival at the test site became a challenging logistical

issue for these tests, and the inflow hydrograph and upstream reservoir elevations experienced unplanned fluctuations away from intended conditions.

These issues make it challenging to interpret the results when attempting to model this test case. When the embankment failed, efforts were made to maintain the upstream water level by releasing large amounts of water from the upstream reservoir. This release of water also was intended to help flush the sediments released during the test downriver and out to sea. However, the control system adopted for the test was unable to respond quickly enough to the rapid variation in conditions, and thus water levels fell and rose rapidly at the test embankment. From an initial assessment it is easy to assume that the entire flood hydrograph represents the breach discharge when in fact it relates mainly to the general release of water through the test site after the breach had already occurred. The hydrograph produced by the breach itself is a relatively small surge in observed flow which occurs around time t = 15,000 s (4 hours 10 minutes) and is then lost in the much larger inflow that arrived at the test site just a few minutes later.

The real challenge for modeling breach in this case is therefore whether the model is able to predict the timing and associated peak of this surge, prior to the arrival of the larger flood hydrograph.

Figure 16.—Breaching of the Norway 1 clay embankment. Note that there is minimal drop in the water surface upstream from the test dam, even after breach is fully complete. The

Modeling with SIMBA

An initial run was made with SIMBA using estimated soil erodibility parameters based on knowledge of the embankment soil type and estimated compaction conditions. Because the soils

were placed and compacted in very difficult working conditions, poor compaction was suspected and a high value of k_d was assumed, 9 cm^3/(N-s). The undrained shear strength, c_u, was estimated at 7.4 kPa based on the reported friction angle (ϕ) and cohesion strength (C) for the material [$c_u = C \cdot \tan(45° + \phi/2)$].

Using these inputs, the initial run predicts breach of the embankment about 40 minutes too soon (Figure 17), which allows the majority of the upstream pool to drain before the arrival of the higher inflows that were actually delivered to the site during the test. The result is a distinct double peak in the outflow hydrograph, whereas the actual outflow hydrograph shows that the rising inflow overwhelms the initial surge in outflow through the breach and the breach peak is barely visible.

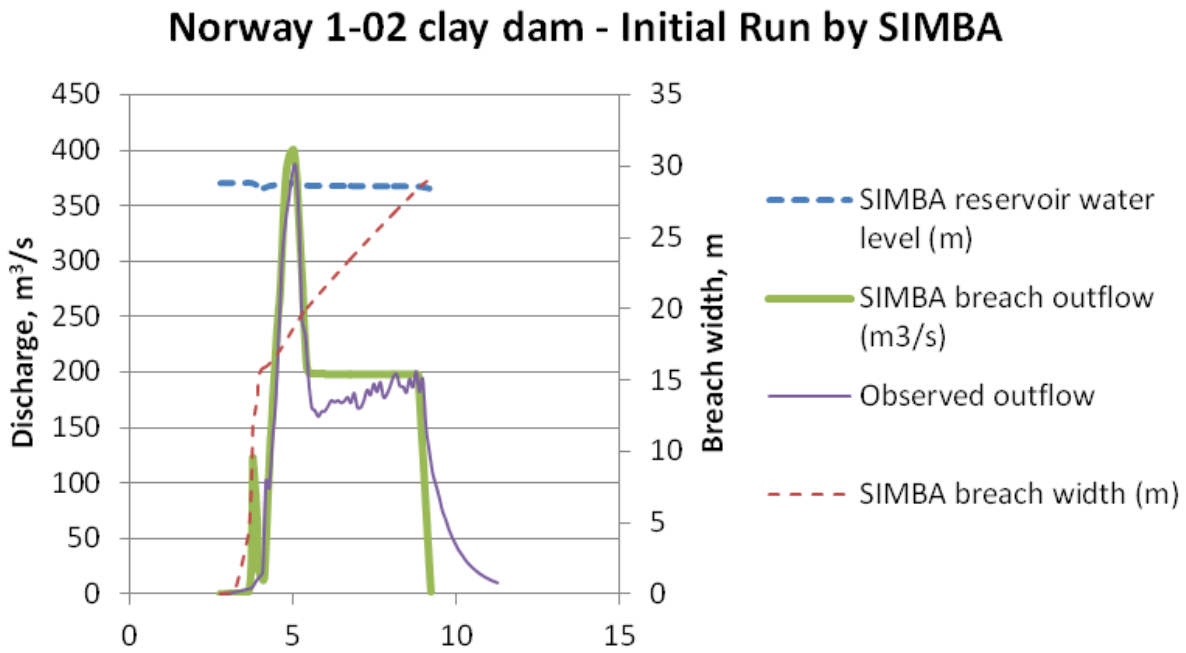

Figure 17.—Comparison of observed data and initial modeling of the Norway clay dam test case with SIMBA. Initial run with SIMBA produces an early breach of the embankment. Inflow matches outflow after the breach event has been completed.

Figure 18 shows the results of an improved run of SIMBA in which k_d was reduced to 5.1 cm^3/(N-s). This run produces accurate timing of the breach. There is still some discrepancy between the observed and simulated reservoir levels. This may be due to inability of the level-pool routing scheme in the SIMBA model to accommodate the dynamics of the rapidly changing inflow hydrograph with a relative small reservoir upstream from the test dam.

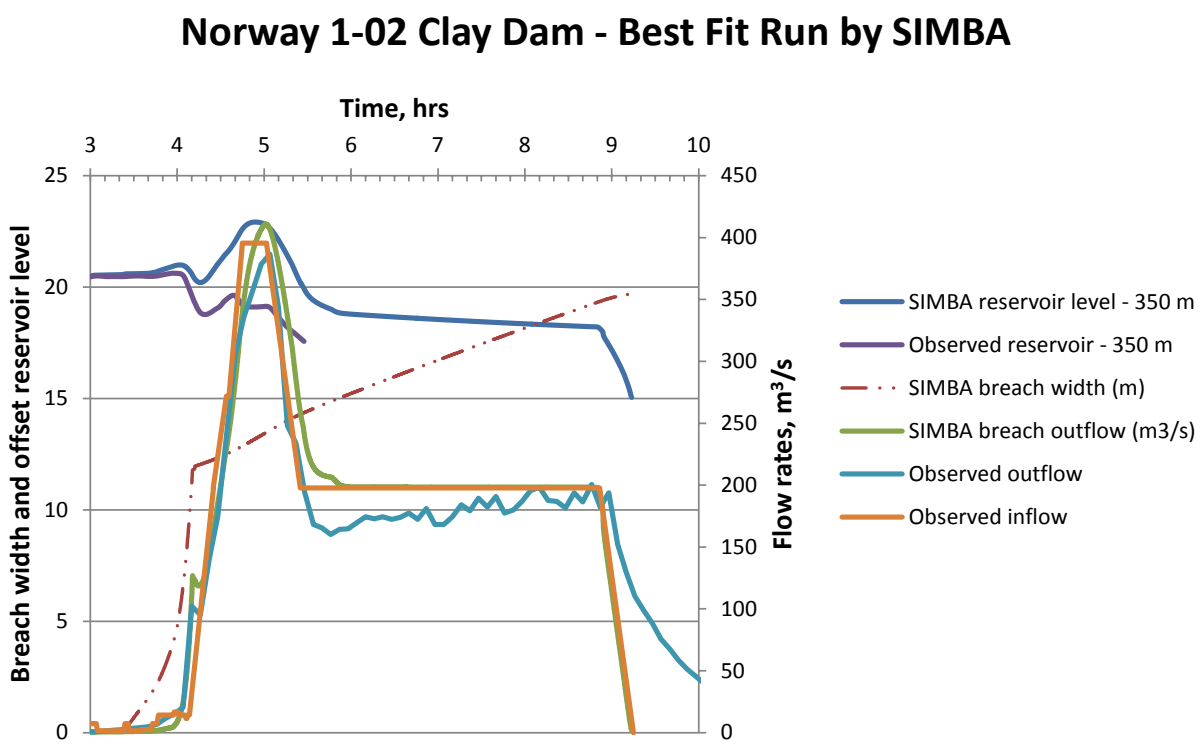

Figure 18.—Comparison of observed and modeled breach behavior for the Norway clay dam.

Modeling with HR BREACH

The initial run was made using the Hanson erosion equation with a k_d value of 1.42 cm^3/(N-s), which is believed to be based on jet tests performed at the site prior to the breach test. This initial run (M2) was made using the surface erosion mode within HR BREACH. While the predicted discharge appears reasonable, a closer look at the reservoir level and breach width shows that the modeled embankment does not fail at t = 15,000 s (as observed) but only later when the larger post-breach increase in inflow arrives at the test site. To obtain a better overall result it appears that the erodibility of the embankment needs to be significantly increased.

Two attempts were made to obtain a better fit to the erosion observations and they were about equally successful. Run M7 uses the Hanson equation with the headcut erosion mode enabled and k_d increased 12-fold to 17.7 cm^3/(N-s). Run M19 uses the Hanson equation with the surface erosion mode and k_d increased 25-fold to 35 cm^3/(N-s). M7 predicts the breach slightly early and a breach discharge slightly less than observed (about 60 instead of 100 m^3/s); M19 predicts breach slightly late and with a discharge slightly higher than observed (about 210 m^3/s). Both duplicate the shape of the upstream reservoir level curve which dips at the time of breach and then rises again as water is released from the upstream reservoir, and finally drops later as the breach widens. It is difficult to choose which modeling approach is preferable, although the headcut mode would be most consistent with the erosion mechanics observed in the test. From a modeling perspective each method requires significant adjustment to match the model results to the observed conditions. For the headcut mode adjustment of k_d and the headcut rate coefficient C is required, and for the surface erosion mode adjustment of the specified breach initiation timing is needed.

Figure 21 shows breach widths simulated in each of the various model runs. It should be noted that the breach widths are reported differently for runs made in surface erosion mode vs. headcut mode. In surface erosion, the breach width is reported as the width of the eroded channel at the critical-flow section that regulates total discharge over the dam. This section can shift as erosion takes place, so the plotted width is not necessarily the width at a fixed cross section. In model run M2 this section is seen to actually oscillate back and forth for about 3.5 hrs between an upstream and downstream section with slightly different widths.

A similar issue arises in headcut mode. The breach width is reported at the headcut location, even if the headcut is downstream from the point of critical-flow control (e.g., headcut on the downstream face when flow passes through critical over the dam crest). Again, the section at which the breach width is being reported will change as the headcut advances.

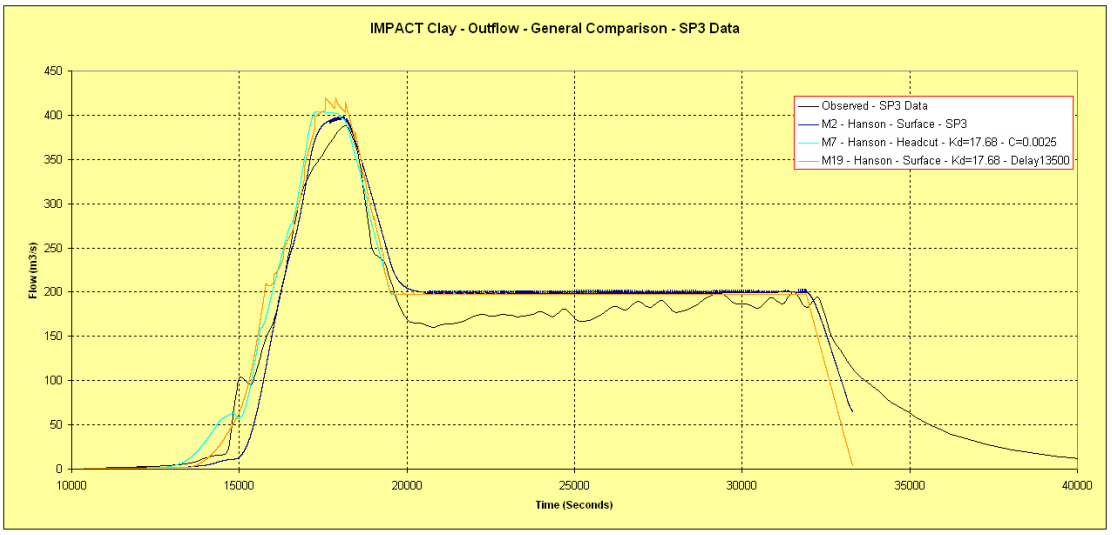

Figure 19.—Breach Outflow – HR BREACH initial and improved runs for Norway 1-02 test case.

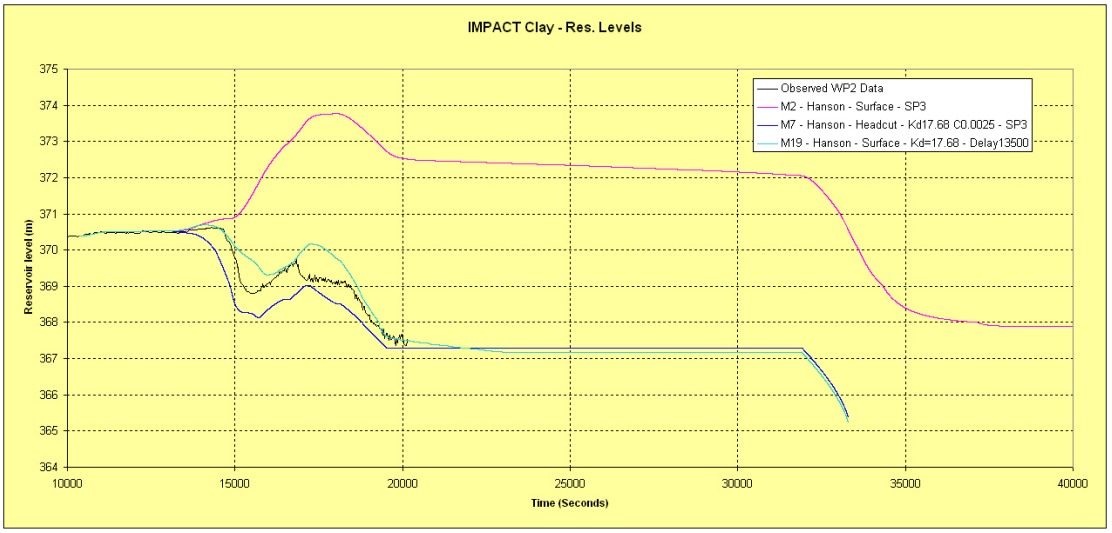

Figure 20.—Water Levels – HR BREACH initial and improved runs for Norway 1-02 test case.

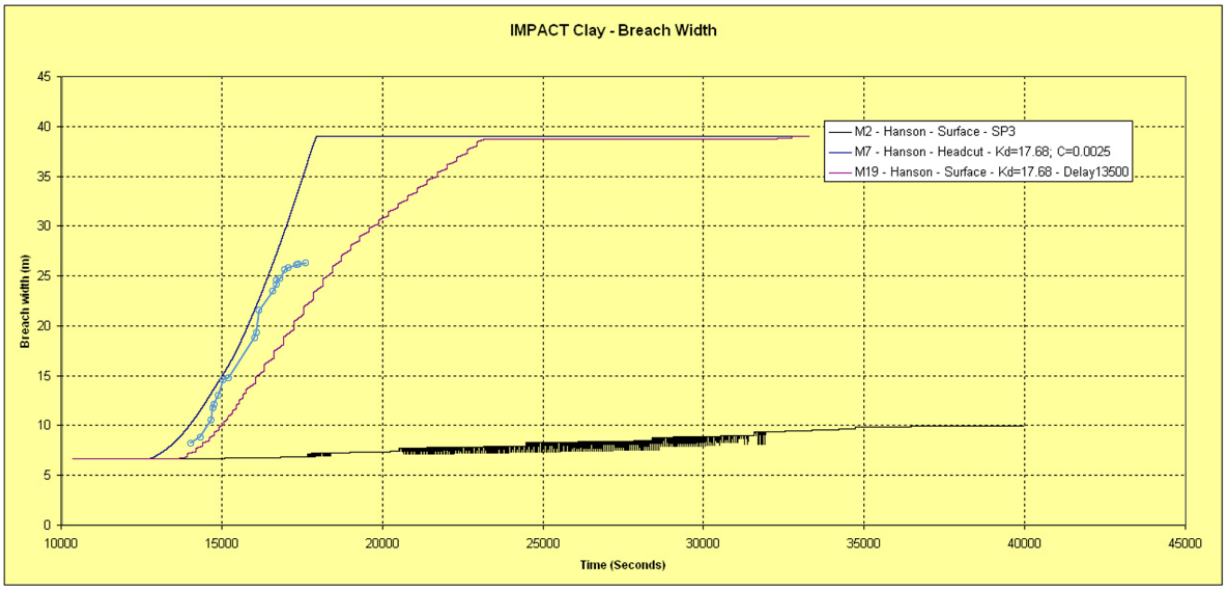

Figure 21.—Breach Widths - HR BREACH initial and improved runs for Norway 1-02 test case. Observed breach widths from field test are plotted with circular symbols (not in legend). Jittery line for the initial (M2) run is due to oscillating variations of the computational section at which critical depth occurs. (In surface erosion mode the breach width is reported at the critical-flow section, which can change from one time step to the next).

Norway 2C-02 (Gravel Dam)

The test designated Norway 2C-02 by Hassan and Morris (2008) was also conducted in 2002. The embankment was 5 m tall with a 2 m crest thickness and slopes of 1.9:1 (upstream) and 1.6:1 (downstream). The embankment was of homogeneous construction using a gravel material with D_{50}=4.75 mm. The soil composition was about 50 percent gravel, 47 percent sand, and 3 percent fines. This embankment was constructed late in the year and the test was conducted on October 16, 2002. Temperatures at the site had dropped low enough that at least the surface of the gravel was frozen. Attempts were made to melt the frozen material by blocking the pilot channel and ponding water within it up to a depth of about 10 cm before the test was started. Video and still photos suggest that frozen soil may have existed deep into the embankment, since a near-vertical headcut was observed. This was not expected given the small fraction of fines (about 3%) in the soil and the fact that the material was nearly 100% coarse-grained. If the gravel was in a frozen condition, this may have contributed sufficient strength to the material so that it was able to stand at a steep slope and develop a headcut. Despite this evidence for some erosion resistance, the breach occurred very quickly. The blockage of the pilot channel was removed at about 12:21 p.m. local time on the day of the test and peak outflow from the breach occurred in about 6 minutes.

The review of data by Hassan and Morris (2008) showed a wide range of uncertainty in the breach outflow hydrograph from this test, with two different hydrographs provided in separate communications, neither of which satisfied a basic continuity check. The true outflow hydrograph is thought to lie somewhere between the two reported hydrographs which are both shown on the plots that follow.

Figure 22.—Photos from the test of the Norway gravel dam, embankment 2C-02.

Modeling

The SIMBA and HR BREACH models were run with a variety of erosion models and material parameters, and with extensive testing, each model was able to produce outflow hydrographs whose peak flow and shape approximated the two observed hydrographs which are believed to bracket the true hydrograph. The timing of the breach was very difficult to model accurately due to the uncertainties related to material erodibility (potential effects of freezing) and the artificial manipulations of the flow through the pilot channel at the start of the test. The only way to truly match the breach timing was to specify the moment of initiation, much as the breach time was forced in the actual test. Neither model was able to completely reproduce the extremely fast rate of increase in breach outflow. Observers of the test and its video records have hypothesized that a massive structural collapse or sliding of the embankment may have occurred as the breach was beginning to enlarge, causing the rate of breach enlargement to exceed anything possible by the erosion processes simulated in the computational models.

Norway 1-03 (Composite Dam)

The Norway 1-03 embankment was designed to be a composite (zoned) structure, failed by overtopping flow. This embankment was constructed with a moraine core and gravel upstream and downstream zones. As with the other Norway tests, there were some differences between the embankment design and the as-built condition, and these are detailed by Hassan and Morris

(2008). Although the embankment was zoned, the differences between the zones may not have been distinct. The moraine material contained no clay-size particles, so the core may not have behaved much differently from the outer zones that included gravel-size material. Post-test photos also raise questions about the accuracy of the construction of the zones, with the gravel zones appearing to be quite thin in some areas. The embankment may have been more nearly homogeneous with just thin zones of gravel on the exterior of the embankment.

Modeling with SIMBA

The SIMBA model is only able to model homogeneous embankments. This zoned embankment was defined in the model with a single set of material properties and with the same basic geometry as the exterior dimensions of the tested embankment. An initial run was performed with k_d=21 cm^3/(N-s) and with the undrained shear strength, c_u, estimated at 49 kPa based on the reported value of cohesion strength and internal friction angle for the core material which was thought to be the controlling aspect of the embankment for erosion modeling purposes. This run caused the breach to occur about 1 hour early, and the resulting peak outflow was about two-thirds of the observed value. The low peak outflow was due to the fact that the inflow to the test site was increased as the breach occurred so that the test would be representative of the breach of a dam retaining a larger reservoir. When the modeled breach occurs too early, this effect is lost and the breach outflow hydrograph represents what would have occurred in the test without manipulation of the inflow.

After some trials, an improved SIMBA run was made with k_d increased to 35 cm^3/N-s and c_u increased to 60 kPa. These are within the range of reasonable values for the materials in this dam, but this was an unusual combination of adjustments to make, since it represents both greater erosion rate and greater shear strength of the soil. The combination works well in this case as it delays the migration of the headcut through the embankment to the proper time, but then allows for relatively rapid breach growth. With these parameters SIMBA is able to reproduce the approximate magnitude of the peak breach outflow, but it does not quite reproduce the detailed shape of the observed outflow hydrograph. The SIMBA hydrograph peaks somewhat late in the breach formation phase, whereas the observed hydrograph peaks at the very start of breach formation, perhaps when the core collapses structurally and the breach width increases dramatically.

Modeling with HR BREACH

This composite structure poses a challenge, with a greater number of variables to consider compared to a homogenous structure. For the HR BREACH model the question was whether to treat the structure as a homogeneous structure with a rock surface layer of protection, or as a zoned structure. Although the original intent when performing the test was to simulate a zoned structure, later analysis of video footage suggests that the outer layer was quite thin in places.

The initial run parameters (M1) were taken from the test description and the embankment was modeled as a zoned structure in which the core has the potential to fail structurally. However, the initial model run failed to even predict that the embankment would breach; the flood hydrograph that was produced was generated through overtopping and the peak flow simply reflects the increased inflow that was provided to the test site to maintain a steady upstream head as the embankment was breached.

Figure 23.—Photos from the test of Norway embankment 1-03.

The improved results (run M19) were achieved after a considerable amount of trial, using both zoned and homogeneous (with rock cover) modeling approaches. With the zoned approach, a range of soil strengths were considered until structural failure of the core was achieved, providing outflow characteristics that match the observations. It is notable that this was the only run that produced the very unique hydrograph shape observed during the test, with a very rapid spike in outflow to reach the peak, followed by a sustained time of high outflow before the reservoir began to drain. Thus, it seems plausible that dual mechanisms of breach formation were at work in this test, an instantaneous collapse of the core followed by a steadier erosion process to clear away the dislodged material and enlarge the breach. This subtle detail may be of importance in some scenarios and less important in others, depending on how close populations at risk are to the dam and how channel attenuation changes the breach outflow hydrograph below the reservoir. It is also possible that the unusual shape of the outflow hydrograph was brought about by the manipulation of the inflow to the test site. The timing of the arrival of increased inflow may have been such that it sustained the breach outflow at a steady level, in a way that is also suggestive of a dual-mechanism failure.

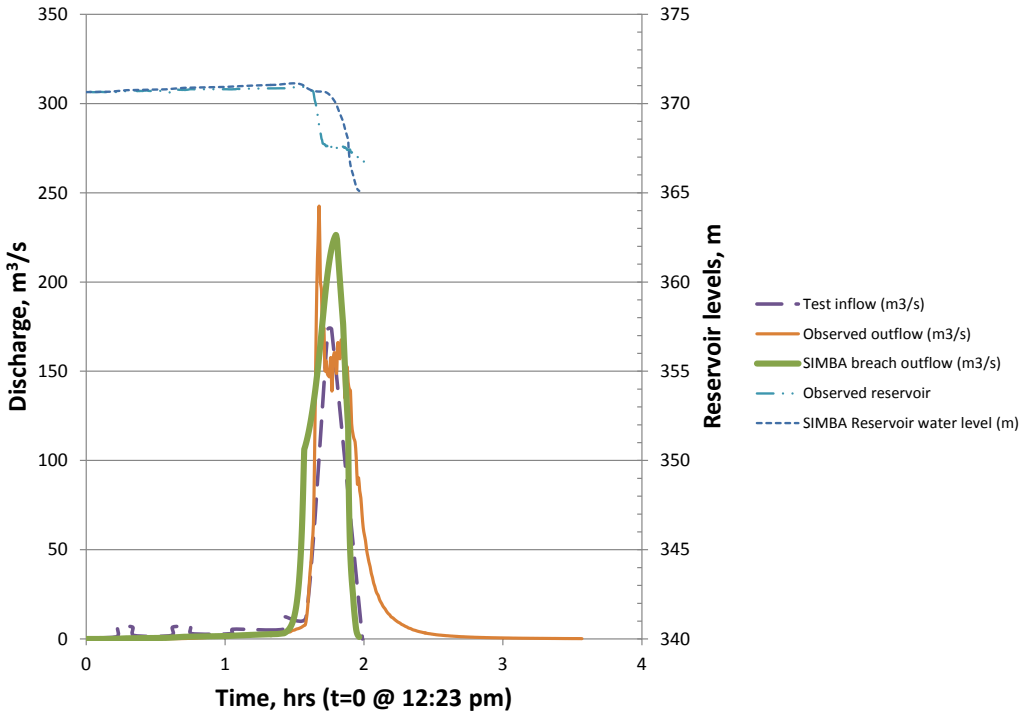

Figure 24.—Improved run of the SIMBA model for the Norway 1-03 composite dam.

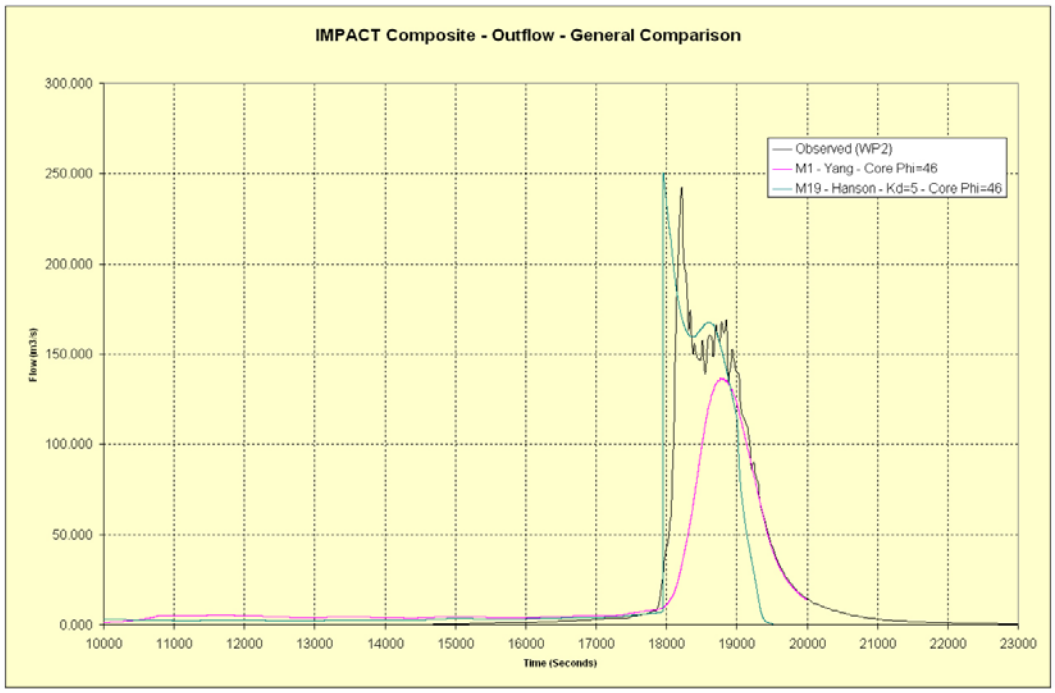

Figure 25.—Plot of outflow – HR BREACH initial and improved runs for the Norway 1-03 composite dam.

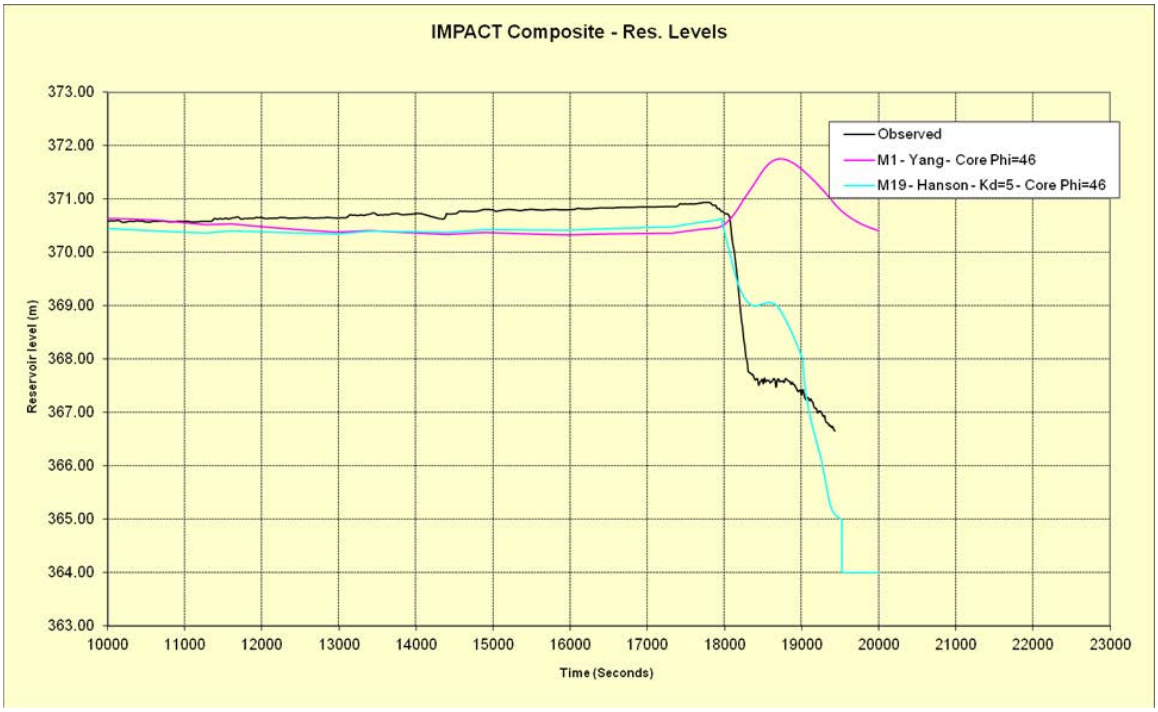

Figure 26.—Plot of water level – HR BREACH initial and improved runs for the Norway 1-03 composite dam. In run M1 the embankment does not breach.

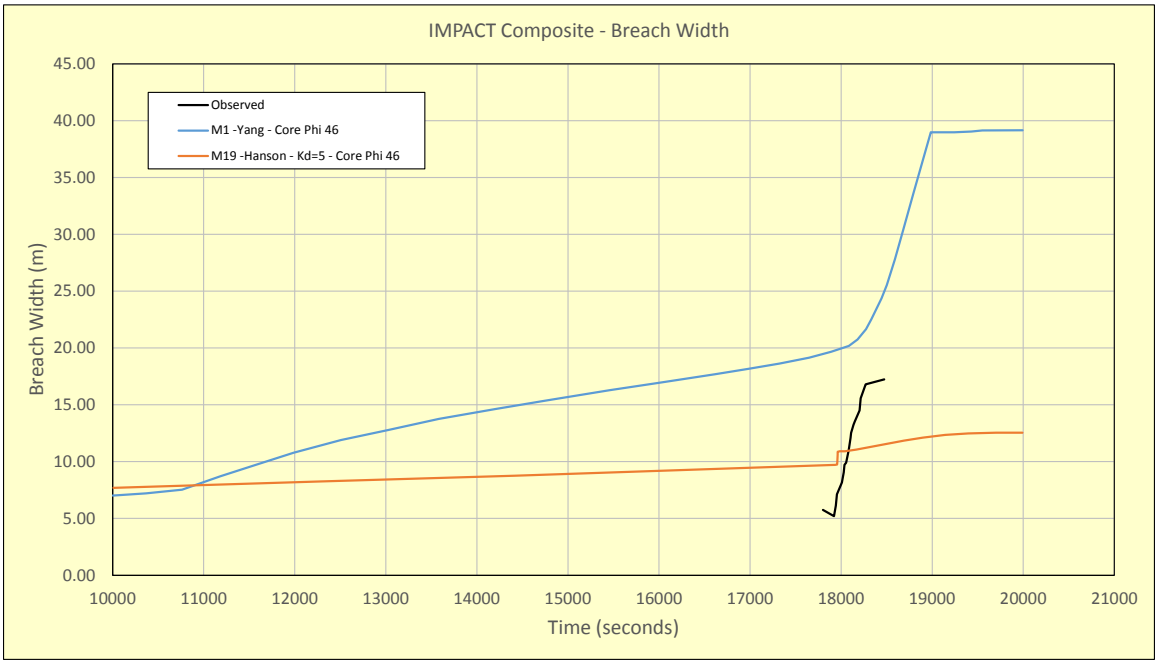

Figure 27.—Plot of breach width - HR BREACH initial and improved runs for the Norway 1-03 composite dam. In run M1 the embankment does not breach, but the model output indicates widening of the section of flow control as the flow exceeds the pilot channel notch and overtops the entire embankment. In the M19 run the change in breach width reported by the model is small in comparison to what was visually observed at the downstream face of the embankment.

Real Dam Failures

Oros Dam – Brazil 1960

Oros Dam in Brazil was a zoned embankment with rockfill and sand outer shells and a thick, clay core. The dam failed in 1960 when it was overtopped while still under construction, following a regional storm that dropped more than 635 mm of rainfall (over 25 inches) in less than a week. For about 4 days preceding the failure, crews worked around the clock in attempt to raise the dam and prevent overtopping. The top section of the dam was raised about 1 meter per day during this time, but was narrow in cross section and probably poorly compacted because of intense rainfall that interfered with the use of heavy equipment. Just prior to failure, a man-made pilot channel was excavated near one abutment to try to force failure to occur through a less erodible section of the dam. The majority of the dam crest was eventually overtopped and a second breach formed in a middle portion of the dam where there was less erosion resistance.

Geometric characteristics, material parameters, inflow hydrographs, and observed data defining the breach process were compiled in phase 1 of the CEATI project (Courivaud 2007) for use in numerical model validation. The greatest uncertainty about this case is the observed peak outflow. Many data compilations report the peak outflow to be about 9,600 m^3/s, but reservoir drawdown records and the area-capacity curve suggest that the peak outflow could have been as great as 58,000 m^3/s (about 6 times greater). However, the very large size of the Oros reservoir is a problem, causing even small errors in reported reservoir level to translate into large changes in peak outflow.

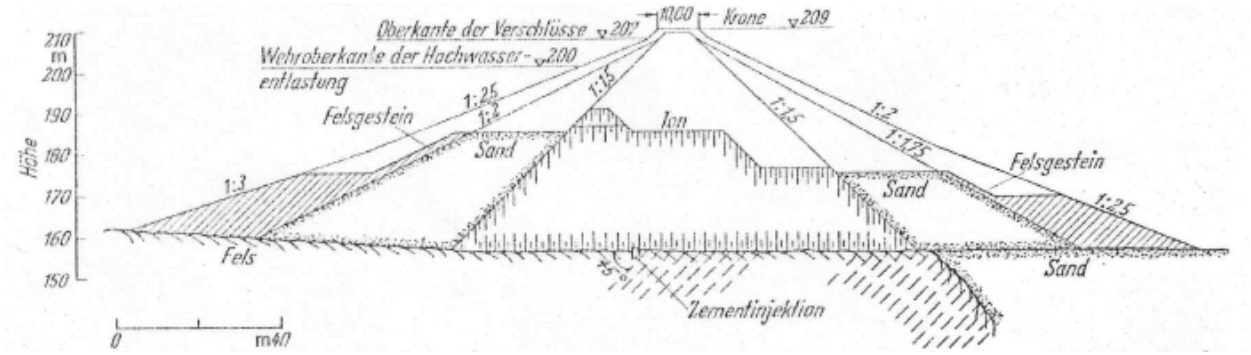

Figure 28.—Embankment geometry of Oros Dam prior to failure. Although this drawing shows the core to have 1.5:1 (H:V) slopes, other information sources report the core to have 1:1 slopes.

Figure 30 shows the recorded reservoir water levels for the event. A sudden 1.7-m drop of the reservoir occurs at time 348.5 hrs. This appears to be an erroneous piece of data or is due to an anomaly in the evolution of the breach. If this data point is ignored, the computed peak outflow drops to about 12,400 m^3/s.

The Oros case study presents a range of modeling challenges:

- The geometry of the embankment was unusual at the time of failure due to the frantic attempts to save the dam,

- There is large uncertainty in the observed peak discharge, with the true value unknown between 9,600 and 58,000 m^3/s,
- The downstream channel may have constricted flow away from the breach and created backwater effects that restricted the outflow and the erosion rate.

Modeling with SIMBA

An initial run of the SIMBA model was made using the following parameters:

- Embankment defined as just the core section with 1:1 slopes, crest thickness = 5 m
- Undrained shear strength computed from reported internal angle of friction and cohesion, $c_u = C \cdot \tan(45° + \phi/2) = 41.2 \text{ kPa} \cdot \tan(45+27/2) = 67.2 \text{ kPa}$
- Estimated erodibility: $k_d = 35 cm^3/(N\text{-}s)$. Critical shear stress $\tau_c = 0$.
- Pilot channel defined as entire crest length, 700 m, with side slopes of 2:1.
-

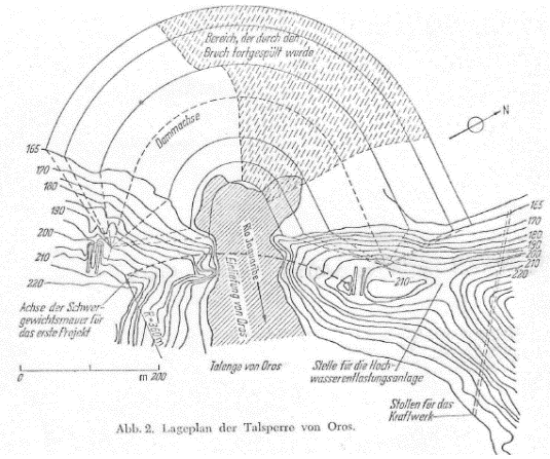

Abb. 2. Lageplan der Talsperre von Oros.

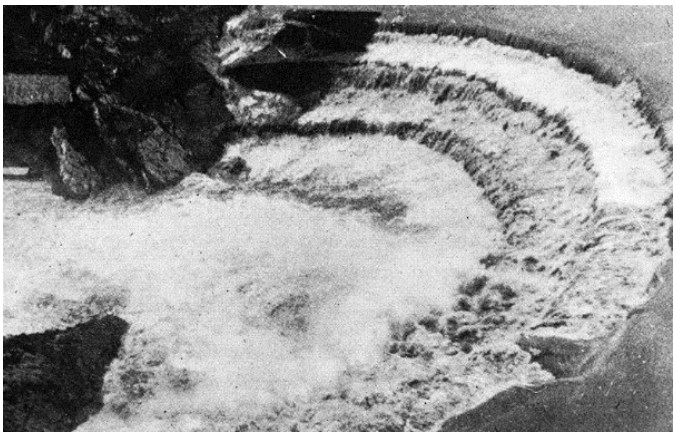

Figure 29.—Overtopping of Oros Dam. The excavated pilot channel is visible at the top of the lower photo, just left of center (right abutment of dam). Flow is overtopping most of the length of the dam. The stepped character of the downstream slope is due to the effort to rapidly construct a narrow embankment section at the upstream edge of the wider embankment section. Also note narrow downstream channel.

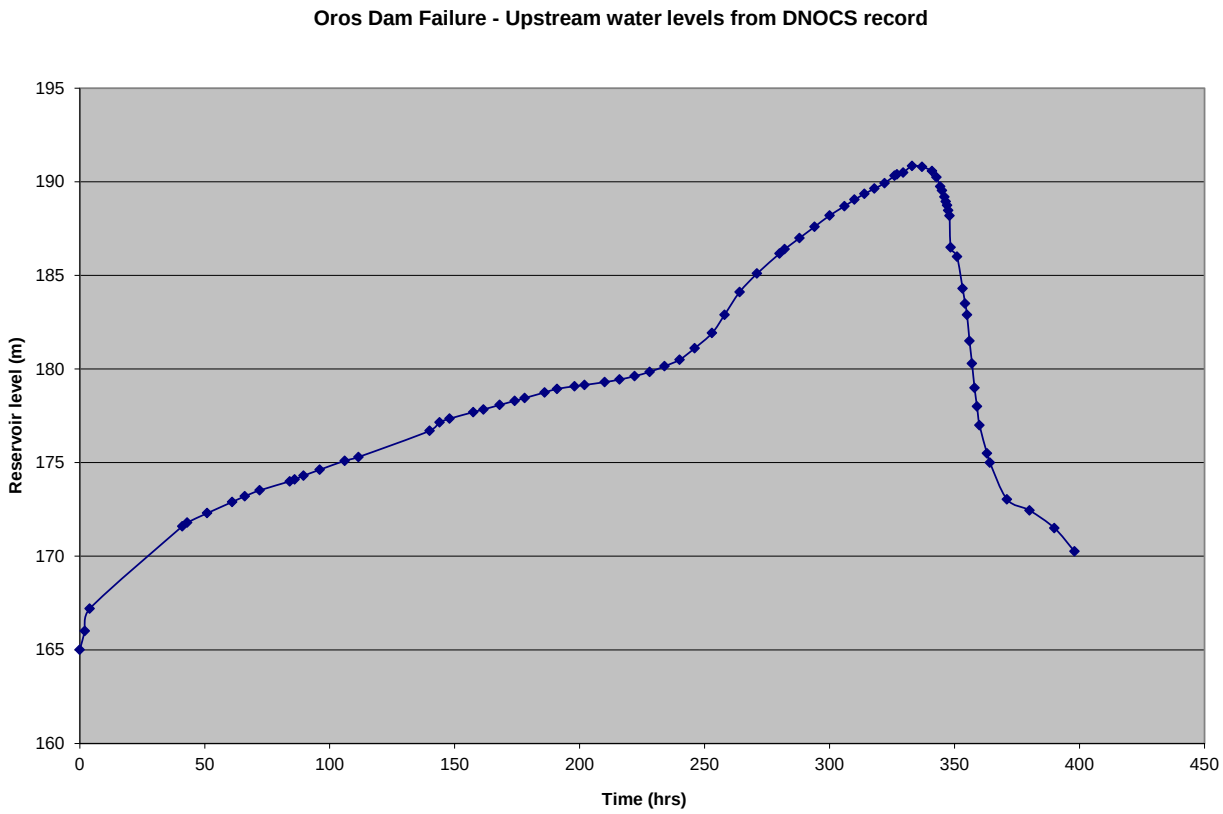

Figure 30.—Water level records from the Oros Dam failure. The computed peak outflow is due to the sudden drop of the reservoir level at time 348.5 hrs (1.7 m in 30 minutes).

The version of SIMBA used for this study did not allow for defining a tailwater rating curve, so there was no consideration for effects of tailwater. The initial run predicted rapid breach development and widening which led to a peak outflow of about 55,000 m^3/s. While this would approximately match the high estimate of peak outflow (which is suspect), the accompanying prediction of the reservoir drawdown rate is also much too fast. In addition, the final reservoir level drops much lower than what was observed, which may be an indication of the importance of tailwater effects and perhaps post-breach deposition of sediments in the tailwater channel.

An improved model run was made by reducing k_d to 1.33 $cm^3/(N\text{-}s)$. While this seems like a relatively low value considering the description of the core material, it may effectively account for other factors that could have reduced the erosion rate, such as tailwater effects and the influence of the outer sand and gravel zones that are not being included in the cross section. The adjustment has the desired effect, as shown in Figure 32. The breach now occurs at approximately the correct time, the reservoir drawdown curve more closely matches the observed reservoir levels, and the peak outflow is consistent with the smoothed estimate of breach outflow. There is still a notable difference in reservoir levels after the breach, and this may indicate tailwater influences, including sediment deposition in the tailwater channel. The other notable difference in this result compared to the initial run is a better prediction of the final breach width. The final run predicts about 95 m, whereas the initial run predicted full washout of the 700-m long dam; different sources put the actual final bottom breach width at 130 to 200 m. It is interesting that as the first real dam failure case modeled, this case gives a good

example of a dam for which the peak breach outflow seems to occur relatively late in the breach development process, since the dam drains slowly. For the model dam experiments considered thus far, the peak breach outflow has tended to occur shortly after the breach entered the reservoir, since the reservoirs drained rapidly before the breaches could fully widen.

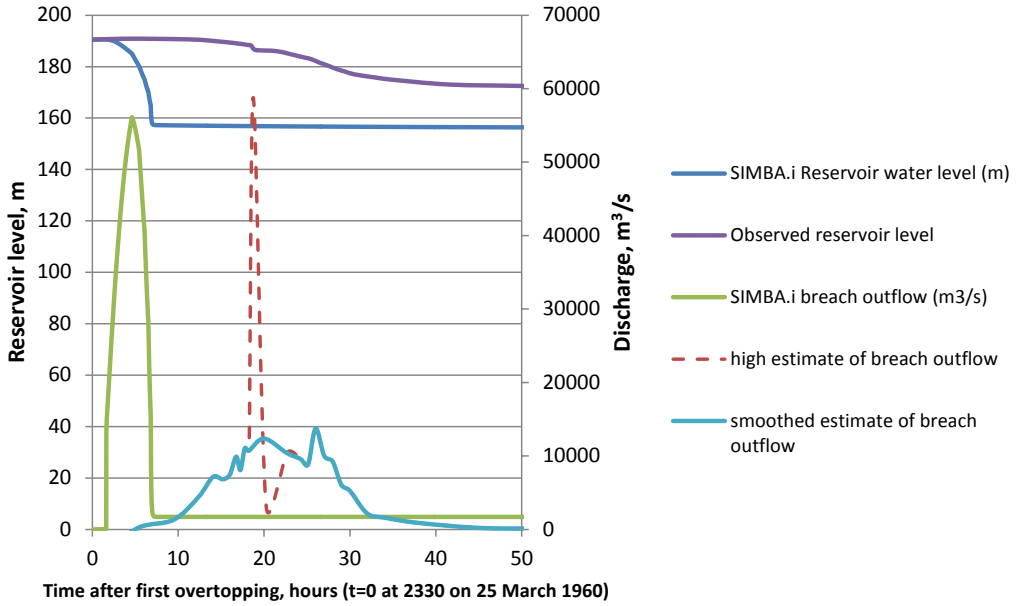

Figure 31.—Initial run of SIMBA model for Oros Dam failure. Breach occurs too soon and breach widening rate is too fast, leading to high peak outflow and drawdown of the reservoir that does not match observed data.

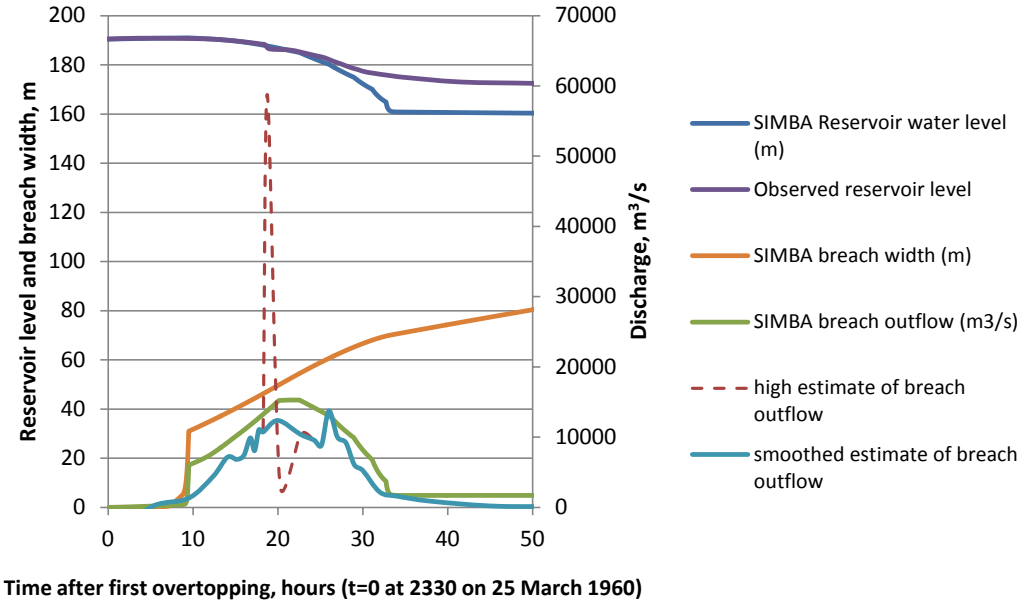

Figure 32.—Improved run of SIMBA model for Oros Dam failure. Breach occurs at approximately the correct time, reservoir drawdown more closely matches the observed reservoir levels, and the peak outflow is consistent with the smoothed estimate of breach outflow.

Modeling with HR BREACH

HR BREACH was applied to the Oros Dam failure using the surface erosion models. An initial model run was made with HR BREACH assuming no downstream influence (i.e. breach opening was not drowned in any way), while subsequent runs included details that allowed the model to predict the effect of drowning. The initial run produced a peak outflow that was near the high end of the uncertainty range for the observed peak outflow, while the later run that included tailwater influences produced a result closer to the low end of the observed peak outflow range. This is believed to be the most plausible result and is considered the improved run.

For the initial estimate the rockfill layer was simulated as a protection layer in the HR BREACH model with D_{50}=100 mm. The Hanson erosion equation was used with what was considered a high erodibility value of k_d=9 cm^3/(N-s), since even the core zone of the dam had a low clay content (about 9%) and low plasticity index, PI=10. With these inputs the model predicts that the dam fails too soon and too rapidly, with a peak outflow of about 55,000 m^3/s. Reservoir water levels and volumes were not matched well with observed values; not only was the timing of the breach wrong, but the rate of reservoir drawdown was much too rapid. This suggests that even if the time of breach could be delayed, a rate of breach development that would lead to a peak outflow in the range of 55-58,000 m^3/s is not consistent with the observed behavior of the reservoir. It was noticeable that observed water levels in the reservoir do not drop below 170 m at the end of the failure. This is believed to be due to tailwater effects from the constricted downstream channel.

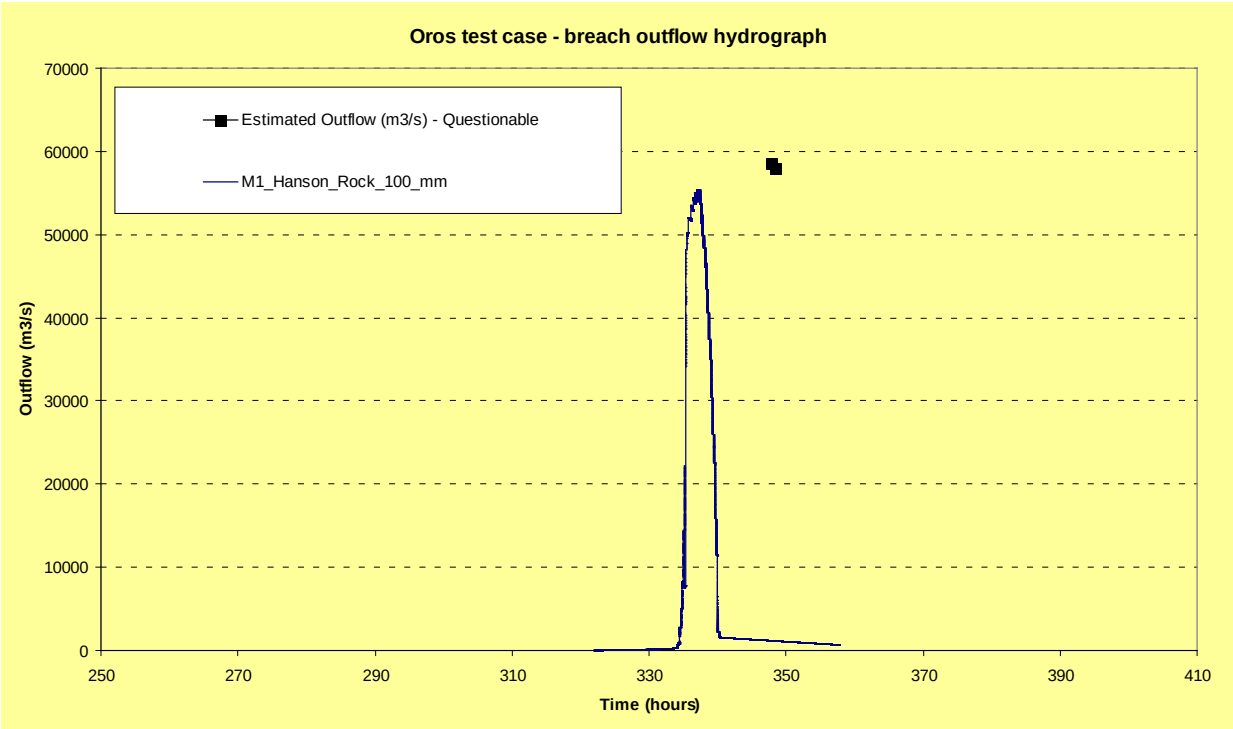

Figure 33.—Breach outflow from Oros Dam for HR BREACH initial run.

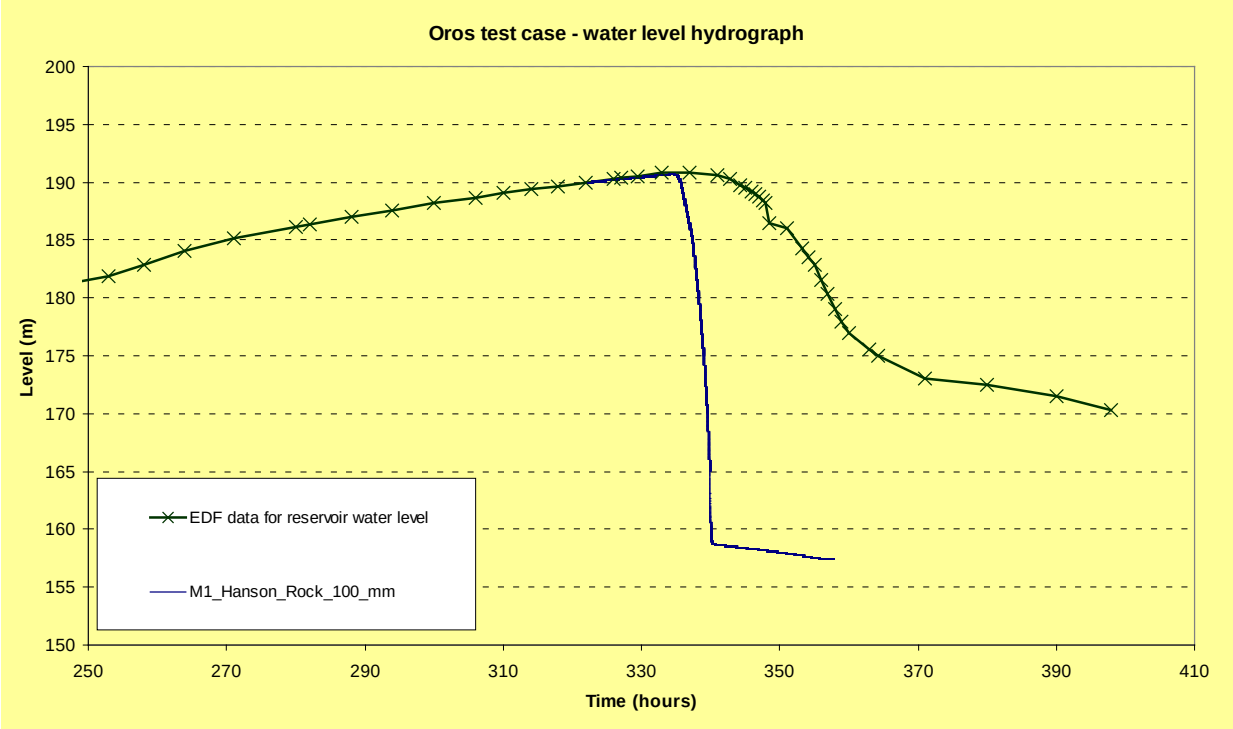

Figure 34.—Water levels upstream from Oros Dam for HR BREACH initial run.

For the improved run the real valley cross section was included. The results show a significant drop in the peak breach outflow, with a value that is consistent with estimates that ignore the anomalous drop in reservoir water level at the 348.5 hr mark. There is also improvement in simulating the drawdown of the reservoir water level and volume, although there is some divergence at the end of the event. This may be due to inaccurate modeling of the invert of the tailwater cross-section. Based upon the results of other trial simulations (not shown here), the D_{50} of the surface protection was also increased to 300 mm and the erodibility coefficient was increased to 18 $cm^3/(N\text{-}s)$, but these changes had relatively minor effects compared to improving the modeling of the tailwater boundary. This combination of adjustments probably allows for somewhat more rapid erosion in the early stages of breach formation, but much slower erosion in latter stages when tailwater suppresses the flow and the erosion rate in the breach. Figure 38 shows the effect of drowning on the breach outflow prediction. The same soil erosion models and parameters are used for each run, and the downstream valley is included in the second run. The downstream valley dramatically chokes the outflow and/or suppresses the erosion rate.

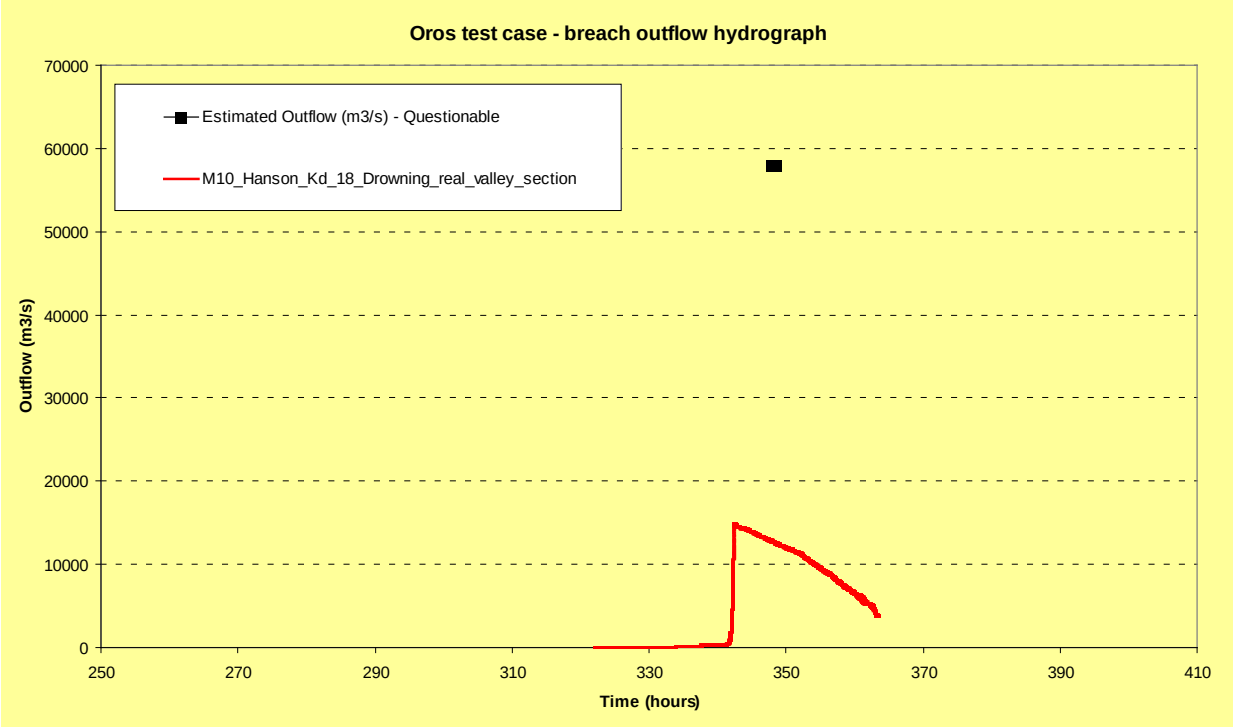

Figure 35.—Breach outflow hydrograph for Oros Dam from the HR BREACH improved run.

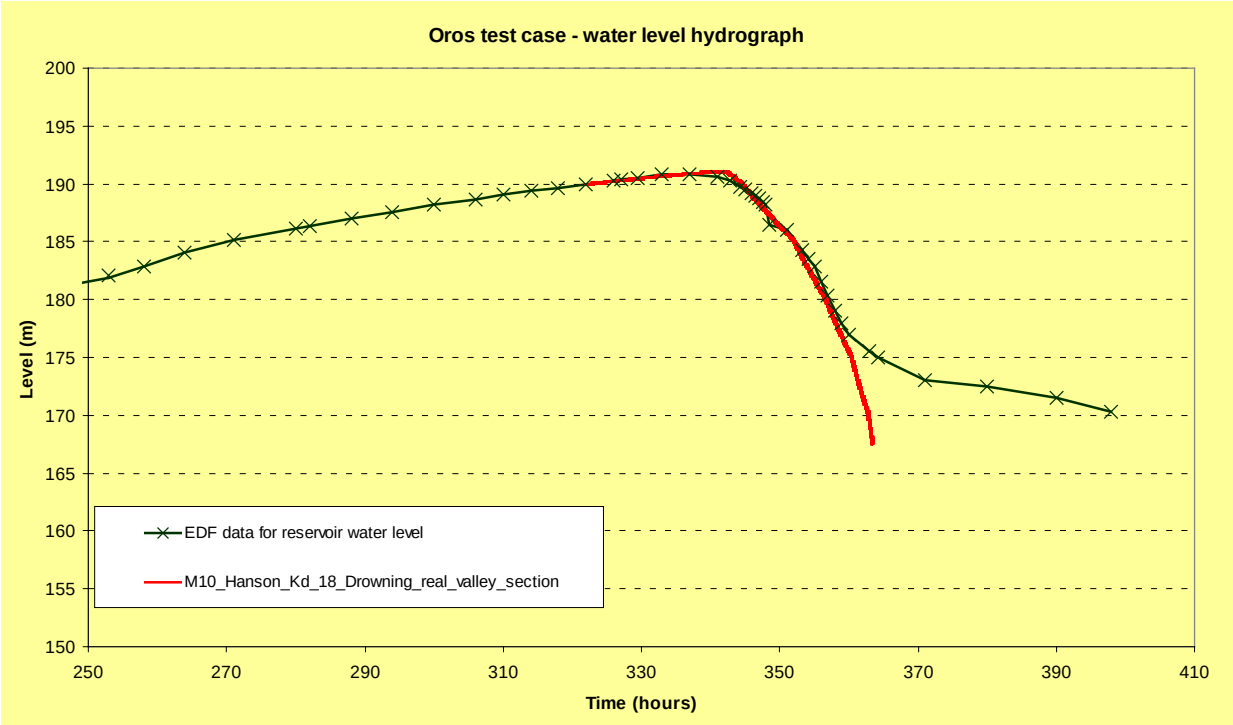

Figure 36.—Reservoir water levels for Oros Dam HR BREACH improved run.

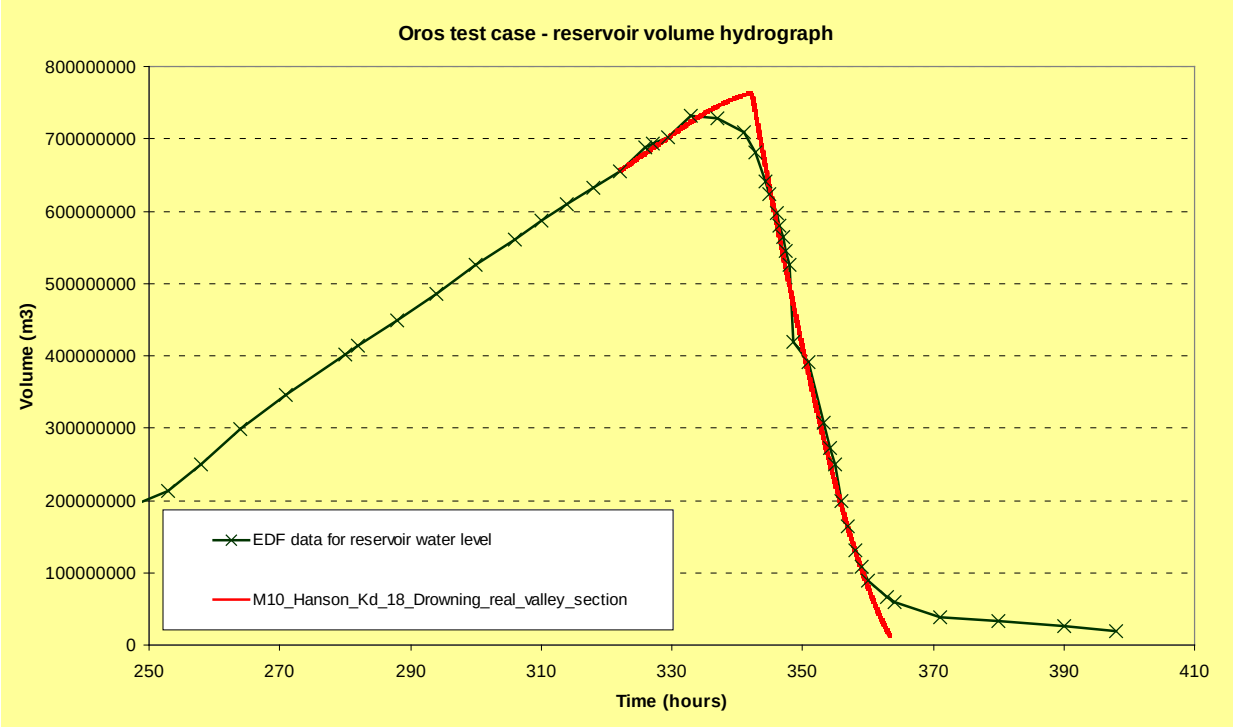

Figure 37.—Reservoir volumes simulated for Oros Dam failure in the HR BREACH improved run.

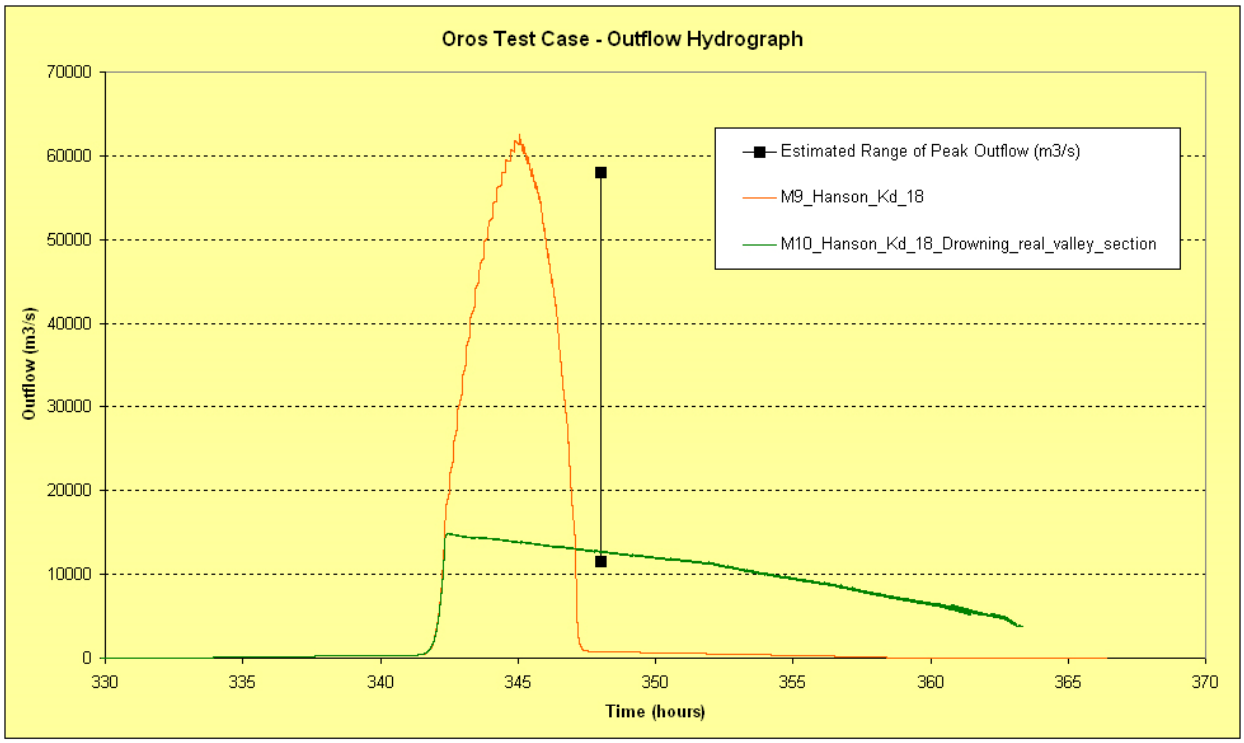

Figure 38.—Effect of breach drowning on predicted outflow for the Oros Dam modeled by HR BREACH.

Banqiao Dam – China 1975

Banqiao Dam was constructed in 1956 by the Chinese government and failed by overtopping during a large regional storm event in 1975. The dam is described as a homogeneous fill with a clay corewall of arenaceous (sandy) shale. The corewall is not believed to have added significant erosion resistance to the dam, and the embankment is believed to have behaved as a homogeneous fill. The dam is thought to have been highly erodible due to the fact that it was manually constructed and compacted only by foot traffic from construction laborers.

Data for the failure of Banqiao Dam were compiled by Courivaud (2008) based on translations of Chinese-language publications. Fujia and Yumei (1994) also provide a useful description of the event. Courivaud (2008) suggested that the breach formation time was most likely about 2.25 hr, and this is consistent with the account by Fujia and Yumei. The dam was equipped with a parapet wall which failed early in the event, suddenly increasing the overtopping depth from about 0.3 to 1.6 m (1 to 5 ft). First overtopping of the parapet wall took place at about 2300 on 7 August, failure of the parapet wall occurred early on 8 August, and complete failure of dam was reported by 0130 on 8 August. Final draining of the reservoir was reported complete about 6 hr after the peak outflow.

Figure 39.—Photo of Banqiao Dam after it failed in 1975 due to overtopping.

As with Oros Dam, a key issue for this case study is the estimated breach outflow hydrograph which is again developed from analysis of reservoir water level records. Figure 40 shows that the reservoir water level curve exhibits anomalies as the breach develops that dramatically affect the calculation of peak outflow. Using the observed water levels directly, a peak flow of about 104,000 m^3/s is obtained. In the study by Electricité de France (Courivaud 2007) a peak outflow of 78,000 m^3/s was suggested. Subsequent analysis shows that with varying degrees of smoothing applied, the peak outflow could be as low as 57,000 m^3/s. The smoothed hydrograph shown in Figure 40 seems realistic and has a peak outflow of 71,800 m^3/s.

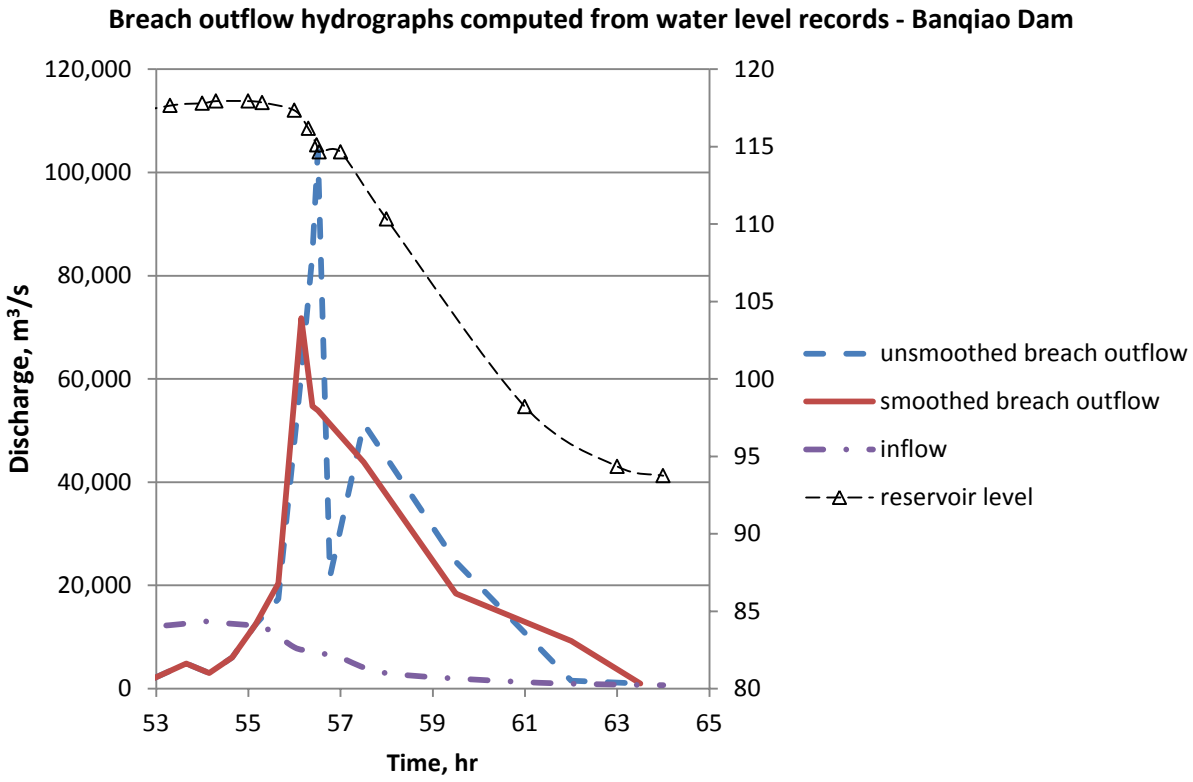

Figure 40.—Potential outflow hydrographs determined from water level records.

Modeling with SIMBA

An initial run of the SIMBA model was made using estimated soil erodibility parameters based on material descriptions: c_u = 24 kPa; total unit weight = 17 kN/m^3; k_d = 35 $cm^3/(N\text{-}s)$; $\tau_c = 0$. The top of the parapet wall was used as the dam crest elevation, and since SIMBA offers no mechanism for triggering failure at a specific time or for removing a parapet wall, this probably delays the breach initiation and slows the early rate of breach development since the modeled overtopping head was significantly less than the actual condition. The resulting peak discharge through the breach is about 35,000 m^3/s and the final breach width is 390 m. Although the discharge is well below what is believed to be a reasonable estimate of the observed breach outflow, the breach width compares well to the observed value of 372 m at the dam crest.

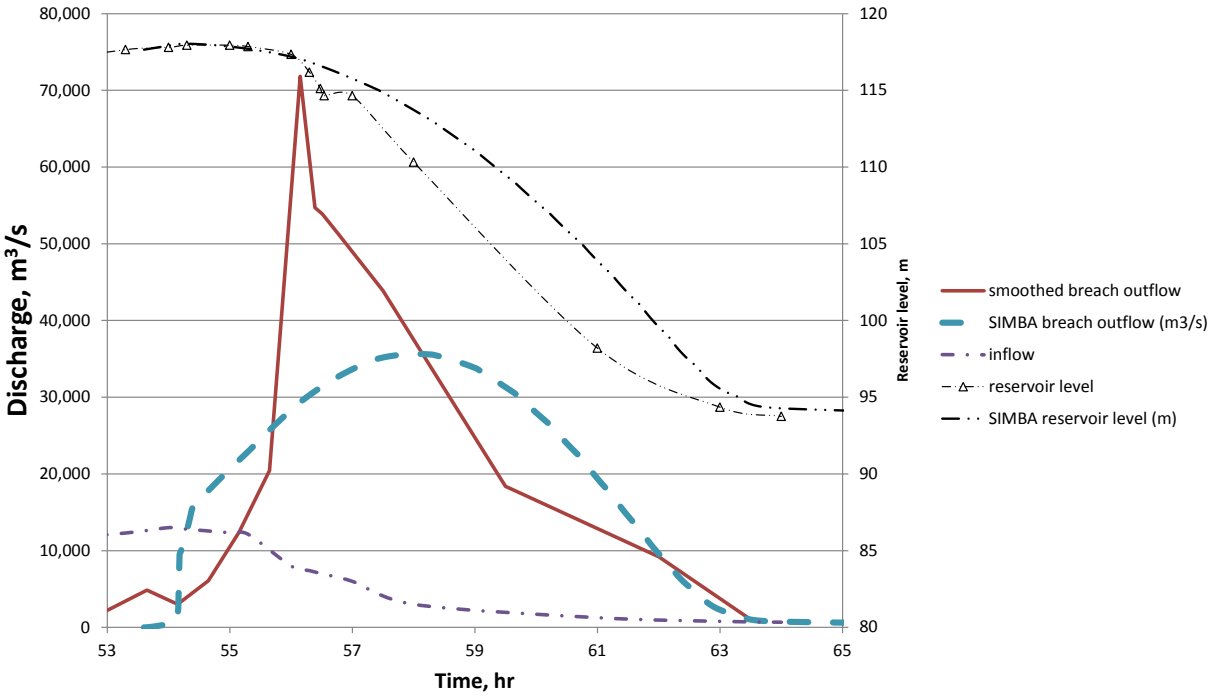

Figure 41.—Initial results from SIMBA for the failure of Banqiao Dam.

A final run of SIMBA was made with the value of k_d increased to 210 $cm^3/(N\text{-}s)$. In this run the peak outflow was about 78,000 m^3/s, close to the smoothed breach outflow hydrograph developed from the reservoir water level data, but the final breach width was 1150 m, about 3 times the observed value. The initiation of breach also seems to occur too soon, although this is difficult to objectively evaluate since the parapet wall failure is not simulated. The uncertainties in the breach outflow hydrograph combined with the inability to fully model the failure sequence of the parapet wall make it difficult to achieve a model run that matches all aspects of the observed data.

Modeling with HR BREACH

The initial run (M1) with HR BREACH used the surface erosion model and a high erodibility of k_d =18 $cm^3/(N\text{-}s)$, as the dam material was reported to be poorly compacted. The time of breach initiation was directly specified. The initial results showed a good match with water levels and reservoir volume, but with the event triggering slightly early. The estimated peak outflow value was about 43,000 m^3/s.

The improved simulation (M6) used the same parameters as the initial run, but the failure initiation was delayed about 35 minutes to improve the prediction of the maximum reservoir water level prior to failure. This run produced a slightly higher peak breach outflow of about 48,000 m^3/s. The reason is not apparent for the spike in outflow seen just after the initial peak in both runs, but it may indicate that model is predicting a slope collapse or other sudden mass wasting event as the breach enlarges. At the time that these runs were made there was still uncertainty regarding the analysis to determine the peak breach outflow, and the result obtained in the M6 run was considered the best that could be achieved with the available information.

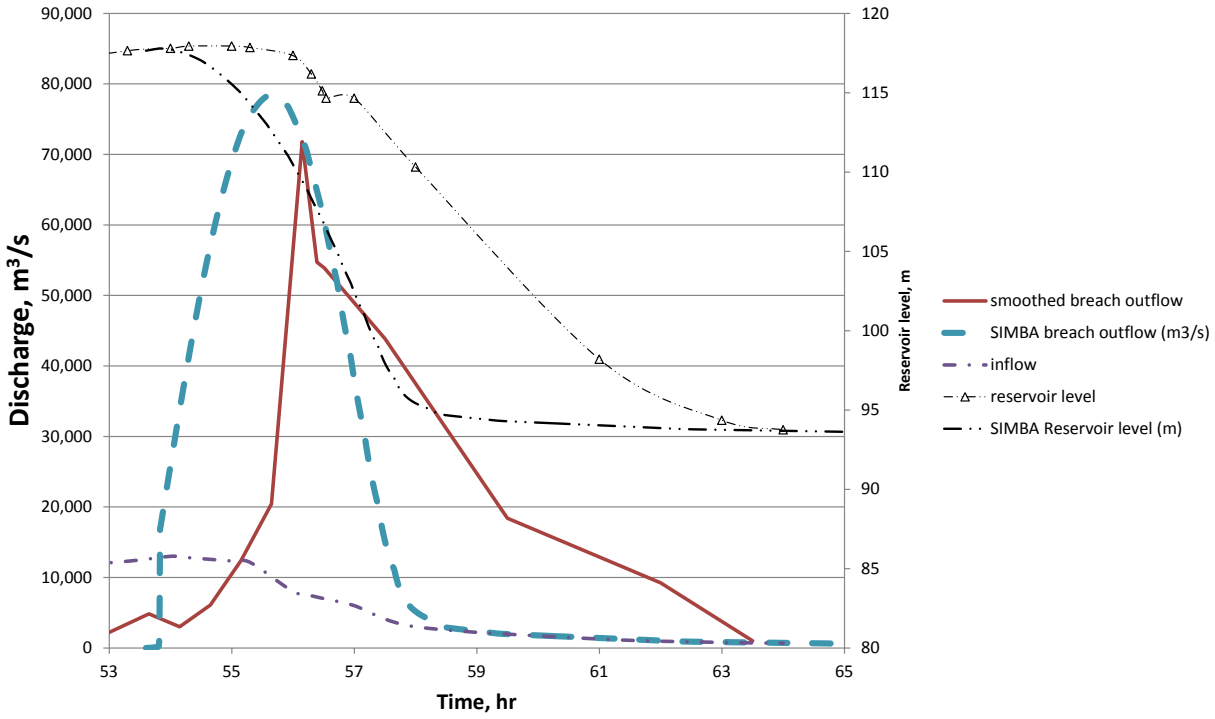

Figure 42.—Final results from SIMBA for the failure of Banqiao Dam.

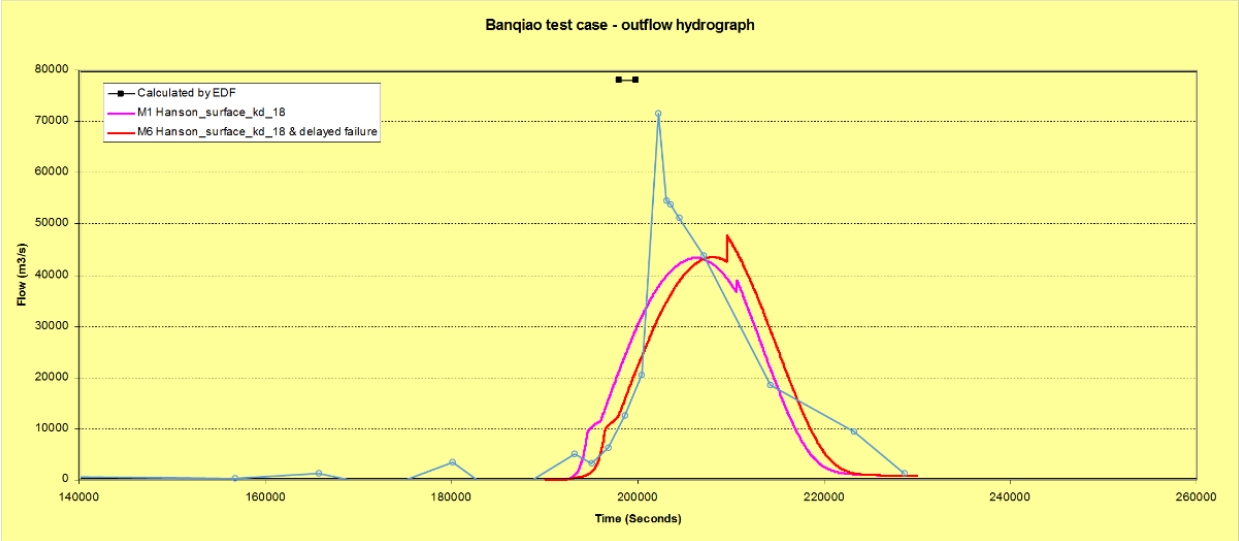

Figure 43.—Banqiao Dam breach outflow hydrographs for HR BREACH initial and improved runs, compared to the smoothed breach outflow hydrograph shown in previous Figures 40-42 (blue line with symbols, not included in legend). Note that the maximum outflow calculated by EDF is incorrectly located on the time axis. It should be located at about 205,200 seconds.

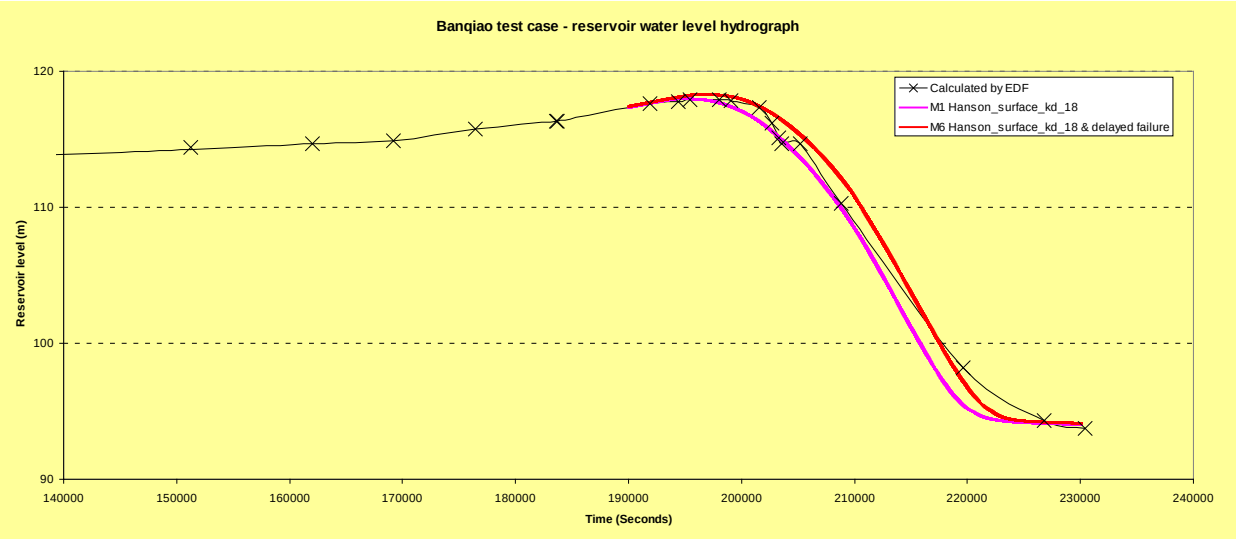

Figure 44.—Banqiao Dam reservoir level graphs for HR BREACH initial and improved runs.

Discussion of Model Performance

Quantitative

To demonstrate the performance of each model in a quantitative way across a range of conditions, the modeling results from each of the individual evaluators in the working group were assembled. The majority of these results came from model runs performed with initial inputs that were based on information that could potentially be available before a dam failure has occurred. These runs were meant to represent the ability of the models to produce accurate results without tuning. In addition, some evaluators were able to complete improved runs in which model input data were adjusted to better represent boundary conditions and material properties, but with the limitation that input parameters should be maintained within physically reasonable bounds. The figures that follow show the ability of each model to predict specific dam breach outputs in both the initial and improved runs.

The specific parameters used for the quantitative evaluation and their working definitions are as follows:

- Breach initiation time, t_i – Ideally this is defined as the elapsed time from first overtopping of the dam until erosion advances past the upstream edge of the dam crest into the reservoir. When the time of erosion breaking through the crest cannot be adequately determined, this can alternately be defined as the elapsed time from first overtopping to when the breach outflow reaches 10% of the eventual peak discharge.
- Breach formation time, t_f – Duration from end of breach initiation to the time at which the breach reaches its approximate maximum dimensions. Since a breach may continue to grow at a very slow rate during the final draining of the reservoir, the end of breach

formation may be practically considered to be the time at which the breach growth rate begins to significantly decelerate.

- Final breach width, B – Final width of the breach at the crest centerline (average of top and bottom widths).
- Breach widening rate – Compute as $B/(t_f-t_i)$, or if possible, define graphically from the slope of the linear portion of the breach width vs. time chart.
- Peak breach outflow – maximum breach outflow rate

It should be noted that in most of the plots that follow, data for only 6 case studies are shown, since the USDA-2 test did not cause a breach of the embankment and did not produce observed values of the parameters described above. For the Norway 2C-02 gravel dam test, the earlier discussion concluded that this case was impossible to adequately model because of uncertainties related to material erodibility, observed breach outflow, and artificial manipulations of the flow at the start of the test, but the results of the evaluators efforts are still included in these plots. Also, the observed values of peak breach outflow for the Oros and Banqiao Dam cases are shown as 58,000 m^3/s and 78,000 m^3/s, respectively, which were the accepted values being used by the evaluators at the time that most of the model runs were completed. As was demonstrated earlier, with adjustment of erosion rate parameters, the models were also able to predict peak outflows that matched the smaller, smoothed estimates of observed peak discharge. This demonstrates both the flexibility of the models and the difficulty of evaluating models against case study data that are highly uncertain.

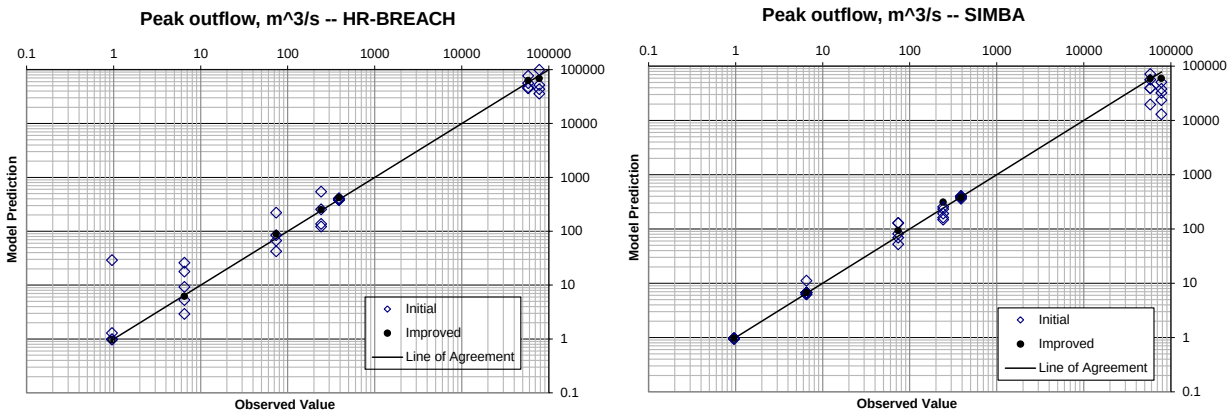

Figure 45.—Model-predicted peak breach outflows versus observed values.

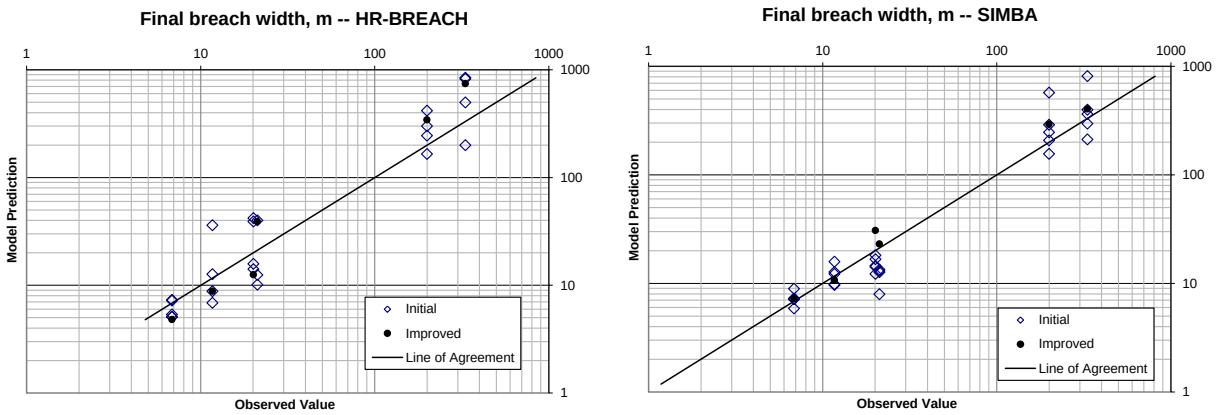

Figure 46.—Model-predicted final breach widths versus observed values.

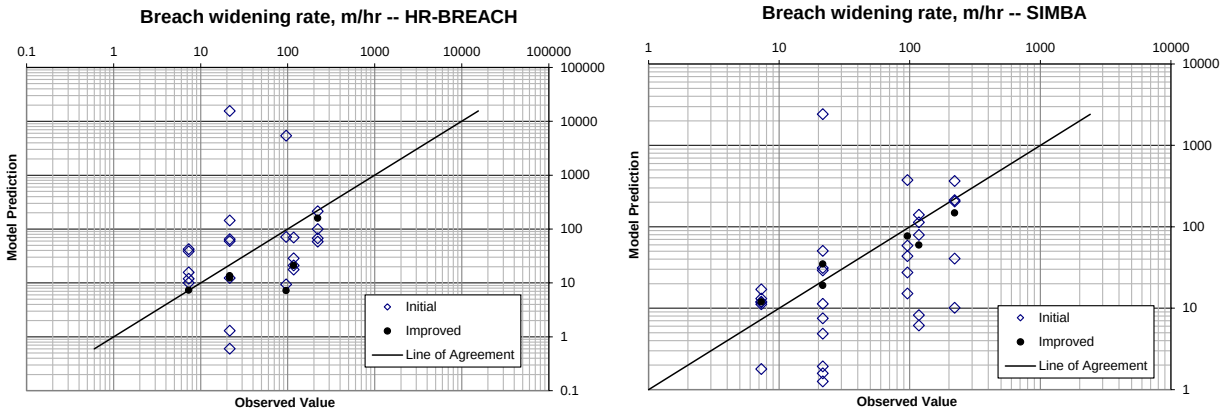

Figure 47.—Model-predicted breach widening rates versus observed values.

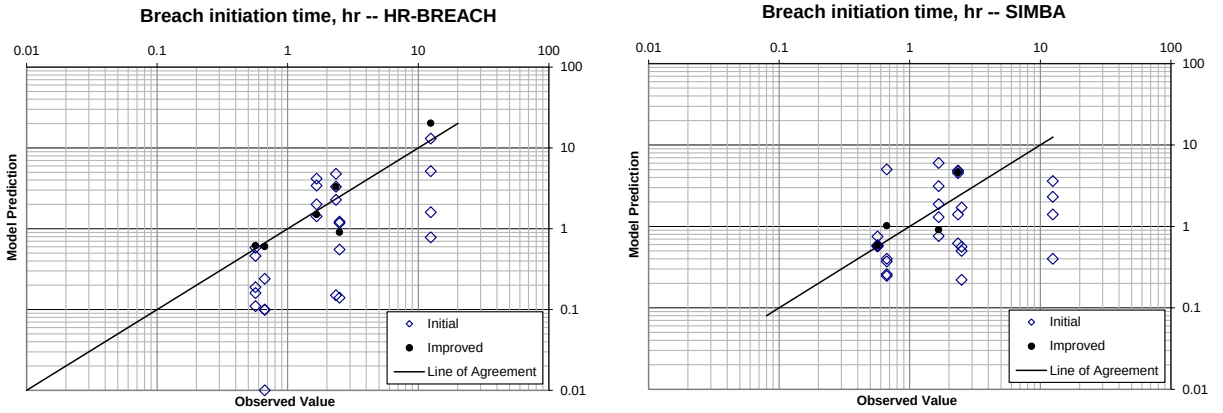

Figure 48.—Model-predicted breach initiation times versus observed values.

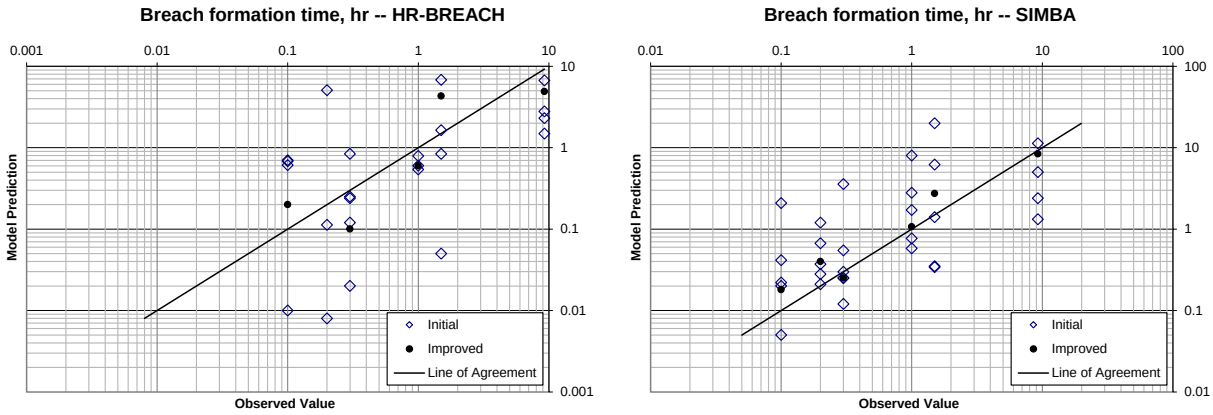

Figure 49.—Model-predicted breach formation times versus observed values.

Table 2.—Observed values of parameters describing the breaches of the dam failure test cases.

Parameter	units	USDA-1	USDA-2	Norway 1-02 (clay)	Norway 2C-02 (gravel)	Norway 1B-03 (zoned)	Oros	Banqiao
breach initiation time, t_i	hr	0.57		1.7	0.67	2.4	12.5	2.5
Breach formation time (t_f-t_i)	hr	0.30		1.0	0.10	0.20	9.25	1.5
Breach widening rate	m/hr	7.3		21.6	117.6	96	21.6	221
Peak outflow	m^3/s	6.5	0.96	390	74	242	58000[a]	78000[b]
Final breach width	m	6.9		21.2	11.7	20.1	200	332

[a]Smoothed estimate of peak outflow was 12,400 m^3/s
[b]Smoothed estimate of peak outflow was 72,000 m^3/s

The ability of both models to consistently predict the peak breach outflow is good in the initial model runs and very good in the improved model runs. This is probably partly due to the fact that matching the peak outflow was a focal point for most of the modelers as they attempted to improve the performance of the models.

Predictions of final breach width by the models were reasonably good also, with SIMBA performing somewhat better, especially in the improved runs. This may be due to the fact that HR BREACH was intentionally run primarily with the surface erosion modeling capabilities, since its headcut erosion module was deemed to have capabilities similar to the headcut erosion model in SIMBA. Similarly, SIMBA was limited only to its deterministic stress-based headcut model; the energy-based model that was disabled for this evaluation may have performed better for some of the cases (that model is included in the WinDAM B model that has since been developed and released by USDA for public use).

Predictions of parameters related to time (breach widening rate, breach initiation time and breach formation time) were less accurate for both models, especially in the initial model runs. The improved model runs exhibited significant improvement, and the errors between predicted and observed values were generally one half order of magnitude or less. Although large, this is better than the prediction errors typically associated with breach formation times resulting from regression equations, which are commonly up to ±1 order of magnitude (Wahl 2004). Prediction errors in the initial runs were comparable to those obtained with regression equations.

Improved model runs provided an opportunity for model users to improve model performance by adjusting input data, such as soil erodibility parameters. For the two USDA model tests, there was not much need for making such adjustments, since jet erosion testing performed during USDA's research programs provided very accurate estimates of soil erodibility characteristics. For the other case studies (the three Norwegian tests and the two real dam failures), information available to the modelers for their initial runs was much less certain, and probably comparable to that which might be available when applying a breach model to a dam for which there has not been any extensive effort to actually measure soil erodibility characteristics. In this respect, the difference between improved model results and initial model results for these cases is probably a good indicator of the potential value that could be obtained from pre-modeling investigations of soil erodibility that utilize physical test methods such as the submerged jet erosion test. Clearly, accurate estimates of soil erodibility are crucial for effective modeling of dam breach events, and although a variety of means exist for estimating erodibility parameters based on general soil properties, knowledge of the construction history of a specific embankment, and engineering judgment, the modelers involved in this study hold the consensus opinion that when soil erodibility characteristics are in doubt, the best approach is always to measure it.

Qualitative

A qualitative assessment of model performance is presented in Table 3 below (Morris et al. 2012). This summarizes the characteristics of the models and highlights their relative strengths.

The model evaluation results showed that the SIMBA and HR BREACH models both performed well on 5 of the 7 test cases. The Banqiao Dam case was poorly modelled by all of the programs, and the quality of the input and observed data are questionable for this case. The evaluators were unable to successfully run the FIREBIRD breach model on most of the test cases. Compared to the other two models, this model has received substantially less organizational support for continued development since it was first created. Although detailed results from running the NWS-BREACH model were not presented in this report, the evaluators typically found it difficult with that model to produce realistic results using reasonable material property inputs.

Headcut erosion was a dominant feature of many of the case studies. The SIMBA model with its deterministic approach to headcut simulation (Hanson et al. 2001) performed very well and exhibited appropriate sensitivity to soil parameters. Only the surface erosion options in HR BREACH were used for these evaluation runs, since HR BREACH's headcut migration model (developed by Temple et al. 2005) is similar to the SIMBA/WinDAM headcut models. In two of the Norway test cases that included non-cohesive materials, surface erosion was a significant process observed during the tests. Here, the HR BREACH model performed very well. SIMBA was also able to do a good job on these cases, but required some user judgment regarding how to model the non-cohesive materials.

Table 3.—Breach model characteristics.

	HR BREACH	SIMBA / WinDAM	FIREBIRD	NWS-BREACH
Erosion Process Models	Good	Good	Fair	Limited
Surface protection	Vegetation (CIRIA) and riprap	Vegetation, riprap in WinDAM	Limited	Yes
Headcut erosion	Good	Best	No	No
Stress-based	—	Yes	—	—
Energy-based	Yes	Yes (in WinDAM)	—	—
Surface erosion	Yes	No	Yes	Yes
Mass-wasting / soil-wasting	Stress-based bank failures and arch failure	Bank failures implicit	Some	Some
Effects of Submergence	Yes	Yes (in WinDAM)	No	Yes
Piping progression	Yes	In development	Some	Yes
Data Input Guidance	Good	Good	Limited	Limited
Ease of Use	Good	Good	Difficult	Difficult
Computational Efficiency	Good	Good	Fair	Good
Documentation	Excellent	Excellent	Limited	Good
Organizational Support for Continued Development	Good	Good	Weak	None
Embankment Geometry Options	Simple Zoning	Homogeneous, (Zoned in future)	Simple Zoning	Primitive Zoning

The Oros case study test highlighted the importance of drowning effects on breach formation. The valley immediately downstream of the Oros Dam poses a tight constriction. In the HR BREACH model, inclusion of this constriction and the subsequent drowning of the breach during the formation process produced prediction results far closer to the observed data than without consideration of drowning effects. In the SIMBA model which did not provide a means to directly simulate a high tailwater condition, reducing the soil erosion rate coefficient produced similar results. In reality, the functional effect of high tailwater levels would be to reduce erosion rates, so the behavior of both models is realistic in this regard.

Sensitivity of the SIMBA and HR BREACH models to changes in soil erodibility parameters was judged to be appropriate and consistent with observed variations in breach development during the laboratory tests. Some model runs proved to be very sensitive to specific parameters when it affected the relative timing of the peak of the inflow hydrograph and the completion of the breach initiation phase. This is a real phenomenon which is often dramatic when trying to simulate a laboratory test, where the inflow hydrograph may vary significantly during the test.

It was clear from the detailed group discussions held when evaluating the various model results against the different test cases, that modeler expertise and understanding of both the models and ways in which dams and levees might fail – and hence how they might apply the models – play a significant role in adopting the right approach and hence the accuracy of the modeling results. With this expertise, also comes an awareness of the sources and magnitude of uncertainty within the different case study data and modeling approaches, which is critical to understand when using modeling results for different end user purposes. The uncertainties in the test case data

made it difficult to specifically evaluate uncertainties in model performance. For this study, data were available with three different quality levels:

- USDA controlled tests – very high quality data with photo and video records of the events, good knowledge of inflow, outflow, and other boundary conditions, and good knowledge of soil properties, including direct measurement of erodibility parameters.
- IMPACT field tests – Controlled experiments with eyewitness measurement, photo and video records, and measured hydraulic parameters, but test control was poor at times, which produced uncertain boundary conditions for the tests. Embankment construction was not always well regulated and documented. Soil properties were known with some uncertainties which allowed estimation of erodibility parameters, but there was no direct measurement of erodibility characteristics.
- Case study data from real dam failures – Limited eyewitness knowledge of the events and considerable data uncertainty relating to all aspects of the cases, including inflow, outflow, reservoir levels, soil characteristics and erodibility, and embankment configuration at time of failure.

Conclusions, Recommendations, and Research Needs

This model evaluation has taken place at a time when practices for the modeling of embankment dam failure are changing rapidly. Models capable of routing dam-break magnitude floods have evolved from early one-dimensional tools (e.g., DAMBRK, FLDWAV) to more sophisticated products with two-dimensional modeling capability, GIS integration, sediment transport capabilities and more. Most of these modern models have included some form of integrated tool for simulating the development of the breach. Many provide capabilities similar to those of DAMBRK and FLDWAV which use breach parameters to relate breach dimensions and enlargement rates parametrically to time, without direct modeling of erosion processes; ultimate size of the breach and the time needed for development from zero size to final size are estimated using regression equations based on dam and reservoir properties. A few models have adopted older physically-based modeling methods to simulate breach development. For example, the commercial FLO-2D model uses an integrated breach model that was developed from the original NWS-BREACH model (O'Brien 2012).

The two models evaluated here represent modern attempts to develop breach modeling capability independently from flood routing capability, with laboratory testing and a fundamental understanding of erosion processes and embankment failure mechanics providing the basis for model development. These models were developed to be applied separately from a flood routing model to generate just the dam breach outflow, but it is also possible that they could be integrated into flood routing models in the future.

The process of evaluating these models has highlighted several things that should be kept in mind as development of physically-based dam breach models continues:

- The usability of models should not be overlooked. FIREBIRD suffered from usability issues and as a result could not be effectively tested in this evaluation.
- User expertise is critical for identifying key physical processes and correctly applying the models, since numerous modeling options and parameters are available.
- A fundamental modeling decision is whether to utilize headcut erosion or surface erosion modeling equations. Surface erosion would generally be appropriate for soils that behave in a noncohesive way and experience erosion continuously along the bed of a sloped channel, whereas headcut erosion is most appropriate when soils exhibit sufficient cohesion to create near-vertical headcuts with erosion localized to the base of the overfall. There is a general understanding that headcut erosion behavior will dominate cohesive soils and surface erosion will dominate decidedly noncohesive soils, but there is also a zone of uncertainty in which it can be difficult to know in advance which erosion mechanism will be most prominent. To address this issue,
    - Research should be undertaken to improve knowledge about this transition and to identify key soil parameters that will allow the dominance of different erosion mechanisms to be predicted in advance,
    - Breach models should incorporate both processes to allow flexibility to analyze a wide variety of embankments.
- Both SIMBA and HR BREACH performed well on many of the different test cases, indicating that there are conditions where both modeling approaches are of value.

Continued Development of Dam Breach Models

The bulk of the work performed to evaluate these dam breach models took place in 2009. The tested models have continued to evolve since that time and have led to the development and release of successor models. Flood routing tools commonly applied to dam-breach modeling problems have also continued to develop, and the scope of potential applications for dam breach models has widened beyond traditional embankment dams to also include levees and canals. The recent developments and opportunities for combining the capabilities of these models are discussed here.

SIMBA / WinDAM Family of Models

The SIMBA model was intended to serve a research function and provided an environment for testing a variety of algorithms and erosion models against data obtained from laboratory tests. The model included specific features of dam breach tests that are typically not relevant to real-world applications, and also omitted some practical capabilities that would be necessary in a model applied to real dam failures. The WinDAM model was the anticipated real-world model and it was developed and released in a phased manner (Visser et al. 2013).

The WinDAM A+ model was released by USDA in 2008, while this project to evaluate the SIMBA model was underway. WinDAM A+ permitted the analysis of vegetation or riprap

protective layers on the downstream face of a dam, but did not perform erosion analysis of the body of the embankment.

WinDAM B was released in 2011, with capabilities to analyze erosion and breach of earthen embankments. This model is the nearest equivalent to the SIMBA model that was evaluated for this project. It incorporates the stress-based headcut erosion model and also provides the option to use an older energy-based headcut erosion model. The model abandons the use of a specified pilot channel but can realistically simulate the increased unit discharge that occurs due to camber and local high and low spots on a dam crest. The model also allows the description of the tailwater channel and its rating curve for more realistic simulation of tailwater effects. The WinDAM B model continued to offer only level-pool reservoir routing, homogeneous cohesive embankment geometry, and overtopping flow to trigger dam failure. WinDAM B was a public-domain product.

WinDAM C version 1.1 was released in May 2016, and can be freely downloaded from http://go.usa.gov/cupCF. This version of the model adds the capability to simulate internal erosion failure of homogeneous cohesive embankments. Laboratory testing to support the development of WinDAM C was reported by Hanson et al. (2010a). Algorithms for WinDAM C have been tested and developed in IE-SIMBA (IE = internal erosion), following a similar development path as that involving SIMBA and WinDAM B.

Further USDA development plans include:

- WinDAM D
  - Potential to initiate failure at the embankment toe, stability berms, or in groin areas (zones of flow and stress concentration during overtopping)
  - Alternative slope protection materials (concrete blocks or reinforced vegetation)
- WinDAM E
  - Embankment overtopping erosion prediction and breach modeling for zoned embankments

Planning for lab work to study physical processes related to the WinDAM D features was started in Oklahoma during the summer of 2015.

HR BREACH Family of Models

At the time of the model evaluation runs in 2009, the HR BREACH model was a more complex model than SIMBA in several ways:

- It allowed the internal erosion failure mode
- It allowed modeling of zoned embankments, with limited geometric options
- It allowed the choice of surface erosion or energy-based headcut erosion models, versus SIMBA's stress-based and energy-based headcut erosion models.
- The model simulates flow and erosion at multiple cross sections down the full length of the flow path, whereas SIMBA and WinDAM simulate flow at the critical-depth flow section and at positions of tracked headcuts.

These differences combine to make HR BREACH a somewhat slower model to execute (although run times are still just a matter of seconds to a few minutes on modern computer hardware). They also make HR BREACH more complex to configure and operate, since there are many modeling options and parameters. For this reason, a new model named AREBA (A Rapid Embankment Breach Assessment) was developed to enable rapid modeling of breach in homogeneous embankments. Computationally the model is much faster (avg. 0.2 sec run-time) since it no longer performs computations at multiple cross sections, but it does retain HR BREACH's flexibility to model internal erosion, or overtopping with either headcut or surface erosion modes. Development of AREBA was funded by the Flood Risk Management Research Consortium (FRMRC), a UK-based group of universities and other organizations pursuing flood-related research. The model is available at this time only to those who funded its development.

Development work on HR BREACH has also continued, and the model has been given a new name, EMBREA. New functionality has been developed to improve the modeling of zoned dams with more options to define a variety of layering and zoning schemes. Some of the new options are especially relevant to typical levee construction practices. The new capabilities can produce very different (but real) results, affecting not only the peak discharge but also the shape and timing of the flood hydrograph (Morris 2011).

Toward Development of a Combined Breach Model

The capabilities of both the WinDAM B/C family of models and the HR BREACH family of models are complementary in many ways, and it seems feasible to develop a single model that could provide a complete selection of modeling alternatives for embankment dams. Both models provide similar capabilities for modeling the erosion of surface protection layers, such as riprap or vegetation. The HR BREACH model provides a means for defining a zoned embankment structure and managing the modeling of different modes of erosion within the zones. For overtopping flow the WinDAM model contains both stress- and energy-based headcut erosion models, and HR BREACH offers surface erosion models. For cases of internal erosion, the capabilities of both models could probably be combined, although the details of each model's approaches were not investigated in this study, so they could be quite different. Finally, HR BREACH contains routines that simulate mass-wasting processes deterministically, while WinDAM implies mass-wasting in the functionality of its headcut erosion routines. These different modeling approaches would need to be reconciled to combine the models.

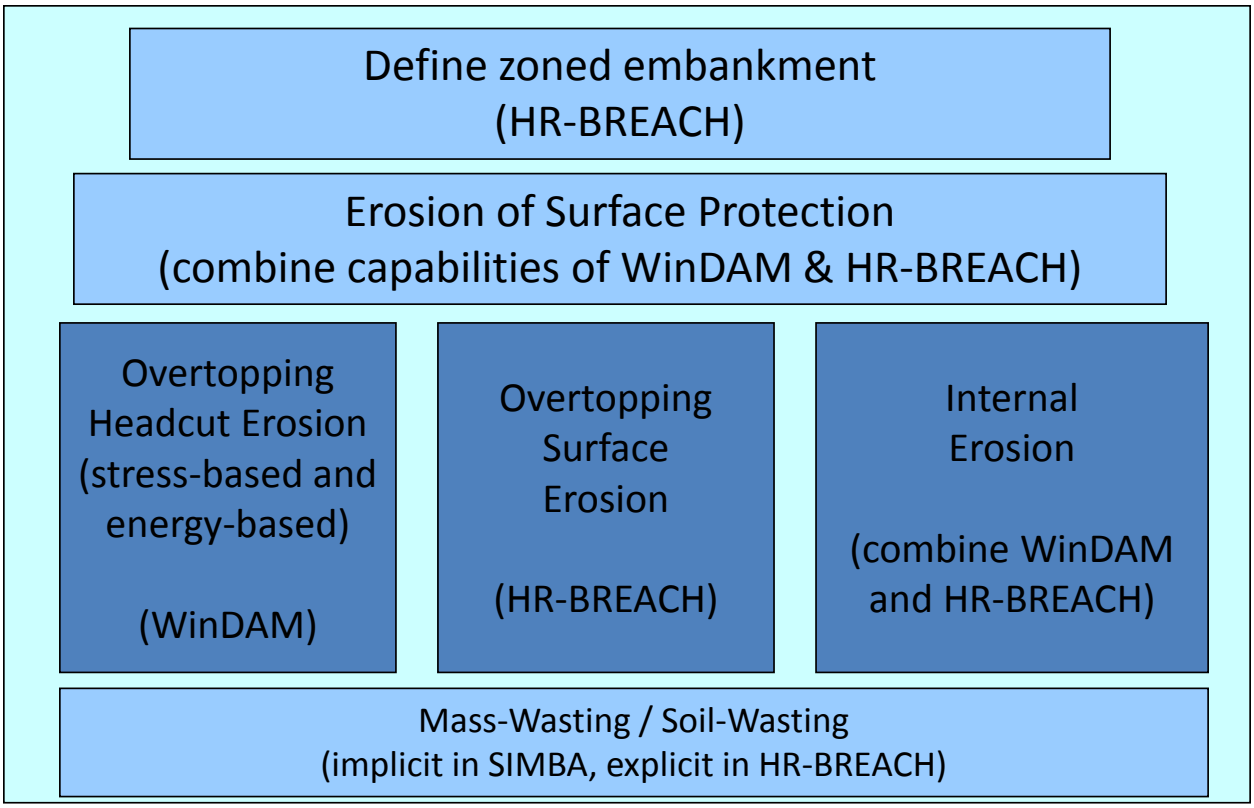

Figure 50.—Conceptual arrangement for a combined breach model.

Both of these models or a combined model are developed to the point that they can be applied as stand-alone products and have a level of organizational support that can provide for maintenance and continued development. It may also prove advantageous from a user standpoint to consider integrating either of these models or a combined model with dedicated flood routing products that have traditionally represented breach development using breach parameters.

References

Brown, C. A., and W. J. Graham, 1988. Assessing the threat to life from dam failure. *Water Resources Bulletin*, vol. 24, no. 6, December, 1988.

Brown, Richard J., and David C. Rogers, 1981, *Users Manual for Program BRDAM*, U.S. Bureau of Reclamation, Denver, Colorado, April 1981, 73 p.

Buchholzer, Y., 2007. *TFE Report: Wave overtopping and breaching models.* Lyon, France: École Centrale de Lyon.

Chang, H. H., 1998. Riprap stability on steep slopes. *International Journal of Sediment Research*, 13(2):40-49.

Chen, Y. H., and Anderson B. A., 1986, "Development of a Methodology for Estimating Embankment Damage Due to Flood overtopping", US Federal Highway Administration Report No. FHWA/RD-86/126, Simons Li & Associates, Fort Collins, Colorado, USA.

Chen, Y.H. and G.K. Cotton, 1988. *Design of Roadside Channels with Flexible Linings*. Hydraulic Engineering Circular No. 15, Second Edition, FHWA-IP-87-7, April 1988, contract number DTFH61-84-C-00055.

Cheng, N.-S., 2002. Exponential formula for bedload transport. Journal of Hydraulic Engineering, 128(10):942-946.

Chow, Ven Te, 1959. *Open-Channel Hydraulics.* McGraw-Hill Book Company.

Courivaud, Jean-Robert, 2007. Analysis of the dam breaching database. CEA Technologies Inc., Dam Safety Interest Group, CEATI Report No. T032700-0207B, 79 pp.

Fread, D.L., 1977, "The Development and Testing of a Dam-Break Flood Forecasting Model," in *Proceedings of the Dam-Break Flood Routing Model Workshop*, Bethesda, Maryland, p. 164-197.

Fread, D.L., 1984, *DAMBRK: The NWS Dam-Break Flood Forecasting Model*, National Weather Service, Office of Hydrology, Silver Spring, Maryland.

Fread, D.L., 1988 (revised 1991), *BREACH: An Erosion Model for Earthen Dam Failures*, National Weather Service, National Oceanic and Atmospheric Administration, Silver Spring, Maryland.

Graham, Wayne J., 1999. *A procedure for estimating loss of life due to dam failure.* Bureau of Reclamation Dam Safety Report DSO-99-06.

Hanson, G. J., K. M. Robinson, and K. R. Cook. 2001. Prediction of headcut migration using a deterministic approach. *Transactions of the ASAE*, 44(3):525-531.

Hanson, G. J., K.R. Cook, and S.L. Britton, 2003. "Evaluating Erosion Widening and Headcut Migration Rates for Embankment Overtopping Tests". American Society of Agricultural Engineers, Meeting Paper No. 032067, ASAE International Meeting, Las Vegas, NV.

Hanson, G.J., and K.R. Cook. 2004. "Apparatus, test procedures, and analytical methods to measure soil erodibility *in situ*." *Applied Engineering in Agriculture*, Vol. 20, No. 4, p. 455-462.

Hanson, G. J., D. M. Temple, M. Morris, M. Hassan, and K. Cook. 2005a. Simplified breach analysis model for homogeneous embankments: Part II, Parameter inputs and variable scale model comparisons. Proceedings of 2005 U.S. Society on Dams Annual Meeting and Conference, Salt Lake City, Utah. p. 163-174.

Hanson, G.J., Cook, K.R., and Hunt, S.L., 2005b. Physical modeling of overtopping erosion and breach formation of cohesive embankments. *Transactions of the ASAE*, 48(5): 1783−1794.

Hanson, G. J., and S. L. Hunt, 2007. Lessons learned using laboratory jet method to measure soil erodibility of compacted soils. *Applied Engineering in Agriculture*, 23(3):305-312.

Hanson, G.J., Tejral, R.D., Hunt, S.L., Temple, D.M., 2010a. Internal erosion and impact of erosion resistance. Proceedings of the United States Society on Dams, 30th Annual Conference, Sacramento, CA April 12-16, 2010.

Hanson, Gregory J., Wahl, Tony L. , Temple, Darrel M., Hunt, Sherry L., and Tejral, Ronald D., 2010b. Erodibility characteristics of embankment materials. In: *Dam Safety 2010* . Proceedings of the Association of State Dam Safety Officials Annual Conference, September 19-23, 2010, Seattle, WA. (CDROM).

Hanson, G.J., Temple, D.M., Hunt, S.L., and Tejral R.D., 2011. Development and characterization of soil material parameters for embankment breach. *Applied Engineering in Agriculture*, 27(4):587-595.

Hassan, Mohamed, and Morris, M.W., 2008. IMPACT Project Field Tests Data Analysis. FLOODsite Report No. T04-08-04, Revision 3_2_P01.

Harris, G.W., and D. A. Wagner, 1967, *Outflow from Breached Earth Dams*, University of Utah, Salt Lake City, Utah.

Hewlett, H. W. M., Boorman, L. A., Bramley, M. E. & Whitehead, E., 1985. *Reinforcement of steep grassed waterways.* CIRIA Technical Note 120. London, UK: CIRIA.

Hewlett, H.W.M., Boorman, L.A., and Bramley, M.E., 1987. *Design of reinforced grass waterways*. CIRIA Report 116, Construction Industry Research and Information Association, London, 116 pp.

Hughes, A. J., 1981. The erosion resistance of compacted clay fill in relation to embankment overtopping. Ph.D., University of Newcastle Upon Tyne.

Hunt, S.L., Hanson, G.J., Cook, K.R., and Kadavy, K.C., 2005. Breach widening observations from earthen embankment tests. *Transactions of the ASAE*, 48(3):1115-1120.

Kahawita, René, 2007. Dam breach modeling – a literature review of numerical models. CEA Technologies Inc., Dam Safety Interest Group, CEATI Report No. T032700-0207C, 68 pp.

Lane, E. W., 1955, Design of stable channels. Transactions of the ASCE, V. 120, p. 1234-1279.

Lou, W.C., 1981, *Mathematical Modeling of Earth Dam Breaches*, Thesis, presented to Colorado State University, at Fort Collins, Colorado, in partial fulfillment of the requirements for the degree of Doctor of Philosophy.

Mohamed, M. A. A., P.G. Samuels, and M.W. Morris, 2001. Uncertainties in Dam Failure Modelling with the US NWS BREACH Model. *In:* First International Conference on River Basin Management, 2001. Cardiff, UK. WIT Press.

Mohamed, M.A.A., 2002. Embankment breach formation and modelling methods. Ph. D. thesis. Open University, UK.

Mohamed, M.A.A., Samuels, P.G., Morris, M.W. and Ghataora, G.S. 2002. Improving the accuracy of prediction of breach formation through embankment dams and flood embankments. Proc. of the Int. Conf. On Fluvial Hydraulics, Louvain-la-Neuve, Belgium, 3-6 Sept. 2002 - River Flow 2002, Bousmar & Zech (editors).

Morris, M. W., 2000. CADAM: A European Concerted Action Project on Dambreak Modelling. *In:* British Dam Society 11th Biennial Conference: Dams 2000, 14-17 June, 2000. Bath, UK. Thomas Telford Ltd.

Morris, M.W., 2011. Breaching of earth embankments and dams. Ph.D. thesis, The Open University, UK.

O'Brien, J.S., 2012. Dam breach mechanism, breach growth and the effect on downstream flooding. ASDSO 2012 Annual Conference, Sept. 16-21, 2012, Denver, Colorado.

Ponce, Victor M., and Andrew J. Tsivoglou, 1981, "Modeling Gradual Dam Breaches," *Journal of the Hydraulics Division, Proceedings of the ASCE*, vol. 107, no. 7, p. 829-838.

Ritchey, J. C., 2001. Embankment dam failure analysis: State assessment criteria, issues and experience - Northeastern United States. *In:* Dam failure analysis research and development topics, 26-28th June, 2001. Oklahoma City, Oklahoma, USA. USDA, pp. 7.

Ritter, A., 1892. Die fortpflanzung der wasserwellen (Propagation of waves), *Zeitschrift des Vereines deutscher Ingenieure*, Vol. 36, No. 33, p. 947-954, Aug. 13, 1892.

Robinson, K. M. 1992. Predicting stress and pressure at an overfall. *Transactions of the ASAE*, 35(2):561-569.

Shuibo, P., Mingsen, Q., Lianxiang, W., Guoyi, X., Yongqiang, S., Longda, X., Cuiyu, M., Loukola, E., Pyyny, J., Reiter, P., Rytkonen, T. & Alanko, M., 1993. *Chinese-Finnish cooperative research work on dam break hydrodynamics. Part I: Investigation report on dam safety research in China.* Helsinki, Finland: National Board of Waters and the Environment.

Singh, V. P. 1996. *Dam Breach Modeling Technology*. Kluwer Academic Publishers. Dordrecht, The Netherlands. 241 p.

Singh, V. P., and P. D. Scarlatos, 1985, *Breach Erosion of Earthfill Dams and Flood Routing: BEED Model*, Research Report, Army Research Office, Battelle, Research Triangle Park, North Carolina, 131 p.

Smart, Graeme M. 1984. Sediment transport formula for steep channels. *Journal of Hydraulic Engineering*, vol. 110, no. 3, March 1984, p. 267-276.

Tejral, Ronald D., Gregory J. Hanson, and Darrel M. Temple. 2009. Comparison of two process based earthen dam failure computation models. In *Dam Safety '09*, Annual Meeting of the Association of State Dam Safety Officials (ASDSO), Sept. 27-Oct. 1, 2009, Hollywood, FL.

Temple, D.M., K.M. Robinson, R.M. Ahring, and A.G. Davis. 1987. *Stability design of grass-lined open channels*. USDA Agriculture Handbook No. 667.

Temple, D. M., G. J. Hanson, M. L. Neilsen, and K. R. Cook. 2005. Simplified breach analysis model for homogeneous embankments: Part I, Background and model components. Proceedings of the 2005 U.S. Society on Dams Annual Meeting and Conference, Salt Lake City, Utah. p. 151-161.

Temple, D.M., Hanson, G.J., Neilsen, M.L. 2006. WINDAM-Analysis of overtopped earth embankment dams. In: ASABE Annual International Meeting, July 9-12, 2006, Portland, Oregon. Paper No. 06-2105. 2006 CDROM.

USDA, NRCS, 1997. *Earth Spillway Erosion Model*. National Engineering Handbook, Part 628 Dams, Chapter 51. United States Department of Agriculture, Natural Resources Conservation Service.

Villemonte, J.R. 1947. Submerged weir discharge studies. *Engineering News Record*. p. 866-869.

Visser, K., G. Hanson, D. Temple, R. Tejral, and M. Neilsen, 2013. Earthen embankment overtopping analysis using the WinDAM B software. National Dam Safety Program Technical Seminar No. 20, Overtopping of Dams, February 20-21, 2013 FEMA National Emergency Training Center, Emmitsburg, MD.

Visser, P. J., 1995. Application of sediment transport formulae to sand-dike breach erosion. Communication on Hydraulic and Geo-technical Engineering, TU Delft, Report no. 94-7.

Visser, P. J., 1998a. *Breach growth in sand dikes.* Ph. D., Delft University of Technology.

Visser, P. J., 1998b. *Breach Growth in Sand-Dikes (Communication on Hydraulic and Geotechnical Engineering).* TU Delft, Report No. 98-1. Delft, The Netherlands.

Yang, C. T., 1979. Unit stream power equation for total load. *Journal of Hydrology*, vol. 40, p. 123-138.

Wahl, Tony L., 1998. Prediction of embankment dam breach parameters: A literature review and needs assessment. Dam Safety Research Report DSO-98-004, U.S. Dept. of the Interior, Bureau of Reclamation, Denver, Colorado, July 1998.

Wahl, Tony L., 2004. Uncertainty of predictions of embankment dam breach parameters. *Journal of Hydraulic Engineering*, Vol. 130, No. 5, p. 389-397.

Wahl, Tony L., 2007. Laboratory investigations of embankment dam erosion and breach processes", CEA Technologies Inc., Dam Safety Interest Group, CEATI Report No. T032700-0207A, 60 pp.

Wahl, Tony L., Regazzoni, Pierre-Louis, and Erdogan, Zeynep, 2008. Determining erosion indices of cohesive soils with the Hole Erosion Test and Jet Erosion Test. Dam Safety Technology Development Report DSO-08-05, U.S. Dept. of the Interior, Bureau of Reclamation, Denver, Colorado, 45 pp.

Wahl, Tony L., 2010. Dam breach modeling – an overview of analysis methods. Joint Federal Interagency Conference on Sedimentation and Hydrologic Modeling, Las Vegas, NV, June 27-July 1, 2010.

Wang, P. and Kahawita, R., 2002. Modeling the hydraulics and erosion process in breach formation due to overtopping. Proceedings of the Symposium held in Monte Verita, Switzerland. Sedimentation and Sediment Transport. Edited by A. Gyr and W. Kinzelbach. September 2002.

Wang, P., Kahawita, R., Mokhtari, A., Phat, T.M. and Quach, T.T., 2006. Modeling breach formation in embankments due to overtopping. ICOLD Conference, Barcelona, Spain, June 2006.

Weisstein, E. W., 2011. *Greens Theorem*. URL: http://mathworld.wolfram.com/GreensTheorem.html [March 2011].

Wilson, K.C., 1987. Analysis of bed-load motion at high shear stress. *Journal of Hydraulic Engineering*, 113(1):97-103.

Wurbs, R. A., 1987. Dam-breach flood wave models. *Journal of Hydraulic Engineering*, 113(1):29-46.

Zhu, Y. H., 2006. *Breach growth in clay dikes.* Ph.D., Delft University of Technology.

APPENDIX A - Detailed Descriptions of Model Physics (2009)

These descriptions of the evaluated models are provided to document the algorithms utilized in the models at the time of the evaluation runs.

HR BREACH

The original HR BREACH model was developed by Mohamed in conjunction with research at HR Wallingford (Mohamed, 2002, Mohamed et al., 2002). Mohamed supported earlier research findings that breach simulation and breach parameter estimation were the greatest source of uncertainty in dambreak flood forecasting (Morris, 2000, Singh, 1996, Wurbs, 1987) and that tools available to predict breach were not very accurate (Mohamed et al., 2001). Having reviewed existing models, the approach taken was to develop a new model rather than modify an existing model. This allowed the simulation of key physical processes to be integrated within the model.

The model integrates hydraulics, soil mechanics and structural failure processes to a broadly consistent degree of complexity. The model undertakes analysis on a section by section basis through the model (Figure A1-1) and, unlike other models such as BRES (Visser, 1998a, Zhu, 2006) or SIMBA (Hanson et al., 2005a, Temple et al., 2005), does not predefine the breaching process in terms of stages and geometry. The 'penalty' for this more detailed approach to analysis is that the model takes a few minutes to run rather than seconds. The model does require the hours of days of computer run time that might be needed by truly three-dimensional computational models.

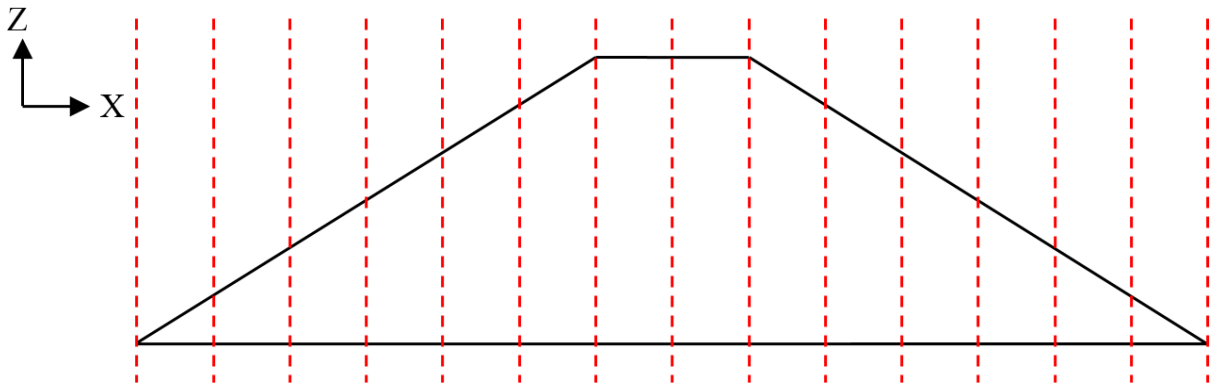

Figure A1-1.—Modeling embankment breach by division of embankment into sections.

Figure A1-2 provides a flow chart showing the order in which the hydraulic, soil and structural processes are analyzed. Each of these stages are considered in more detail below.

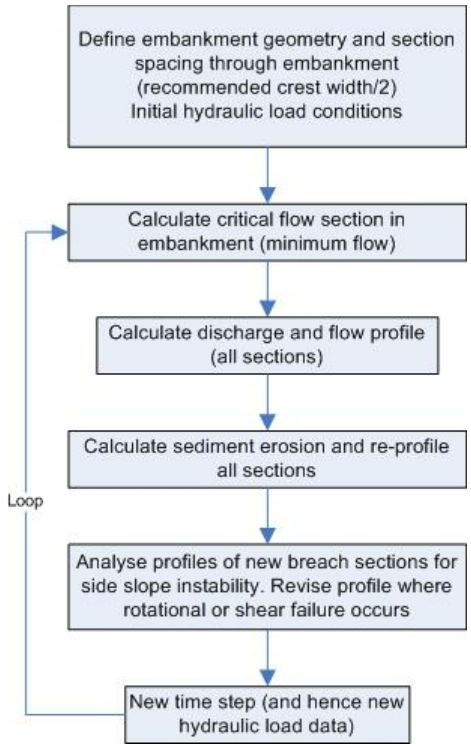

Figure A1-2.—HR BREACH model processes.

Geometry and Section Spacing

The breach model works by initially requiring the user to define a notch (breach initiation notch) through the embankment crest (and along the downstream face), through which the initial overtopping flow runs. This provides a focus for the flow and allows calculation of flow and erosion conditions at each cross section, leading to prediction of progressive erosion, breach growth and subsequent catastrophic failure of the embankment or dam.

Hence, the embankment profile used for flow calculation (Figure A1-3) has a slightly different profile to the outer profile used to define the embankment shape in general (Figure A1-1). The flow profile is defined by points A, B`, C`, D` rather than A,B,C,D. Since the initiation notch is not present in the upstream face, and the notch depth is parallel to both the crest and the downstream face, the modified profile results in different offsets for points B → B` and C → C`, hence a small change in crest width.

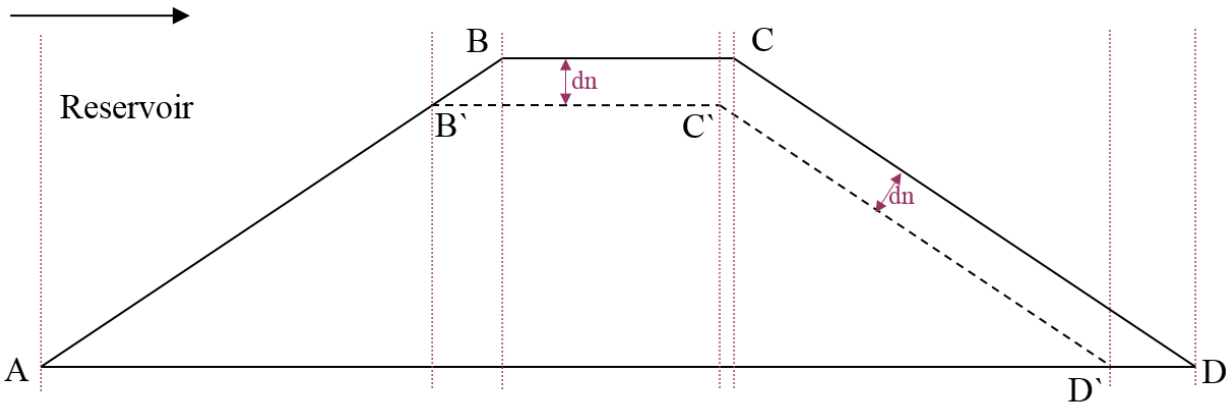

Figure A1-3.—Embankment profile showing breach initiation notch.

When running the model, the user is asked to define the section spacing (dx). User dx is typically defined as half the crest width, hence (B-C)/2. In order to identify specific section locations for modeling that also coincide with the key geometry points A, B`, C`, D` the following rules are applied:

1. User defines 'User dx';
2. Calculate the number of sections between A – B` (i.e. [(A-B`) / User dx]). Round up to the nearest whole number. This defines 'Model dx' for the upstream slope.
3. Repeat process for crest, B`-C` - this defines 'Model dx' for the crest;
4. Repeat process for downstream slope, D`-C` - this defines 'Model dx' for the downstream slope;
5. Compare the three 'Model dx' values and select the smallest (Min dx). (This normally equates to the crest Model dx since this is typically the smaller length subdivided into dx.);
6. Calculate specific section locations across the entire embankment working from:
    a. Upstream crest (B`)→ upstream toe (A);
    b. Downstream crest (C`) → upstream crest (B`);
    c. Downstream toe (D`) → downstream crest (C`);

Where spacing does not allow an exact fit of sections using Min dx, the last three spaces are divided into two sections (i.e. two sections with spacing > Min dx, rather than two sections of dx plus one undefined remainder).

Critical Flow Section

The model assumes that flow through the breach transforms from sub to supercritical flow as it passes across the embankment crest section; this may be the original crest or an eroded profile that is controlling the breach flow. The flow profile is obtained by calculating the surface profile up and downstream from this critical section.

There are five different methods provided within the HR BREACH model to locate the critical flow section. Correct identification of this section is important within the model because once identified, the flow profile is calculated upstream (sub critical) and downstream (super critical)

from this section. The section flow conditions define shear stress and hence soil erosion at each section. The five approaches comprise:

1. Up and downstream slopes;
2. Up to downstream slope;
3. Upstream edge of downstream face;
4. Maximum energy;
5. Minimum flow.

Up and downstream slopes

This method considers how the eroding embankment slope changes between sections, with the goal of identifying the crest, either side from which the sections slope downwards. For each section, the critical slope is calculated using the Manning's equation. Slopes between this and adjacent sections are then calculated and compared to determine whether the flow might transition from a subcritical to supercritical state at that particular section (Figure A1-4).

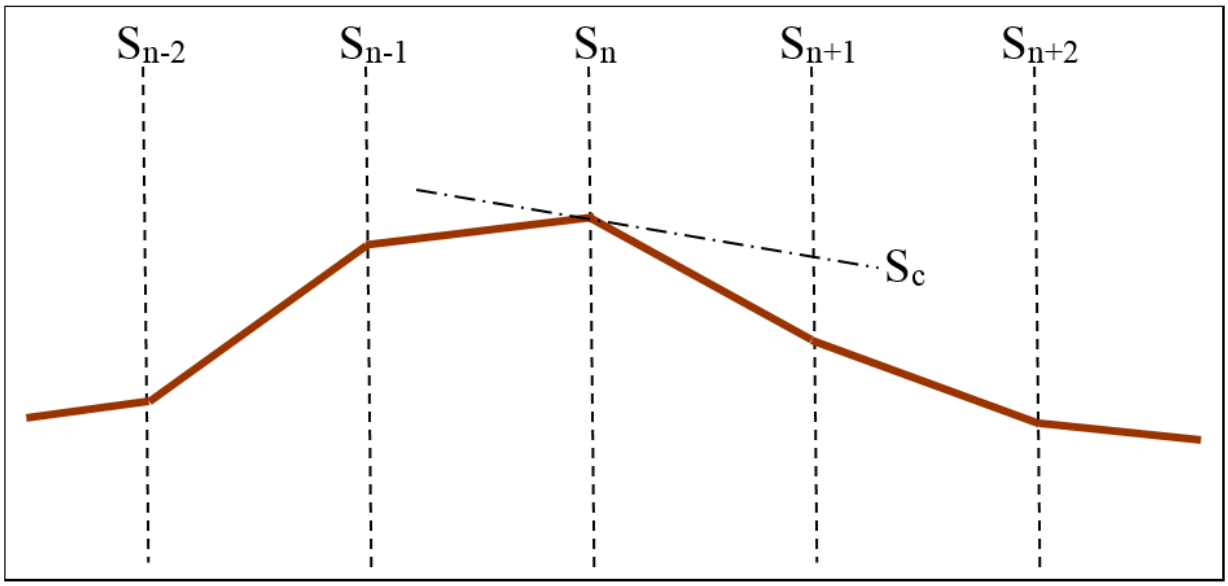

Figure A1-4.—Critical section - up and downstream slope method.

Up to downstream slope

This method calculates the average slope between upstream and downstream sections and then compares this slope to the critical slope for the section S_n. If the average slope exceeds the critical slope, then it is assumed that section S_n is the approximate location of the critical flow section.

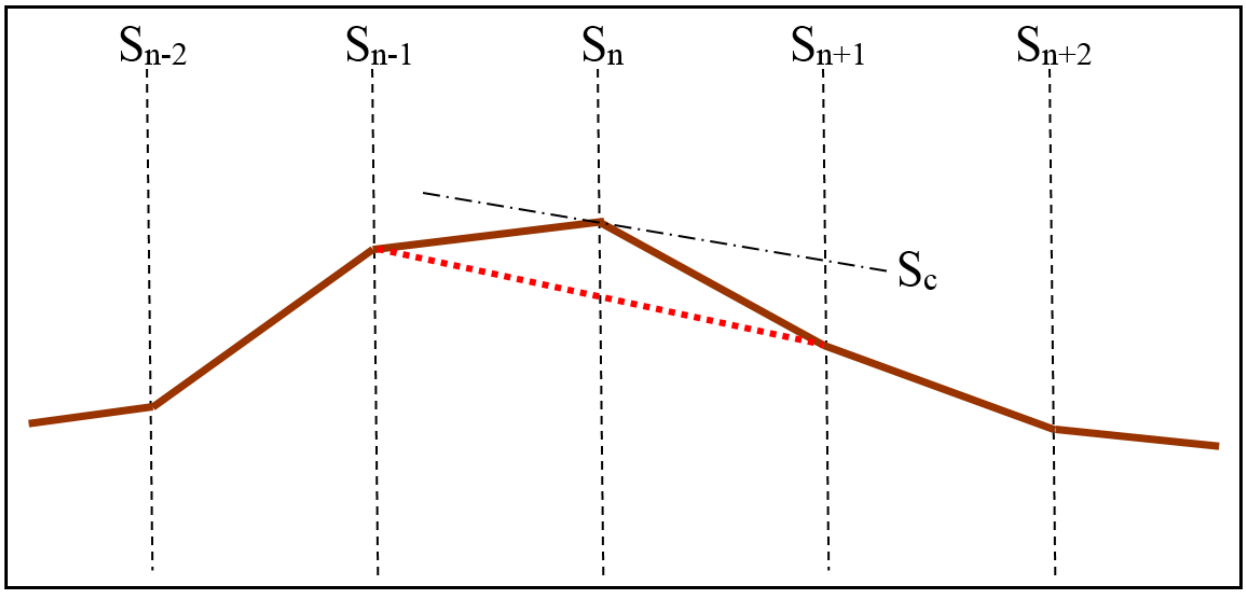

Figure A1-5.—Critical section - up to downstream slope method.

Upstream edge of downstream face

This simple approach looks at the downstream slope of each section and the section bed level in order to identify the upstream edge of the downstream face. This analysis starts from the downstream toe and works upstream until a suitable section is identified. Since this method will be 'trapped' into a false answer if a dip in section bed levels is found, this method should only be used if the other approaches fail.

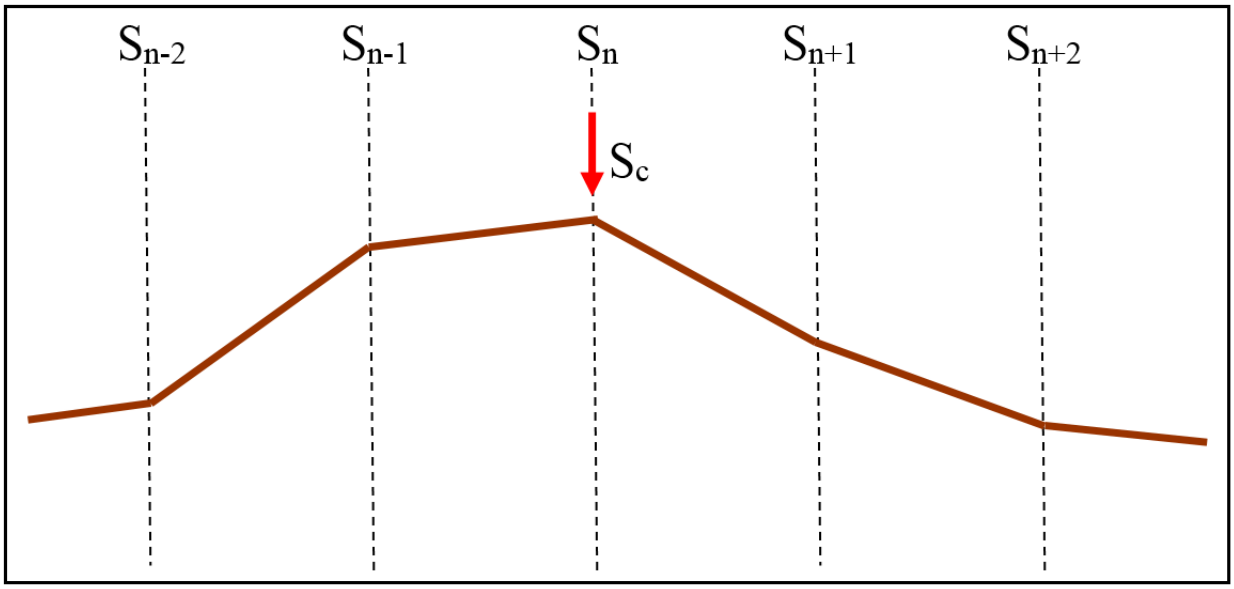

Figure A1-6.—Critical section – upstream edge of downstream face method.

Maximum energy

This method assumes that the critical section can be defined as the section with the maximum energy in the system. Therefore, the critical energy is calculated for all sections, based on the Bernoulli equation, and the section with the maximum energy is assumed to be the critical section.

Minimum flow

This method assumes that the critical section can be defined as the section with the minimum flow in the system. By definition, this is the section that would regulate flow through the breach. A potential head of water is calculated for each section by comparing the water level in the reservoir and the lowest elevation point of each breach cross section. The water head (h) is calculated for each section through the embankment and the weir formula is used to calculate the potential flow at each section using the section average width (h). The section that gives the minimum flow value is assumed to be the critical section. This method is the preferred approach for calculating the critical flow section within the breach model.

Discharge and Flow Profile

Breach models typically use one of the following approaches to calculate flow conditions through the breach (Table 2-5)

- 1D or 2D Saint Venant equations;
- The steady uniform flow equation;
- The steady non-uniform flow equation.

HR BREACH uses a weir flow equation (Eq A1-1) to calculate discharge at the critical flow section and a form of the non-uniform flow equation (Chow 1959) (Eq A1-2) to map the flow profile:

$$Q_b = C_d B_b H_b^{3/2} \qquad \textbf{(A1-1)}$$

where: Q_b Flow through breach m^3/s
C_d Discharge coefficient -
B_b Section averaged breach width m
H_b Total head over the breach m

$$Y_1 + \frac{U_1^2}{2g} = Y_2 + \frac{U_2^2}{2g} + S_f \Delta x \qquad \textbf{(A1-2)}$$

where: Y_1 : Water level at an upstream section
Y_2 : Water level at a downstream section
U_1 : Mean flow velocity at an upstream section
U_2 : Mean flow velocity at a downstream section
g : Acceleration due to gravity
Δx : Distance between the two sections
S_f : The friction slope that can be represented by the Manning's equation:

$$S_f = \frac{U_m^2 n^2}{R_m^{4/3}} \quad \text{(A1-3)}$$

where: U_m : Average mean velocity = $(U_1+U_2)/2$
R_m : Average hydraulic radius = $(R_1+R_2)/2$
n : Manning's roughness coefficient

The equations are solved iteratively with the computations proceeding in the upstream direction for the sub-critical flow zone and in the downstream direction for the supercritical flow zone.

Sediment Erosion and Section Profile

The model predicts erosion of the breach section by calculating the shear stress distribution around the flow section and then calculating sediment removal based upon a user selected sediment transport or erosion equation. This process leads to undercutting of the breach sides, as observed in many of the IMPACT project field tests (Section 2.4). Figure A1-7 shows how the process is replicated within the model. At an initial time step the section and water level is defined by seven points. During each time step the model calculates a new breach section profile, and subsequently a new water level at the start of the next time step. Each loop potentially adds two more points to the definition of the breach geometry. This is not sustainable for a model which will run many hundreds or thousands of time steps, hence when a section is defined by 9 points this is reduced back to 7 points (Figure A1-8).

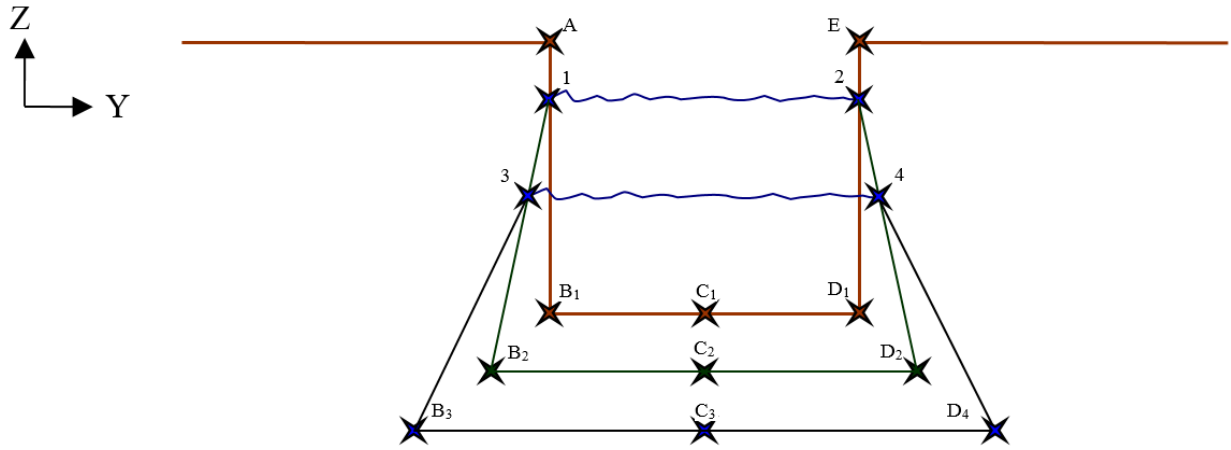

Figure A1-7.—Existing modeling process for calculating growth of breach section.

The initial breach section is shown by the profile A-B_1-C_1-D_1-E. The water level within this section is defined by the line 1-2. Note that point C_1 is specified as a low point in the section, and is established 1mm below the horizontal defined by B_1–D_1. This assists in maintaining the stability of model flow calculations with negligible effect on the breach profile. Hence, the initiation notch is defined by 5 points and the water level by an additional 2 points, giving 7 points in total at time step t_0. Having established an initial breach section profile, a new profile may be calculated for the given flow conditions. This is shown by the profile of 7 points A-1-B_2-C_2-D_2-2-E. Subsequently, at t_1, a new water level may be established (line 3-4). The breach

profile is now determined by 9 points, and the calculation process predicts a new eroded profile defined by the line A-1-3-B_3-C_3-D_3-4-2-E. At this point, the section is redefined (using Green's theorem(Weisstein, 2011)) so as to maintain the same area of the soil wedge but to only use 7 points, as for example profile A-1-B_2-C_2-D_2-2-E. The transformation between a 9 point and a 7 point definition is shown in Figure A1-8. Notation is consistent with Figure A1-7. The wedge of soil defined by A-1-3-B_1 is replaced by the wedge defined by A-N-B_1 which maintains the same wedge area. Analysis has shown the effect on subsequent hydraulic calculations to be negligible (Buchholzer, 2007).

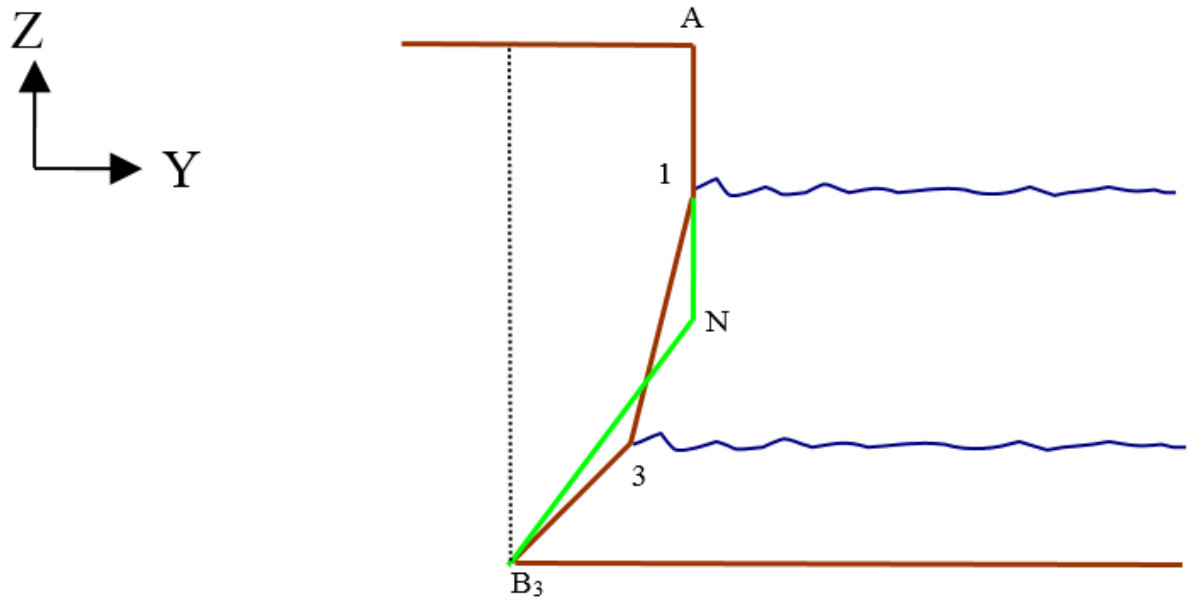

Figure A1-8.—Process for maintaining breach section description between 7 and 9 points.

While the erosion rate is calculated section by section through the embankment, large variations in erosion rate between adjacent sections are avoided by applying an averaged value at each section rather than the individual section specific value. Hence, the erosion rate at any given (internal) section is taken as the average value of that section plus the section up and downstream.

Breach Stability

A number of stability calculations are performed within the breach model. For breach development through a homogeneous embankment, breach side slope stability is assessed according to potential rotational and shear failure modes.

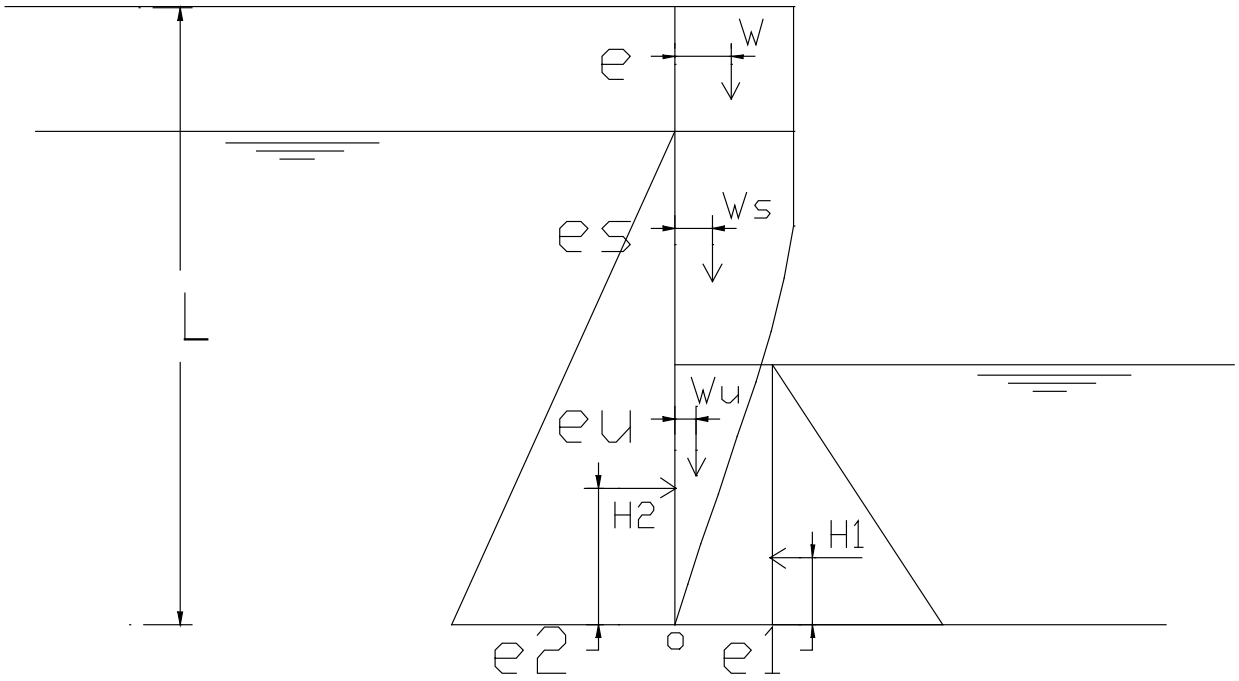

Figure A1-9.—Rotational or bending slope failure (Mohamed, 2002).

Rotational, or bending, failure occurs when the balance of forces on an overhanging block result in a force that exceeds the tensile strength of the soil.

$$M_o = W \cdot e + W_s \cdot e_s + W_u \cdot e_u + H_2 \cdot e_2 - H_1 \cdot e_1 \quad \textbf{(A1-4)}$$

where: M_o : Moment about point o
W : Weight of dry block of the soil.
Ws : Weight of saturated block of the soil.
Wu : Weight of submerged block of the soil.
H_1 : Hydrostatic pressure force in the breach channel
H_2 : Hydrostatic pressure force inside the embankment.
E, e_s,e_u : Weight forces eccentricities.
E_1, e_2 : Hydrostatic pressure forces eccentricities.
L : Length of the failure plane.

Based on the above analysis, the maximum actual tensile stress ($\sigma_{t(actual)}$) on the plane of failure can be computed as follows:

$$\sigma_{t(actual)} = (H_2 - H_1)/L + 6M_0/L^2 \quad \textbf{(A1-5)}$$

Assuming that the allowable soil tensile strength ($\sigma t_{(soil)}$) is known, then failure occurs when $\sigma t_{(actual)}$ exceeds $\sigma t_{(soil)}$.The modeler can then select whether the failed block of soil remains within the breach for subsequent erosion or is removed instantly.

A similar approach may be adopted for the analysis of block failure due to shear (Figure A1-10), including the following assumptions:

- Suction is neglected in the zone above the water level inside the embankment and this zone is considered dry.
- Changes in water level inside the embankment during the embankment failure are slow to respond and can be neglected.

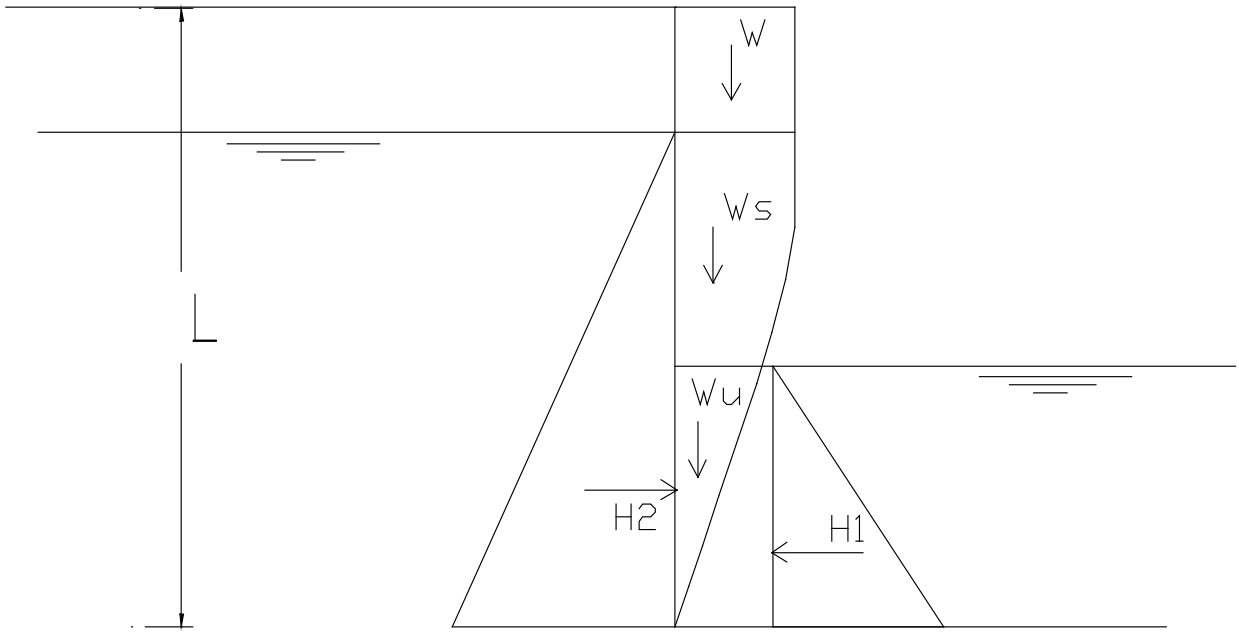

Figure A1-10.—Slope failure due to shear (Mohamed, 2002).

$$FOS = \frac{c * L + H_1 \tan\phi}{W + W_s + W_u + H_2 \tan\phi} \qquad \textbf{(A1-6)}$$

where:
- c : Soil cohesion.
- ϕ : Soil angle of friction.
- W : Weight of dry block of the soil.
- W_s : Weight of saturated block of the soil.
- W_u : Weight of submerged block of the soil.
- H_1 : Hydrostatic water pressure in the breach channel.
- H_2 : Hydrostatic water pressure in the embankment.
- L : Length of the failure plane.

Further structural failure modes are considered for composite embankment structures (i.e. embankments with a core of relatively thin, but stronger, less erodible material). In these cases it is assumed that the core controls the rate of overall breach failure by withstanding erosion relative to the weaker, more erodible supporting material. Hence the model simulates erosion of the supporting material and structural failure of the core material. This process is clearly

demonstrated by the scouring time contours from large scale testing on the Yahekou Dam, China (Shuibo et al., 1993) and can also be seen in dam failure case studies by Ritchey (Ritchey, 2001).

Failure mechanisms that are analysed include sliding of the clay core wall, overturning of the clay core wall and bending failure of the core wall (Hughes, 1981). Details of the force balance equations are provided by Mohamed (Mohamed, 2002).

Surface Protection Layers

In addition to analysis of breach growth processes, the HR BREACH model also includes analysis of the role of surface protection layers comprising either grass or rock cover. The model allows calculation of the flow profile but prevents any breach erosion until flow conditions exceed the design stability of the grass or rock cover. At this point the cover layer is assumed to fail and breach initiation and growth processes continue unrestricted. The performance of grass cover is simulated using the CIRIA grass performance curves (Hewlett et al., 1985); the performance of rock cover is simulated using the semi empirical formula developed by Chang (Chang, 1998) for the design of riprap on steep slopes.

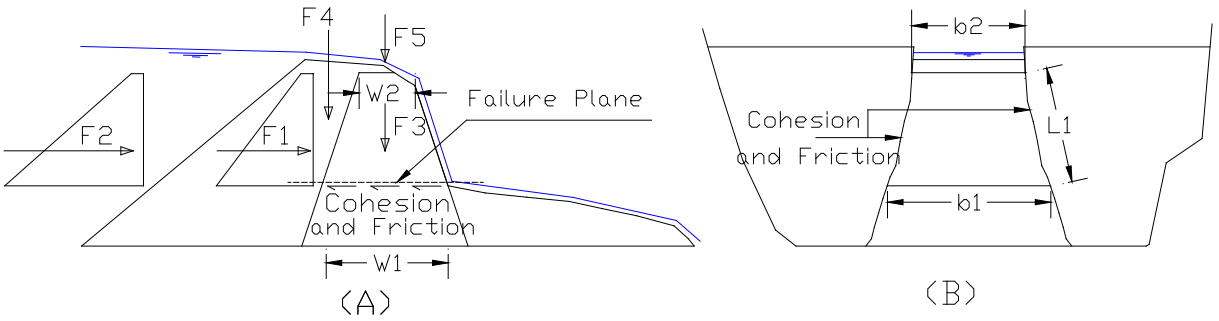

a) Shear failure of core: forces acting on clay core wall

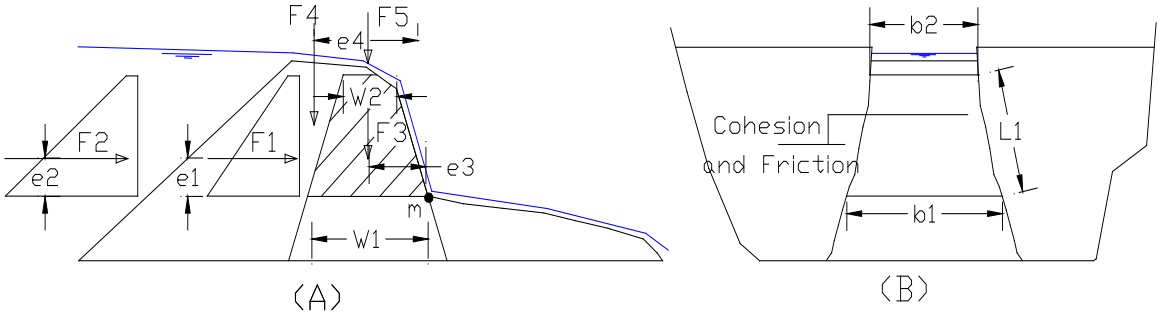

b) Overturning failure of core: forces acting on the clay core wall

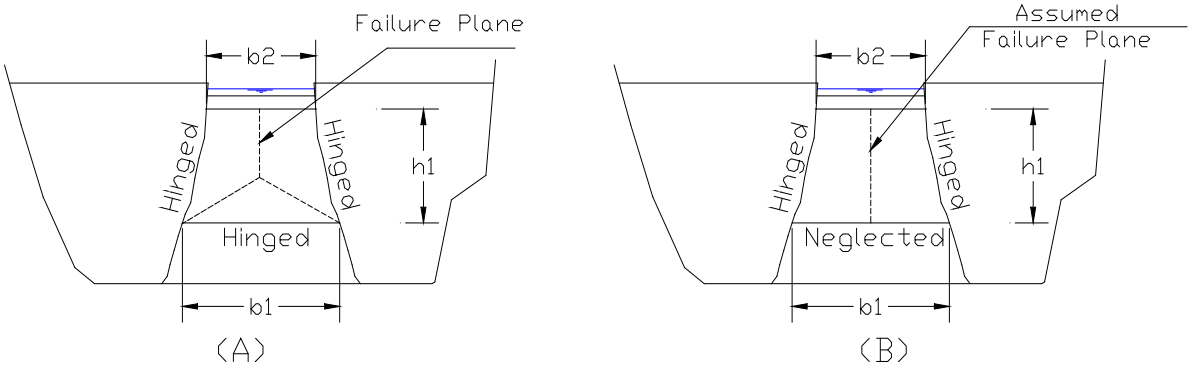

c) Bending failure of the core: assumed failure planes

Figure A1-11.—Structural failure mechanisms used for composite dam breach (Mohamed, 2002).

SIMBA

SIMBA simulates headcut development and headcut advance through the embankment and the widening of the breach and release of the reservoir storage to yield a breach outflow hydrograph. WinDAM additionally evaluates erosional failure of embankment surface layers (vegetation or riprap) preceding headcut development.

Reservoir routing

SIMBA incorporates a level surface reservoir routing model using the assumption of stepwise steady state conditions. During computation, inflow, reservoir water surface elevation, and other conditions, including the geometry of the developing breach erosion area, are known at the beginning of any time step. Conditions at the beginning of the time step are treated as constant during that time step for purposes of erosion computation, allowing the geometry at the end of the time step to be computed as described later. Discharge at the end of the time step may then be computed as a function of reservoir water surface; in turn allowing the water surface elevation to be determined through a mass balance with both inflow and outflow averaged over the time step.

SIMBA allows flow only over the top of the dam through a pre-formed pilot channel, and through the developing breach area. The WinDAM B model that has incorporated SIMBA erosion technology also allows for flow through spillways.

Computation of the discharge through the breach area, if any, is based on unit discharge, with the eroded geometry and effective width of the breach area determined as described later in this report. During breach initiation, the unit discharge in the breach area is computed as for other overtopped areas of the dam using the eroded cross section. Since the breach will tend to form at the point of maximum overtopping, the breach area unit discharge will always be greater than or equal to the maximum overtopping unit discharge. Once breach is initiated, lowering the hydraulic control, energy losses are ignored, and the breach area unit discharge is computed using the assumption of hydrostatic pressure and an energy coefficient of 1.0 at the hydraulic control section. Flow depth at the control section is the greater of that implied by critical flow conditions or downstream tailwater. Total discharge through the breach area is computed as the product of the computed unit discharge and the width of the breach area. To obtain the total discharge associated with overtopping, including that through the breach area, the previously computed discharge associated with flow over the top of the dam is reduced by the product of the maximum overtopping unit discharge and the width of the breach area and added to the breach area discharge. This approximation is consistent with those used in computing the progressive breach erosion as subsequently described.

Embankment overtopping analysis

The downstream embankment slope may be either unprotected or protected by vegetation. WinDAM B will also consider embankments protected by riprap on the downstream slope.

The embankment overtopping erosion analysis is focused on the determination of the timing of a potential breach and development of the resulting outflow hydrograph. The embankment erosion model in SIMBA is therefore directly integrated into the routing model, with the extent of erosion allowed to impact the magnitude of outflow in the breach area. As previously noted, the approach taken is to treat the attack, and therefore erosion rates, as constant over the computational time step. This allows the breach geometry at the end of the time step to be determined and used in the computation of discharge through the breach area at the end of that time step. The computed discharge and geometry are then used to compute erosion rates for the next time step.

The breach erosion model incorporated into SIMBA (and later WinDAM) divides the breach process into four stages (Hanson et al., 2003). These stages are: 1) Failure of any slope protection (WinDAM only) and formation of a headcut on the downstream face of the embankment; 2) Progression of the headcut through the crest of the embankment to initiate breach; 3) Continued progression of the headcut into the reservoir with resulting lowering of the hydraulic control until the embankment is entirely removed in the breach area; and 4) Widening of the breach area during drain-down of the reservoir. The end of stage 2 defines the breach initiation time: the time elapsed prior to the release of stored water. The end of stage 3 defines the breach formation time: the time elapsed prior to complete local removal of the embankment.

Breach Stage 1

Stage 1 of the embankment breach process may be divided into two phases: a) the failure of slope protection, if any, on the downstream face; and b) surface erosion resulting in the development of a headcut. Note that this approach to breach initiation implies that areas of concentrated attack such as toe, berm, and groin areas are submerged or otherwise protected. The location of the surface failure and headcut development is taken to be the point of minimum embankment crest elevation the furthest from an abutment at the most upstream point on the dam face. This location represents the point of maximum discharge over the embankment with the minimum distance for headcut movement to initiate breach and the maximum potential for breach area widening before encountering an abutment.

WinDAM is capable of evaluating the protective capability of grassy vegetation on the downstream face of the embankment or as an unprotected soil surface. For each condition, the approach taken is to assume development of normal flow on the slope resulting in maximum erosive attack. Assignment of these conditions to the upstream end of the reach as described in the previous paragraph represents a worst case simplification of actual flow conditions.

For vegetation, the basis for evaluation is that applied to phase 1 (surface) failure of vegetated earth spillways (USDA NRCS, 1997). Both the time integral of the erosionally effective stress and the maximum gross stress are evaluated. Erosionally effective stress is computed using the relations presented for grass-lined channels by Temple et al. (1987). The vegetal cover is classified as uniform, having minor discontinuities, or having major discontinuities, and the computed erosionally effective stress is adjusted as described in USDA NRCS (1997). The erosionally effective stress is numerically integrated assuming stepwise steady flow conditions. The value of the time-stress integral corresponding to failure is a function of the plasticity index

of the soil material as developed from experience with vegetated spillways (USDA NRCS, 1997).

In evaluating the potential for gross stress to fail the vegetal protection, adequate rooting on the slope is assumed and the limiting value is taken to be 650 Pa (13.5 lb/ft^2). When the gross stress at the beginning of a given time step exceeds this value, failure is assumed to take place during the time step. Conditions at the end of the time step are then those associated with vegetal failure. Vegetal failure is assumed to result in removal of the soil and vegetation to a depth of 0.15 m (0.5 ft). Width of this initial failure area is assumed to be 1.4 times the depth (Temple et al., 2006).

When the downstream embankment face is unprotected, implying exposed bare soil, surface erosion is assumed to be initiated at the beginning of the first time step in which the computed hydraulic shear exceeds the critical shear stress for the soil. The depth of the eroding area is set to zero at the beginning of the time step and an erosion depth computed for the time step. Width at the end of the time step is again calculated to be 1.4 times the computed depth.

For purposes of computing surface erosion, the erosionally effective stress on the soil is assumed to be equal to the gross shear stress, implying that the flow is capable of detaching "particles" of the size governing flow resistance. For purposes of these computations, Manning's *n* representing the eroding soil surface is set to a value of 0.02. The erosion rate expressed in volume per unit area (erosion depth change) per unit time is computed using the excess shear relation:

$$E_r = k_d(\tau_e - \tau_c) \quad (1)$$

where

τ_e= the erosionally effective stress on the soil (total stress for bare soil conditions),

E_r = the soil detachment rate in volume per unit area per unit time,

k_d = a detachment rate coefficient,

τ_c= the critical shear stress,

The detachment rate coefficient and the critical shear stress are material properties and are user inputs to the computational model. Determination of these parameters is discussed by Hanson and Cook (2004) and Hanson and Hunt (2007).

Stage 1, surface erosion will continue to increase the depth and width of the eroding (breach) area until the erosion depth is greater than the critical flow depth associated with the unit discharge in the breach area. Unit discharge is treated as constant over the width of the breach area. Since the eroding surface is now a bare soil condition, erosionally effective stress is assumed equal to gross stress and the change in erosion depth is computed by multiplying the erosion rate, E_r, by length of the time step. In computing width change, each side of the eroding area is assumed to progress at approximately 0.7 times the rate of downward erosion. This rate

is based on observation and an approximation of Lane's (1955) work on stress distribution assuming a rectangular channel and erosionally effective stress much greater than critical stress. Widening is suppressed when the edge of the eroding area reaches an abutment and when the elevation of the crest of the dam is greater than the elevation of the reservoir water surface at the edge of the eroding area.

When the eroded depth exceeds the critical flow depth with the elevation of the downstream tailwater below the crest of the headcut, the flow will tend to develop a plunging action capable of causing the headcut to progress upstream into the crest of the embankment. This represents the end of stage 1 and the beginning of stage 2 of the breach process. The original embankment crest is treated as being erosion resistant such that the erosion depth during stages 1 and 2 is also the height of the developing headcut.

Breach Stage 2

During stage 2 of the breach process, the headcut (breach area) widens, deepens, and progresses upstream through the crest of the embankment. During this stage, the height of the headcut will normally be greater than the critical depth of flow over the crest and the plunging action of the flow will govern the erosion process. If a rising reservoir should result in submergence of the headcut during this stage, headcut advance is temporarily halted, and the deepening and widening is computed as described for stage 1. If downstream tailwater submerges the crest, both headcut advance and downcutting are suppressed.

For plunging flow, the downward erosion lowering the headcut base is again computed using equation 1. The applied stress for use in equation 1 is the greater of that computed for erosion on the slope below the headcut and that computed using the equations developed by Robinson (1992) for stress at the base of an idealized overfall. The width change of the breach area associated with the plunging flow action is taken to be equal to the headcut advance and will usually govern for plunging flow conditions. Computationally, the width change of the breach area over the time step is taken to be the maximum width change associated with either plunging action, approach flow conditions, or exit flow conditions. One half of the computed width change is assigned to each side of the headcut and widening suppressed when the side of the headcut reaches the abutment or the elevation of the dam crest is locally above the reservoir water surface.

For computation of headcut advance, SIMBA uses a deterministic, stress-based headcut advance model. A semi-empirical energy-based model has also been developed, but was disabled for the DSIG model evaluation work. The energy-based model is available in the WinDAM B model which was completed using technology developed in SIMBA. The stress-based model represents the physics of the observed breach erosion processes more directly than the energy-based model.

The stress-based headcut model is fundamentally that presented by Hanson et al. (2001). The headcut is assumed to advance through a series of mass failures driven by erosion at the base as indicated by the sketch presented as figure 1.

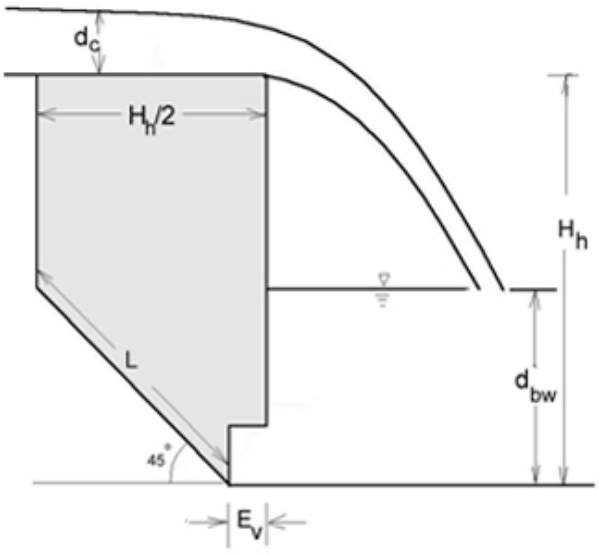

Figure A1-12.—Sketch of headcut failure form used in formulation of Hanson/Robinson headcut advance model.

Hydraulic shear stresses are assumed to erode the base, increasing the distance E_v and shortening distance L, until gravitational forces exceed the soil strength resulting in failure. Soil tensile strength is assumed to be negligible. The hydraulic shear stress driving the erosion on the face of the headcut to increase E_v is computed by the relations developed by Robinson (1992). For the condition represented by Figure 1, these relations may be expressed as:

$$C_n = 0.146 + 27.5[(H_h - d_{bw})/H_h]\left(\frac{d_c}{H_h}\right)^{0.852} e^{-6.1(H_h - d_{bw})/H_h} \tag{2}$$

$$X_{ws} = d_c\left[\frac{0.823 + \frac{H_h - d_{bw}}{d_c}}{0.483}\right]^{\frac{1}{C_n + 1.6}} \tag{3}$$

$$S_{ws} = -0.483(C_n + 1.6)\left(\frac{X_{ws}}{d_c}\right)^{(C_n + 0.6)} \tag{4}$$

$$X_p = X_{ws} - \frac{d_{bw}}{S_{ws}} - 0.411 d_c \tag{5}$$

$$\tau_{hf} = 0.025\gamma d_c \left(\frac{H_h}{d_c}\right)^{0.026} \left(\frac{d_c}{X_p}\right)^{1.06} \left(\frac{d_{bw}}{d_c}\right)^{0.221} \quad (6)$$

where:

C_n = a correction factor associated with the assumption of an incompletely vented nappe at the overfall,

X_{ws} = the relative position of the entry of the jet into the tailwater,

S_{ws} = the slope of the jet upon entry into the tailwater,

X_p = the approximate stagnation pressure of the jet at the headcut base with eccentricity and contraction of the jet ignored as secondary effects,

τ_{hf} = the stress on the headcut face driving the undercutting erosion to increase distance E_v,

γ= the unit weight of the water

d_{bw} = the depth of backwater relative to the base of the headcut (limited to a minimum value equal to critical depth).

and the other variables are as previously defined. τ_{hf} is used as the erosionally effective stress in equation 1 to compute the rate of erosion associated with the increase in distance E_v with time.

The value of E_v corresponding to incipient mass failure for the condition shown in figure 1 may be computed from the quadratic equation solution form (Hanson et al., 2001):

$$E_v = \frac{-b - \sqrt{b^2 - 4ac}}{2a} \quad (7)$$

with

$$a = \frac{\gamma_t}{2} \quad (7a)$$

$$b = \gamma d_c - \frac{\gamma_t H_h}{2} - 2c_u \quad (7b)$$

$$c = c_u H_h + \frac{\gamma}{2} d_{bw}^2 - 0.375 \gamma_t H_h^2 - \frac{\gamma}{2} d_c H_h \quad (7c)$$

where

γ_t = the total unit weight of the soil mass,

c_u=the undrained shear strength of the soil,

a, *b*, and *c* are intermediate terms in the solution of the quadratic equation, and the other variables are as previously defined. Use of d_c rather than d_{bw} in computation of the *b* term implies a conservative application ignoring the stabilizing effect of high tailwater on the mass balance.

The implied average headcut advance rate may then be computed as:

$$\frac{dX}{dt} = \left(\frac{H_h}{2E_v} \right) k_d (\tau_{hf} - \tau_c) \quad (8)$$

With the rate equal to zero when the erosionally effective stress on the face, τ_{hf}, is less than the critical stress for the soil,τ_c.

Equation 8 is applicable only to plunging flow with headcut height and soil strength such that the computed value of E_v is greater than zero. A value of E_v approaching zero implies an unstable vertical face. Physical observations of headcut advance under these conditions are extremely limited, but the expected mode would be cascading flow down the unstable near vertical face. Therefore, the headcut advance model as implemented in WinDAM assumes an upper limit on the headcut advance rate computed by equation 8 equal to the rate associated with normal depth erosion on a 0.5H:1V slope using the assumptions previously described for bare soil. The 0.5H:1V slope is based on the erosion feature created in the failure process described in figure 1. In recognition of the fact that this represents only an approximation of the physics and actual geometry for these high headcuts, E_r from equation 1 is used directly as the advance rate without correction for the assumed geometry.

Breach Stage 3

Stage 3 of the breach erosion process begins when the headcut has advanced through the upstream edge of the embankment crest. Further advance results in a lowering of the hydraulic control and an associated increase in discharge through the breach area. The time associated with the end of stage 2 and beginning of stage 3 is referred to as the breach initiation time.

During stage 3, the headcut may continue to advance as in stage 2 or it may experience downcutting of the crest due to stress-based erosion of the hydraulic control. When the flow is

determined to be plunging, the downcutting of the crest is computed from the frictional hydraulic stress associated with critical flow conditions. When this rate of decrease in the hydraulic control elevation is greater than that associated with headcut advance due to the plunging action of the flow, this change in hydraulic control is considered to govern and the headcut is treated as having advanced the distance that would result in the equivalent drop in hydraulic control. The breach area widening and deepening rates are limited to those that would be computed for plunging flow conditions. Headcut height is allowed to decrease only when the headcut base has reached the dam base elevation. Once the headcut has entered the reservoir, widening of the breach area is suppressed only when the headcut reaches an abutment.

Once the elevation of the headcut base reaches the elevation of the base of the dam, further downward erosion of the base is suppressed and continuing erosion decreases the headcut height. This will eventually result in submergence of the plunging action driving the associated headcut advance rate to zero and causing the downward erosion of the headcut crest to govern using the criteria described in the previous paragraph. When the elevation of the downstream tailwater is greater than the elevation of the water surface associated with critical flow over the crest of the headcut, the flow depth at the hydraulic control is taken to be the difference between the elevations of the crest of the headcut and the tailwater.

Breach Stage 4

Stage 3 is complete when the headcut has advanced to the upstream toe of the embankment indicating complete removal of the embankment in the breach area. During stage 4, erosion associated with breach outflow serves to widen the breach. The rate of widening is computed as for submerged headcut conditions during stage 3. Energy losses associated with flow through the breach are ignored and the flow depth at the hydraulic control section is taken to be the greater of critical depth or the difference between the elevation of the downstream tailwater and the base of the dam. The slope of the energy grade line at the hydraulic control is computed using Manning's equation and the maximum boundary frictional stress is computed as the product of the unit weight of water, the flow depth, and the energy slope. The associated erosion rate is computed from equation 1. The rate of expansion of each edge of the breach area is taken to be 0.7 times the computed maximum erosion rate. Expansion is suppressed when the edge of the breach area reaches an abutment.